UNIVERSITY OF CALIFORNIA
RIVERSIDE

Characterization and Estimation of Greenhouse Gas and Ammonia Emissions From California Dairy Farms

A Dissertation submitted in partial satisfaction
of the requirements for the degree of

Doctor of Philosophy

in

Environmental Sciences

by

Valerie Carranza

March 2023

Dissertation Committee:
Dr. Francesca M. Hopkins, Chairperson
Dr. Peter M. Homyak
Dr. Raymond G. Anderson

The Dissertation of Valerie Carranza is approved:

_____

_____

_____

Committee Chairperson

University of California, Riverside

ACKNOWLEDGMENTS

The author would like to thank all the scientists and collaborators who supported the technical and intellectual content of this research including Dr. Francesca Hopkins, Dr. Ray Anderson, Dr. Deanne Meyer, Dr. Akula Venkatram, Dr. Marc Fischer, Dr. Amy Townsend-Small, Isis Frausto-Vicencio, Talha Rafiq, Michael Rodriguez, and Ranga Thiruvenkatachari. A special thanks to our dairy collaborators in Central and Southern California for site access and collaboration. The author also thanks Casaundra Caruso, Yifan Ding, Sajjan Heerah, Celia Limón, Alison Marklein, and Cindy Yañez for help with field work.

This work was supported by the University of California, Office of the President, Laboratory Fee Research Program (grant LFR-18-548581). The author also acknowledges funding from the National Science Foundation Graduate Research Fellowship Program and the University of California, Riverside Environmental Dynamics and GeoEcology (EDGE) Institute. Work at Lawrence Berkeley National Laboratory was also supported by Contractor Supporting Research (CSR) under Contract No.DE-AC02-05CH11231. The authors' views and opinions expressed herein do not necessarily state or reflect those of the United States Government or any agency thereof, or The Regents of the University of California.

The second chapter of this dissertation, in full, is a reprint of the material as it appears in “Isotopic Signatures of Methane Emissions From Dairy Farms in California’s San Joaquin Valley” published within Journal of Geophysical Research: Biogeosciences

in 2022 which was authored by Valerie Carranza, Brenna Biggs, Deanne Meyer, Amy Townsend-Small, Ranga Rajan Thiruvenkatachari Akula Venkatram, Marc L. Fischer, and Francesca M. Hopkins.

DEDICATION

There are many who I want to thank for their immense support, encouragement, and inspiration in my pursuit to a Ph.D.. To my parents, thank you for your unconditional love and for all your sacrifice. I would not be where I am if it were not for your courage to take a leap of faith in another country for a better life. Mamá, gracias por siempre apoyarme en todos mis sueños, por acompañarme en todas mis desveladas, y por nunca dejarme rendir cuando más lo necesitaba. Papá, gracias por todos tus sacrificios en el trabajo y por todo tu apoyo incondicional—me enseñaste el valor del trabajo y que todo es posible si le echas muchas ganas. Los quiero mucho.

To my brother, Daniel, thank you for being there for me, especially this year, when I needed it most and for your support throughout my Ph.D.. You witnessed my lows and highs and were always there whenever I needed an extra hand. Thank you. To my cousin, Junior, thank you for always encouraging me to follow my dreams and for being an amazing role model. To Ellie, for her unconditional love, support, and for always reminding me the simple joys of life.

I would like to especially thank Dr. Francesca Hopkins for believing in me when I was a community college student interning at UC Irvine. Thank you for all your guidance, patience, and support throughout the last 9 years. Thank you for inspiring me to be a scientist when I was a community college student who had never met a female scientist before. From an intern at UC Irvine and JPL to a PhD at UC Riverside, thank you for helping me develop into a scientist full of curiosity and hope.

I would like to thank my lab mates, who have also become my closest friends: Isis Frausto-Vicencio, Talha Rafiq, Michael Rodriguez, Alondra Moreno, Cindy Yañez, Celia Limón, and Michelle Carr. I could not imagine a better lab group than the one I was so lucky to be a part of. We shared so much laughter, frustrations, and adventures together. Thank you for being an amazing support network during graduate school. I wish you all success and satisfaction in all your personal and career endeavors.

Lastly, I would like to thank all my mentors who have supported and inspired me to become a scientist. To my community college professors, Professors Dr. Becky Green-Marroquin, Meredith Leonard, and George Leddy, thank you for inspiring me to pursue environmental sciences as a career and for opening my world to research. To my JPL mentors, Dr. Chip Miller, Riley Duren, and Dr. Kristal Verhulst, thank you for your mentorship during my internships at JPL and for encouraging me to publish my first scientific paper. Dr. Peter Kareiva, I am incredibly grateful for all your mentorship at UCLA, all our intellectual conversations, and for encouraging me to pursue a Ph.D.. To my dissertation committee members, Dr. Francesca Hopkins, Dr. Peter Homyak, and Dr. Ray Anderson, for their insight on my dissertation and all their advice throughout my Ph.D. career. I am grateful for all of you.

ABSTRACT OF THE DISSERTATION

Characterization and Estimation of Greenhouse Gas and Ammonia Emissions From California Dairy Farms

by

Valerie Carranza

Doctor of Philosophy, Graduate Program in Environmental Sciences
University of California, Riverside, March 2023
Dr. Francesca M. Hopkins, Chairperson

Dairies are an important source of greenhouse gas and air pollutant emissions, such as methane (CH_4), nitrous oxide (N_2O), and ammonia (NH_3), but these emissions remain highly uncertain across spatial and temporal scales. Stable isotope measurements and enhancement ratios between different trace gases can be used to characterize and identify relative magnitudes, trends, and sources of emissions. In the first study, CH_4 emissions from enteric fermentation and manure management source areas from dairy farms in California's San Joaquin Valley (SJV) are characterized using isotopic signatures of CH_4 ($\delta^{13}C_{CH4}$). Methane from manure lagoons was more enriched in $\delta^{13}C$ than CH_4 from enteric fermentation across seasons on average by 14 ± 2‰. The second study quantified and characterized seasonal CH_4, N_2O, and NH_3 emissions from SJV dairy farms using enhancement ratios of trace gases (ΔN_2O:ΔCH_4; ΔNH_3:ΔCH_4). The average ΔNH_3:ΔCH_4 from freestall barns and corrals observed across all seasons is 0.58 ± 0.19 ppbv $ppbv^{-1}$ and 0.48 ± 0.05 ppbv $ppbv^{-1}$, respectively. Manure lagoons had an average ΔNH_3: ΔCH_4 of

0.09 ± 0.01 ppbv ppbv^{-1} , whereas dry bedding had ΔNH_3:ΔCH_4 of 2.71 ± 0.85 ppbv ppbv^{-1}. ΔN_2O:ΔCH_4 also show distinct signatures between livestock housing, manure management, cropland, and silage, with the highest enhancement ratios observed in cropland (1.65 ± 0.17 ppbv ppbv^{-1}). The third study estimated seasonal and diurnal CH_4 fluxes from dairy manure lagoons in Southern California. Diurnal CH_4 fluxes were closely correlated with latent heat fluxes and show a positive relationship with lagoon temperatures and wind speed; however, the temperature relationship differs at seasonal timescales. Methane fluxes decreased over the study period, with the highest CH_4 fluxes measured during the spring season (6.89 µmol $m^{-2}s^{-1}$; 95% CI: 6.41 - 7.45 µmol $m^{-2}s^{-1}$), following precipitation events. These findings highlight how isotopic measurements and enhancement ratios of co-located emissions can be used for source apportionment of dairy emissions. Lastly, it underscores the importance of long-term measurements of CH_4 fluxes from dairy manure lagoons to determine the principal environmental factors influencing the magnitude of seasonal and diurnal trends.

Table of Contents

List of Figures

List of Tables

1. Introduction

Agricultural practices impact and influence climate change and air quality, with an estimated 23% of total anthropogenic greenhouse gas (GHG) emissions stemming from Agriculture, Forestry and Other Land Use (AFOLU) (IPCC, 2019). In the United States alone, livestock contributes an estimated 66% of total agricultural GHG emissions (USDA, 2016). The primary emissions stem from greenhouse gases, such as methane (CH_4), nitrous oxide (N_2O), carbon dioxide (CO_2), as well as air pollutants, such as ammonia (NH_3), a gas-phase precursor to fine particulate matter. CH_4 is more efficient at trapping infrared radiation than CO_2, with a lifetime of about 10 years in the troposphere and a global warming potential (GWP) about 28 times that of CO_2 on a 100-year scale (IPCC, 2013). Since 2007, the global mole fraction of atmospheric CH_4 has steadily increased from 1781 ppb to 1895 ppb. Meanwhile, the $^{13}C/^{12}C$ isotopic ratio of CH_4 (expressed as $\delta^{13}C_{CH4}$) has shifted to more negative values, suggesting a shift towards more biogenic sources that may include an increase in agricultural sources (Nisbet et al., 2019). Atmospheric N_2O levels are about 334 ppb and have increased by more than 20% since 1750, with a GWP 265 times that of CO_2. The agricultural sector contributes an estimated 52% of anthropogenic N_2O emissions (Tian et al., 2020). In addition, global emissions of NH_3 have doubled in the last 70 years, and are expected to rise, posing a concern for poor air quality (Bauer et al., 2016; Lamarque et al., 2010).

In the United States, California leads the nation in dairy production, with 1.8 million milk cows and $6.5 billion in milk sales (USDA NASS, 2019). In the last decade, the State of California has emerged as a leader in GHG reduction strategies. Under

California's Global Warming Solutions Act of 2006 [Assembly Bill 32 (AB 32)], the State mandates that GHG emissions are reduced to 1990 levels by 2020 (California Assembly Bill No. 32-Global Warming Solutions Act of 2006, 2006). Additionally, in 2016, Legislature passed SB 32, which directs the State to reduce GHG emissions 40% below 1990 levels by 2030, along with SB 1383, which directs efforts towards reducing short-lived climate pollutants (e.g., CH_4) that have a strong climate forcing potential. The dairy sector contributes a substantial amount of CH_4, N_2O, and NH_3 emissions, and as such are important to study to meet these requirements. For instance, dairy enteric fermentation and manure management, account for an estimated 27% and 25% of total CH_4 emissions in the State inventory, respectively (CARB, 2015). Although N_2O is not yet targeted by SB 1383, it is estimated that N_2O emissions from manure management account for about 13% of the statewide total N_2O (CARB, 2015). However, there is high uncertainty in emission estimates of CH_4, N_2O, and NH_3 from dairy farms in California, in large part due to a dearth of measurements conducted at the facility level and across timescales. So far, there have only been two studies that have investigated on-farm seasonal CH_4 emissions in California (Arndt et al., 2018; Amini et al., 2022). In addition, there have only been two source attribution studies in California that have used isotopic signatures of CH_4 (Townsend-Small et al., 2012; C. Viatte et al., 2016) that were conducted in Southern California. Another useful source attribution method is to use enhancement ratios, which are defined as ratios between enhancements of trace gases (i.e., atmospheric mole fractions of a given trace gas (e.g., CH_4, N_2O, and NH_3) above atmospheric background mole fractions) (D. J. Miller et al., 2015; Eilerman et al., 2016). There has only been one such study investigating

dairy farms in California, but was limited to only one season during winter (D. J. Miller et al., 2015)

Anaerobic microbial breakdown of carbohydrates in the digestive tract of cattle produces about 30-40% of CH_4 as a by-product (Bréas et al., 2001). Ruminants, such as cattle, have large fermentative cavities in the beginning of the digestive tract that break down carbohydrates and plant cell walls, and form acetate, propionate, butyrate, succinate, H_2, and CO_2 through the Embden-Meyerhof-Parnas pathway (Immig, 1996). Methanogens then use the by-product H_2 and reduce CO_2 into CH_4 (T. L. Miller & Wolin, 1986). The other by-products, acetate and butyrate, help induce methanogenesis.

Manure management systems vary among dairy farms but generally consist of dry and wet management practices (Kaffka et al., 2016). Dry manure management consists of deep pits, solid manure storage, dry lots, and daily spread (CARB, 2015). In a wet manure management system, manure waste from animal housing areas are washed and typically collected in manure lagoons, where anaerobic conditions produce CH_4 (Kaffka & Barzee, 2016). Manure can also be diverted to anaerobic digesters and converted to useable energy. Dry manure handling practices reduce anaerobic conditions since they do not flush waste with water. Methane emissions from dairy operations are thought to depend on the type of manure management used (Kaffka et al., 2016). So far, however, there are only two studies on seasonal CH_4 emissions from anaerobic lagoons in California, but none have studied emissions from all four seasons (Arndt et al., 2018; Amini et al., 2022). Measuring and modeling emissions from dairy manure management are challenging given the variability of practices (Owen & Silver, 2015). It is only recently that mobile measurement campaigns

measured CH_4 emissions from a small number of dairies with anaerobic lagoons (Camille Viatte et al., 2017; Thiruvenkatachari et al., 2020).

Isotopic signatures of CH_4 can help resolve and identify sources of CH_4 emissions. The $\delta^{13}C_{CH4}$ denotes the abundance of ^{13}C relative to ^{12}C in CH_4, expressed as:

$$\delta^{13}C_{CH4} = \left\{ \frac{\left(\frac{\delta^{13}C}{\delta^{12}C}\right)_{sample}}{\left(\frac{\delta^{13}C}{\delta^{12}C}\right)_{standard}} - 1 \right\} \times 1000‰ \quad \text{(Eq.1)}$$

$\delta^{13}C_{CH4}$ is in units of permil, or ‰, and the standard values come from the Vienna Pee Dee Belemnite (VPDB) standard (Arata et al., 2016). The δD can also be used to characterize CH_4 emissions using a similar equation as Eq.1 measuring the abundance of ^{2}H relative to ^{1}H in CH_4 with the standard Vienna Standard Mean Ocean Water (VSMOW). Stable isotopes of CH_4, $\delta^{13}C$ and δD ratios, can characterize microbial sources of CH_4, with $\delta^{13}C$ values typically between -50‰ and -110‰ and δD values of -150‰ to -400‰ (Stevens & Rust, 1982; Cicerone & Oremland, 1988; P. D. Quay et al., 1991; P. Quay et al., 1999; Bréas et al., 2001; Whiticar & Schaefer, 2007; Dlugokencky et al., 2011).

Isotopic signatures of CH_4 can also elucidate information about the methanogenic pathways in a source system and the associated fractionation factors. The bacterial reduction of CO_2 to CH_4 can lead to depleted $\delta^{13}C_{CH4}$ values as negative as -110‰, whereas the fermentation of methylated substrates can produce $\delta^{13}CH_{4values}$ of -50‰ to -60‰ (Whiticar, 1999). Methanogenesis of methylated substrates can produce δD_{CH4} values as negative as -531‰, meanwhile the CO_2-reduction pathway produces δD_{CH4} values between -170‰ to -250‰ (Whiticar, 1999). As an example of isotopic signatures of CH_4 emitted

from dairy farms, Levin et al. (1993) found that the isotopic signature $\delta^{13}C$ of CH_4 from cattle strongly depended on the feedstock composition (i.e., C3 diet vs. C4 diet). A diet consisting of 100% C3 plants produced $\delta^{13}C$ of -65.1±1.7‰, but a 60-80% C4 diet produced $\delta^{13}C$ of -55.6±1.4‰. This isotopic difference is on par with the difference of $\delta^{13}C$ of the two plant types (i.e., ~10‰). The δD values of CH_4 from cattle and dairy wastes were similarly depleted, with values of -300±10‰ and -298±6‰, respectively, suggesting that the primary methanogenic pathway is from acetate fermentation (Levin et al., 1993).

Atmospheric N_2O emissions from dairies arise from wet and dry manure management practices. Given that field data is still variable, the majority of N_2O emissions is estimated to originate from barns, unlike dairy CH_4 emissions, which are mostly expected from anaerobic lagoons and slurry systems (Owen & Silver, 2015). The next largest emitter of N_2O from dairy manure management is estimated to come from corrals and solid manure piles (Owen & Silver, 2015). Corrals include loafing pens, hardstandings, and dry lots. Studies have also measured N_2O emissions from anaerobic lagoons and slurry stores, which was unexpected since anaerobic conditions are dominant in wet manure storage (Sneath et al., 2006; Bjorneberg et al., 2009; Borhan et al., 2011a, 2011b; Leytem et al., 2011). In anaerobic wet manure, nitrogen is mostly found in the form of ammonium (NH_4^+) and organic nitrogen, but denitrification is possible at inlets from wet manure storage systems if aerobic conditions are present (Owen & Silver, 2015). Nitrous oxide can also form through the denitrification of nitrate (NO_3^-) generated by Feammox, Mnammox, or anammox in the cases where NO_3^- is present (Mulder et al., 1995; Engström et al., 2005; Yang et al., 2012). Nitrification can also occur under aerobic conditions, where N_2O is

emitted as a by-produced when NH_4^+ is first oxidized to nitrite and then converted to NO_3^- (Broucek, 2016). Crop fields fertilized by manure and other synthetic fertilizers near dairies also emit N_2O (Davidson, 2009).

Ammonia is formed and volatilized from dairy manure almost immediately after urine and feces are excreted. Ammonia travels to the manure surface via diffusion and is released to the atmosphere via convective mass transfer (Ni, 1999). In general, NH_3 volatilization increases with higher concentrations of NH_4^+/NH_3, substrate temperature, wind speed and turbulence (Olesen & Sommer, 1993; Teye & Hautala, 2008). The pH at the surface of manure impacts the amount of NH_3 that is volatilized. Ammonia emissions are highest between a pH of 7 to 10 and decrease with lower pH and is impacted by the pKa (~9) of the reaction (Saggar et al., 2004; Hristov et al., 2011).

The overarching objective of this dissertation was to characterize and quantify CH_4, N_2O, and NH_3 emissions from California dairy farms. The dissertation chapters are the following:

- Isotopic Signatures of Methane Emissions from Dairy Farms in California's San Joaquin Valley (Chapter 2)
- Characterization of Ammonia, Nitrous Oxide, and Methane Emissions from California Dairy Farms Using Enhancement Ratios (Chapter 3)
- Seasonality of Methane Fluxes from Dairy Manure Lagoons: A Case Study from a Southern California Dairy (Chapter 4)

For the first investigation, we hypothesized that $\delta^{13}C_{CH4}$ can be used to differentiate observations of atmospheric CH_4 enhancements between anaerobic decomposition in

manure lagoons and enteric fermentation. In addition, we expected that seasonality may affect $\delta^{13}C_{CH4}$ from dairy farm sources if, for example, there are large differences in diet composition between seasons. Lastly, we hypothesized that $\delta^{13}C_{CH4}$ source signatures from enteric fermentation and anaerobic lagoons at the farm scale can help explain the dominant source of CH_4 plumes downwind of dairy farms at the regional scale.

For the second investigation, we hypothesized enhancement ratios can be used for source apportionment and identification of relative emission trends between sources of dairy emissions. We expected different sources at a dairy farm to have distinct enhancement ratios between NH_3 and CH_4 (ΔNH_3:ΔCH_4) and N_2O and CH_4 (ΔN_2O:ΔCH_4). We also hypothesized that seasonality may impact enhancement ratios from dairy farm sources.

For the third investigation, we expected CH_4 emissions from manure lagoons to follow seasonal patterns, with higher fluxes in spring and summer when manure substrate availability and temperature are higher. We also predicted that higher wind speeds would increase CH_4 fluxes through increased turbulence and mixing of the lagoon surface. Lastly, we hypothesized that manure management practices would have a measurable impact on measured CH_4 emissions.

As more nations and cities move towards meeting GHG and air pollution reduction goals, it is critical to gain a better understanding of the magnitude and drivers of emissions. Different biogeochemical processes, environmental factors, and temporal and spatial variability can impact emission estimates, making it challenging to assess mitigation efforts across regions and timescales (Hristov et al., 2011; Owen & Silver, 2015; Broucek, 2018).

The objective of these investigations is to gain a comprehensive understanding of seasonal and diurnal patterns of CH_4 fluxes from dairy manure lagoons and provide source apportionment tools that may be used to distinguish between co-located dairy emissions.

1.1 References

Amini, S., Kuwayama, T., Gong, L., Falk, M., Chen, Y., Mitloehner, Q., Weller, S., Mitloehner, F. M., Patteson, D., Conley, S. A., Scheehle, E., & FitzGibbon, M. (2022). Evaluating California dairy methane emission factors using short-term ground-level and airborne measurements. *Atmospheric Environment: X*, *14*(November 2021), 100171. https://doi.org/10.1016/j.aeaoa.2022.100171

Arata, C., Rahn, T., & Dubey, M. K. (2016). Methane Isotope Instrument Validation and Source Identification at Four Corners, New Mexico, United States. *Journal of Physical Chemistry A*, *120*(9), 1488–1494. https://doi.org/10.1021/acs.jpca.5b12737

Arndt, C., Leytem, A. B., Hristov, A. N., Zavala-Araiza, D., Cativiela, J. P., Conley, S., Daube, C., Faloona, I., & Herndon, S. C. (2018). Short-term methane emissions from 2 dairy farms in California estimated by different measurement techniques and US Environmental Protection Agency inventory methodology: A case study. *Journal of Dairy Science*, *101*(12), 11461–11479. https://doi.org/10.3168/jds.2017-13881

Bauer, S. E., Tsigaridis, K., & Miller, R. (2016). Significant atmospheric aerosol pollution caused by world food cultivation. *Geophysical Research Letters*, *43*(10), 5394–5400. https://doi.org/10.1002/2016GL068354

Bjorneberg, D. L., Leytem, A. B., Westermann, D. T., Griffiths, P. R., Shao, L., & Pollard, M. J. (2009). Measurement of atmospheric ammonia, methane, and nitrous oxide at a concentrated dairy production facility in southern idaho using open-path FTIR spectrometry. *Transactions of the ASABE*, *52*(5), 1749–1756.

Borhan, M. S., Capareda, S. C., Mukhtar, S., Faulkner, W. B., McGee, R., & Parnell, C. B. (2011a). Greenhouse gas emissions from ground level area sources in dairy and cattle feedyard operations. *Atmosphere*, *2*(3), 303–329. https://doi.org/10.3390/atmos2030303

Borhan, M. S., Capareda, S., Mukhtar, S., Faulkner, W. B., McGee, R., & Parnell, C. B. (2011b). Determining Seasonal Greenhouse Gas Emissions from Ground-Level Area Sources in a Dairy Operation in Central Texas. *Journal of the Air & Waste Management Association*, *61*(7), 786–795. https://doi.org/10.3155/1047-3289.61.7.786

Bréas, O., Guillou, C., Reniero, F., & Wada, E. (2001). The global methane cycle: Isotopes and mixing ratios, sources and sinks. *Isotopes in Environmental and Health Studies*, *37*(4), 257–379. https://doi.org/10.1080/10256010108033302

Broucek, J. (2016). Nitrous Oxide Production from Cattle and Swine Manure. *Journal of Animal Behaviour and Biometeorology*, *5*(1), 13–19. https://doi.org/10.14269/2318-1265/jabb.v5n1p13-19

Broucek, J. (2018). Nitrous oxide production in ruminants - A review. *Animal Science Papers and Reports*, *36*(1), 5–19.

CARB. (2015). *California Greenhouse Gas Emissions Inventory: 2000– 2015*.

Cicerone, R. J., & Oremland, R. S. (1988). Biogeochemical aspects of atmospheric methane. *Global Biogeochemical Cycles*, *2*, 299–327. https://doi.org/10.1029/GB002i004p00299

Davidson, E. A. (2009). The contribution of manure and fertilizer nitrogen to atmospheric nitrous oxide since 1860. *Nature Geoscience*, *2*(9), 659–662. https://doi.org/10.1038/ngeo608

Dlugokencky, E. J., Nisbet, E. G., Fisher, R., & Lowry, D. (2011). Global atmospheric methane: budget, changes and dangers. *Philosophical Transactions of the Royal Society A: Mathematical, Physical and Engineering Sciences*, *369*(1943), 2058–2072. https://doi.org/10.1098/rsta.2010.0341

Eilerman, S. J., Peischl, J., Neuman, J. A., Ryerson, T. B., Aikin, K. C., Holloway, M. W., Zondlo, M. A., Golston, L. M., Pan, D., Floerchinger, C., & Herndon, S. (2016). Characterization of Ammonia, Methane, and Nitrous Oxide Emissions from Concentrated Animal Feeding Operations in Northeastern Colorado. *Environmental Science and Technology*, *50*(20), 10885–10893. https://doi.org/10.1021/acs.est.6b02851

Engström, P., Dalsgaard, T., Hulth, S., & Aller, R. C. (2005). Anaerobic ammonium oxidation by nitrite (anammox): Implications for N2 production in coastal marine sediments. *Geochimica et Cosmochimica Acta*, *69*(8), 2057–2065. https://doi.org/10.1016/j.gca.2004.09.032

Hristov, A. N., Hanigan, M., Cole, A., Todd, R., McAllister, T. A., Ndegwa, P. M., & Rotz, A. (2011). Review: Ammonia emissions from dairy farms and beef feedlots. *Canadian Journal of Animal Science*, *91*(1), 1–35. https://doi.org/10.4141/CJAS10034

Immig, I. (1996). The rumen and hindgut as source of ruminant methanogenesis. *Environmental Monitoring and Assessment*, *42*(1–2), 57–72. https://doi.org/10.1007/BF00394042

IPCC. (2013). Carbon and Other Biogeochemical Cycles. In: Climate Change 2013: The Physical Science Basis. Contribution of Working Group I to the Fifth Assessment Report of the Intergovernmental Panel on Climate Change. *Cambridge University Press*, *9781107057*, 465–570. https://doi.org/10.1017/CBO9781107415324.015

IPCC. (2019). *Summary for Policymakers. In: Climate Change and Land: an IPCC special report on climate change, desertification, land degradation, sustainable land management, food security, and greenhouse gas fluxes in terrestrial ecosystems*. https://doi.org/10.1002/9781118786352.wbieg0538

Kaffka, S., & Barzee, T. (2016). *Evaluation of Dairy Manure Management Practices for Greenhouse Gas Emissions Mitigation in California*.

Lamarque, J.-F., Bond, T. C., Eyring, V., Granier, C., Heil, A., Klimont, Z., Lee, D., Liousse, C., Mieville, A., Owen, B., Granier, C., Mieville, A., Schultz, M. G., Shindell, D., Smith, S. J., Stehfest, E., Van Aardenne, J., Cooper, O. R., Kainuma, M., … Van Vuuren, D. P. (2010). Historical (1850–2000) gridded anthropogenic and biomass burning emissions of reactive gases and aerosols: methodology and application. *European Geosciences Union*, *10*(15), 7017–7039. https://doi.org/10.5194/acp-10-7017-2010

Levin, I., Bergamaschi, P., Dörr, H., & Trapp, D. (1993). Stable isotopic signature of methane from major sources in Germany. *Chemosphere*, *26*(1–4), 161–177. https://doi.org/10.1016/0045-6535(93)90419-6

Leytem, A. B., Dungan, R. S., Bjorneberg, D. L., & Koehn, A. C. (2011). Emissions of Ammonia, Methane, Carbon Dioxide, and Nitrous Oxide from Dairy Cattle Housing and Manure Management Systems. *Journal of Environmental Quality*, *40*(5), 1383–1394. https://doi.org/10.2134/jeq2009.0515

Miller, D. J., Sun, K., Tao, L., Pan, D., Zondlo, M. A., Nowak, J. B., Liu, Z., Diskin, G., Sachse, G., Beyersdorf, A., Ferrare, R., & Scarino, A. J. (2015). Ammonia and methane dairy emission plumes in the San Joaquin Valley of California from individual feedlot to regional scales. *Journal of Geophysical Research: Atmospheres*, *120*(18), 9718–9738. https://doi.org/10.1002/2015JD023241

Miller, T. L., & Wolin, M. J. (1986). Methanogenesis in human and animal intestinal tracts. *Systematic and Applied Microbiology*, *7*, 223–229.

Mulder, A., van de Graaf, A. A., Robertson, L. A., & Kuenen, J. G. (1995). Anaerobic ammonium oxidation discovered in a denitrifying fluidized bed reactor. *FEMS Microbiology Ecology*, *16*(3), 177–184.

Ni, J. (1999). Mechanistic models of ammonia release from liquid manure: a review. *Journal of Agricultural Engineering Research*, *72*(1), 1–17. https://www.sciencedirect.com/science/article/pii/S0021863498903420

Nisbet, E. G., Manning, M. R., Dlugokencky, E. J., Fisher, R. E., Lowry, D., Michel, S. E., Myhre, C. L., Platt, S. M., Allen, G., Bousquet, P., Brownlow, R., Cain, M., France, J. L., Hermansen, O., Hossaini, R., Jones, A. E., Levin, I., Manning, A. C., Myhre, G., … White, J. W. C. (2019). Very Strong Atmospheric Methane Growth in the 4 Years 2014–2017: Implications for the Paris Agreement. *Global Biogeochemical Cycles*, *33*(3), 318–342. https://doi.org/https://doi.org/10.1029/2018GB006009

Olesen, J. E., & Sommer, S. G. (1993). Modelling effects of wind speed and surface cover on ammonia volatilization from stored pig slurry. *Atmospheric Environment Part A, General Topics*, *27*(16), 2567–2574. https://doi.org/10.1016/0960-1686(93)90030-3

Owen, J. J., & Silver, W. L. (2015). Greenhouse gas emissions from dairy manure management: A review of field-based studies. *Global Change Biology*, *21*(2), 550–565. https://doi.org/10.1111/gcb.12687

California Assembly Bill No. 32-Global Warming Solutions Act of 2006, 5 Secretary 38500 (2006).

Quay, P. D., King, S. L., Stutsman, J., Wilbur, D. O., Steele, L. P., Fung, I., Gammon, R. H., Brown, T. A., Farwell, G. W., Grootes, P. M., & Schmidt, F. H. (1991). Carbon isotopic composition of atmospheric CH 4 : Fossil and biomass burning source strengths. *Global Biogeochemical Cycles*, *5*(1), 25–47. https://doi.org/10.1029/91GB00003

Quay, P., Stutsman, J., Wilbur, D., Snover, A., Dlugokencky, E., & Brown, T. (1999). The isotopic composition of atmospheric methane. *Global Biogeochemical Cycles*, *13*(2), 445–461. https://doi.org/10.1029/1998GB900006

Saggar, S., Bolan, N. S., Bhandral, R., Hedley, C. B., & Luo, J. (2004). A review of emissions of methane, ammonia, and nitrous oxide from animal excreta deposition and farm effluent application in grazed pastures. *New Zealand Journal of Agricultural Research*, *47*(4), 513–544. https://doi.org/10.1080/00288233.2004.9513618

Sneath, R. W., Beline, F., Hilhorst, M. A., & Peu, P. (2006). Monitoring GHG from manure stores on organic and conventional dairy farms. *Agriculture, Ecosystems & Environment*, *112*(2–3), 122–128. https://doi.org/10.1016/J.AGEE.2005.08.020

Stevens, C. M., & Rust, F. E. (1982). The carbon isotopic composition of atmospheric methane. *Journal of Geophysical Research*, *87*(C7), 4879. https://doi.org/10.1029/JC087iC07p04879

Teye, F. K., & Hautala, M. (2008). Adaptation of an ammonia volatilization model for a naturally ventilated dairy building. *Atmospheric Environment*, *42*(18), 4345–4354. https://doi.org/10.1016/j.atmosenv.2008.01.019

Thiruvenkatachari, R. R., Carranza, V., Ahangar, F., Marklein, A., Hopkins, F., & Venkatram, A. (2020). Uncertainty in using dispersion models to estimate methane emissions from manure lagoons in dairies. *Agricultural and Forest Meteorology*, *290*, 108011. https://doi.org/10.1016/j.agrformet.2020.108011

Tian, H., Xu, R., Canadell, J. G., Thompson, R. L., Winiwarter, W., Suntharalingam, P., Davidson, E. A., Ciais, P., Jackson, R. B., Janssens-Maenhout, G., Prather, M. J., Regnier, P., Pan, N., Pan, S., Peters, G. P., Shi, H., Tubiello, F. N., Zaehle, S., Zhou, F., … Yao, Y. (2020). A comprehensive quantification of global nitrous oxide sources and sinks. *Nature*, *586*(7828), 248–256. https://doi.org/10.1038/s41586-020-2780-0

Townsend-Small, A., Tyler, S. C., Pataki, D. E., Xu, X., & Christensen, L. E. (2012). Isotopic measurements of atmospheric methane in Los Angeles, California, USA: Influence of "fugitive" fossil fuel emissions. *Journal of Geophysical Research: Atmospheres*, *117*(D7). https://doi.org/10.1029/2011JD016826

USDA. (2016). U . S . Agriculture and Forestry Greenhouse Gas Inventory 1990–2013. In *United States Department of Agriculture, Office of the Chief Economist, Climate Change Program Office*.

USDA NASS. (2019). United States Summary and State Data. In *2017 Census of Agriculture* (Vol. 1, Issue April 2019). https://www.nass.usda.gov/Publications/AgCensus/2017/Full_Report/Volume_1,_Chapter_1_US/usv1.pdf

Viatte, C., Lauvaux, T., Hedelius, J. K., Parker, H., Chen, J., Jones, T., Franklin, J. E., Deng, A. J., Gaudet, B., Verhulst, K., & Duren, R. (2016). *Methane emissions from dairies in the Los Angeles Basin*. https://doi.org/10.5194/acp-2016-281

Viatte, Camille, Lauvaux, T., Hedelius, J. K., Parker, H., Chen, J., Jones, T., Franklin, J. E., Deng, A. J., Gaudet, B., Verhulst, K., Duren, R., Wunch, D., Roehl, C., Dubey, M. K., Wofsy, S., & Wennberg, P. O. (2017). Methane emissions from dairies in the Los Angeles Basin. *Atmospheric Chemistry and Physics*, *17*(12), 7509–7528. https://doi.org/10.5194/acp-17-7509-2017

Whiticar, M. (1999). Carbon and hydrogen isotope systematics of bacterial formation and oxidation of methane. *Chemical Geology*, *161*(1–3), 291–314. https://doi.org/10.1016/S0009-2541(99)00092-3

Whiticar, M., & Schaefer, H. (2007). Constraining past global tropospheric methane budgets with carbon and hydrogen isotope ratios in ice. *Philosophical Transactions of the Royal Society A*, *365*, 1793–1828. https://doi.org/10.1098/rsta.2007.2048

Yang, W. H., Weber, K. A., & Silver, W. L. (2012). Nitrogen loss from soil through anaerobic ammonium oxidation coupled to iron reduction. *Nature Geoscience*, *5*(8), 538–541. https://doi.org/10.1038/ngeo1530

2. Isotopic Signatures of Methane Emissions From Dairy Farms in California's San Joaquin Valley

Carranza, V., Biggs, B., Meyer, D., Townsend-Small, A., Thiruvenkatachari, R. R., Venkatram, A., Fischer, M.L., Hopkins, F.M. (2022). Isotopic signatures of methane emissions from dairy farms in California's San Joaquin Valley. Journal of Geophysical Research: Biogeosciences, 127, e2021JG006675. https://doi.org/10.1029/2021JG006675

2.0 Acknowledgement of Co-Authorship

This work was completed with contributions from Valerie Carranza, Brenna Biggs, Deanne Meyer, Amy Townsend-Small, Ranga Rajan Thiruvenkatachari, Akula Venkatram, Marc L. Fischer, Francesca M. Hopkins

2.1 Abstract

In this study, we present seasonal atmospheric measurements of $\delta^{13}C_{CH4}$ from dairy farms in the San Joaquin Valley of California. We used $\delta^{13}C_{CH4}$ to characterize emissions from enteric fermentation by measuring downwind of cattle housing (e.g., freestall barns, corrals) and from manure management areas (e.g., anaerobic manure lagoons) with a mobile platform equipped with cavity ring-down spectrometers. Across seasons, the $\delta^{13}C_{CH4}$ from enteric fermentation source areas ranged from -69.7 ± 0.6 per mil (‰) to -51.6 ± 0.1‰ while the $\delta^{13}C_{CH4}$ from manure lagoons ranged from -49.5 ± 0.1‰ to -40.5 ± 0.2‰. Measurements of $\delta^{13}C_{CH4}$ of enteric CH_4 suggest a greater than 10‰ difference between cattle production groups in accordance with diet. Isotopic signatures of CH_4 were used to characterize enteric and manure CH_4 from downwind plume sampling of dairies.

Our findings show that $\delta^{13}C_{CH4}$ measurements could improve the attribution of CH_4 emissions from dairy sources at scales ranging from individual facilities to regions and help constrain the relative contributions from these different sources of emissions to the CH_4 budget.

2.2 Introduction

Methane (CH_4) is the second most important anthropogenic greenhouse gas after carbon dioxide and is increasingly becoming a critical priority for near-term climate action, given its relatively short lifetime and substantial potential for rapid mitigation (United Nations, 2021). Over the last several decades, the growth rate of atmospheric CH_4 has significantly changed, reaching stable zero growth from 1999 to 2006, followed by an increase beginning 2007 (Dlugokencky et al., 1998; Nisbet et al., 2014; Lan et al., 2021a). This rise in the global mole fraction of atmospheric CH_4 has been the subject of several studies that focus on explaining this phenomenon, without a definitive explanation. A rise in CH_4 emissions could be indicative of changes in total emissions from various sources, including from biogenic, thermogenic, and pyrogenic CH_4 and/or changes in the atmospheric sink of CH_4 (Zheng et al., 2016; Rigby et al., 2017; Turner et al., 2017; Worden et al., 2017; Nisbet et al., 2019; Naus et al., 2019).

The isotopic signature of CH_4 is an important tool to diagnose the source of this increase in CH_4 (Dlugokencky et al., 2011). The global stable carbon isotope ratio of atmospheric CH_4, expressed as $\delta^{13}C_{CH4}$, has shifted towards more negative values simultaneously with the rise of the atmospheric mole fraction of CH_4 (Schaefer et al.,

2016). Recent isotopic evidence suggests that this rise in CH_4 is likely dominated by increased emissions of biogenic CH_4, which are more depleted in ^{13}C relative to fossil and pyrogenic CH_4 sources (Schaefer et al., 2016; Zheng et al., 2016; Fujita et al., 2020). Based on this explanation, possible biogenic sources responsible for the rise in atmospheric CH_4 include ruminants, rice paddies, and wetlands, among others, (Dlugokencky et al., 2011; Schaefer et al., 2016; Zheng et al., 2016). Previous work have shown that isotopic signatures of CH_4 emitted by enteric fermentation depend on the carbon isotopic ratio of diet composition, driven by the proportion of plants with C3 and C4 photosynthetic pathways, with estimates $\delta^{13}C_{CH4}$ of about -60‰ for C3-fed ruminants and about -50‰ for C4-fed ruminants (Metges et al., 1990; Levin et al., 1993; Schulze et al., 1998; Bilek et al., 2001; Dlugokencky et al., 2011; Schwietzke et al., 2016). Other conflicting hypotheses about the CH_4 budget include an underestimate of fossil-derived sources in CH_4 inventories based on an isotope mass balance (Schwietzke et al., 2016). Further studies, however, show that an increase in fossil-derived CH_4 emissions is inconsistent with the observed trend in atmospheric $\delta^{13}C_{CH4}$ (Fujita et al., 2020; Lan et al., 2021b). Additionally, there are large uncertainties in the magnitude and trends of atmospheric sinks of CH_4 (Rigby et al., 2017; Gromov et al., 2018; Nicely et al., 2018; Lan et al., 2021a). Given that our understanding of the CH_4 budget remains incomplete, there is a clear need for sufficient in situ isotopic characterization of CH_4 at the local level to identify the location and type of sources that dominate the current rise in global CH_4 emissions (Nisbet et al., 2019, 2021). Even at local to regional scales, the budgets of both CH_4 and its stable carbon isotope remain uncertain (Townsend-Small et al., 2012). Improved knowledge is particularly

important for ensuring effective mitigation of CH_4 at scales where policies to reduce CH_4 are being enacted (Hopkins et al., 2016a).

In California, there are statewide efforts underway to reduce CH_4 emissions, but it remains challenging to accurately monitor progress given the large inconsistencies between atmospheric observations and greenhouse gas inventories (Jeong et al., 2013; Duren et al., 2019). Atmospheric observations have inferred higher CH_4 emissions than reported in GHG inventories at the statewide and regional levels and from individual sectors, including dairies (Cui et al., 2017; Jeong et al., 2016; Miller et al., 2013; Trousdell et al., 2016; Wecht et al., 2014). However, there is little information about the processes that produce this apparent discrepancy. The California Air Resources Board (CARB) GHG inventory estimates that dairies contribute about half of statewide CH_4 emissions, with contributions from enteric fermentation by ruminant gut microbes and manure managed in anaerobic conditions. However, these estimates are based on emission factors derived from a few pilot and lab-scale studies conducted outside of California and thus likely not representative of California's climate and unique biogeography (Owen & Silver, 2015). Given that mitigation practices are targeted towards the biogeochemical and management processes that produce CH_4, new tools for source apportionment and process understanding are required (Nisbet et al., 2020). Stable isotopes of CH_4 may be a promising way forward.

The few studies that have measured isotopic signatures of CH_4 from dairies in California were done in the Los Angeles Basin. Townsend-Small et al. (2012) investigated the isotopic signature of major sources of CH_4 in the Los Angeles megacity and found that

isotopic values of $\delta^{13}C_{CH4}$ from fields applied with cow manure were characterized by values between -62.1 per mil (‰) to -59.2‰, whereas $\delta^{13}C_{CH4}$ of manure biofuel from a manure digester facility ranged from -52.4‰ to -50.3‰. Cow breath, on the other hand, had more depleted $\delta^{13}C_{CH4}$ source signatures between -64.6‰ and -60.2‰. A more recent study by Viatte et al. (2017) measured isotopic signatures of $\delta^{13}C_{CH4}$ from the largest dairy farms in Southern California, and observed values between -65‰ to -45‰, attributing the most depleted observations to enteric fermentation.

In Europe, previous research has shown that $\delta^{13}C_{CH4}$ signatures vary dependent on the type of dairy manure storage. In Heidelberg, Germany, Levin et al., (1993) observed more enriched $\delta^{13}C_{CH4}$ from manure piles (-45.5±1.3‰) and a biogas generator (-51.8±2.8‰) than liquid manure (-73.9±0.7‰). Two recent studies used mobile surveys to measure $\delta^{13}C_{CH4}$ in Europe. In Germany, Hoheisel et al. (2019) conducted mobile measurements to determine $\delta^{13}C_{CH4}$ signatures around Heidelberg and in North Rhine-Westphalia. The $\delta^{13}C_{CH4}$ signatures ranged from -66.0‰ to -40.3‰ for three dairy farms with biogas plants. More enriched $\delta^{13}C_{CH4}$ signatures were observed from plumes downwind of the biogas plant relative to plumes downwind of the animal housing. In Northern England, Lowry et al., (2020) found that methane plumes downwind of dairy farms had $\delta^{13}C_{CH4}$ signatures from -67‰ to -58‰. Atmospheric measurements downwind of manure piles were more enriched in $^{13}C_{CH4}$ with values close to -50‰ relative to cow breath, which were close to -70‰. Isotopic endmembers were variable downwind of animal housing dependent on the cattle population and amount of manure waste present. In general, CH_4 from barns with fewer cows and more manure waste were more enriched

in ^{13}C. In comparison, beef cattle feedlots have isotopic signatures within the range of expected enteric fermentation, with $\delta^{13}C_{CH4}$ signatures of -66.7 ± 2.4‰ in Alberta, Canada (Lopez et al., 2017) to -56.2‰ ± 1.2‰ in the Colorado Front Range, USA (Townsend-Small et al., 2016). Beef cattle are generally pasture raised until they are sent to feedlots, where their diet is primarily maize with varying proportions of wheat (Drouillard, 2018).

In this study, we present seasonal atmospheric measurements of $\delta^{13}C_{CH4}$ from dairy farms located in the San Joaquin Valley, California, where 91% of the state's dairy herd resides (Mullinax et al., 2020). Our primary objective was to measure $\delta^{13}C_{CH4}$ emitted from anaerobic manure lagoons and enteric fermentation source areas across seasons. Our second objective was to use $\delta^{13}C_{CH4}$ source signatures from enteric fermentation and anaerobic lagoons to identify the dominant source responsible for CH_4 hotspots detected from downwind plume sampling of other dairies in the region. We hypothesized that the $\delta^{13}C_{CH4}$ signatures from dairy anaerobic manure lagoons and enteric fermentation can be used to apportion CH_4 emissions between these two dairy farm source processes. These isotopic signatures can help contribute to the body of knowledge that aims to resolve the CH_4 budget in California and globally.

2.3 Methodology

2.3.1 Study Site

Ground-based mobile measurements were collected at a dairy in Tulare County (San Joaquin Valley), California, in the fall, spring, summer, and winter seasons from 2018 to 2020. Hereafter, we will refer to this dairy as the reference test site farm. Figure 2.1

shows a schematic of the reference test site farm layout. The reference test site has on average 3070 milking cows that spend most of their time in freestall barns, with an additional ~400 dry cows and ~3000 heifers that are primarily in open lots (corrals). Manure waste is handled using a combination of wet and dry manure management practices (Meyer et al., 2019). Wet manure management is used for waste deposited in the freestall barns, where manure waste is flushed from barn floors and diverted to a processing pit. Wastewater from the milking parlor also enters the processing pit. Processing pit water is reused to flush lanes or is pumped over stationary inclined screen (manure separator). A manure separator then removes coarser solids (17% of total solids) from liquid effluent, which gravity flows into cell 1. The liquid manure navigates from separation cell 1, cell 2, the primary lagoon, and finally into a holding pond via gravity, decreasing the content of suspended volatile solids through anaerobic decomposition and settling as it moves from one component to the next. Water waste from the holding pond is later used as irrigation water for cropland. Hereafter, manure lagoons refer to cell 1, cell 2, primary lagoon, and the holding pond. Dry manure management refers to the fraction of waste that is separated from the liquid waste stream, which is spread out on the ground and solar dried. Once dry, this manure is distributed into freestall beds (bedding) or stacked and covered in the dry bedding. The primary forages are wheat and maize preserved as silage. Silage piles are covered with a double layer of plastic.

The feed composition for different seasons was obtained by weighing each feed ingredient as it was included into the mixer wagon. All weights were transferred electronically to feed management software (VAS FeedWatch). FeedWatch data were

retrieved once monthly for ingredient identification, quantity fed per pen, pen population and dry matter composition. Each ingredient was identified as C3 or C4 except for distiller's grain, which could be a changing combination of C3 and C4 sources. Sum of dry weights by pen for C3, C4, distillers feeds were calculated. The feed composition by cattle production group is presented in .

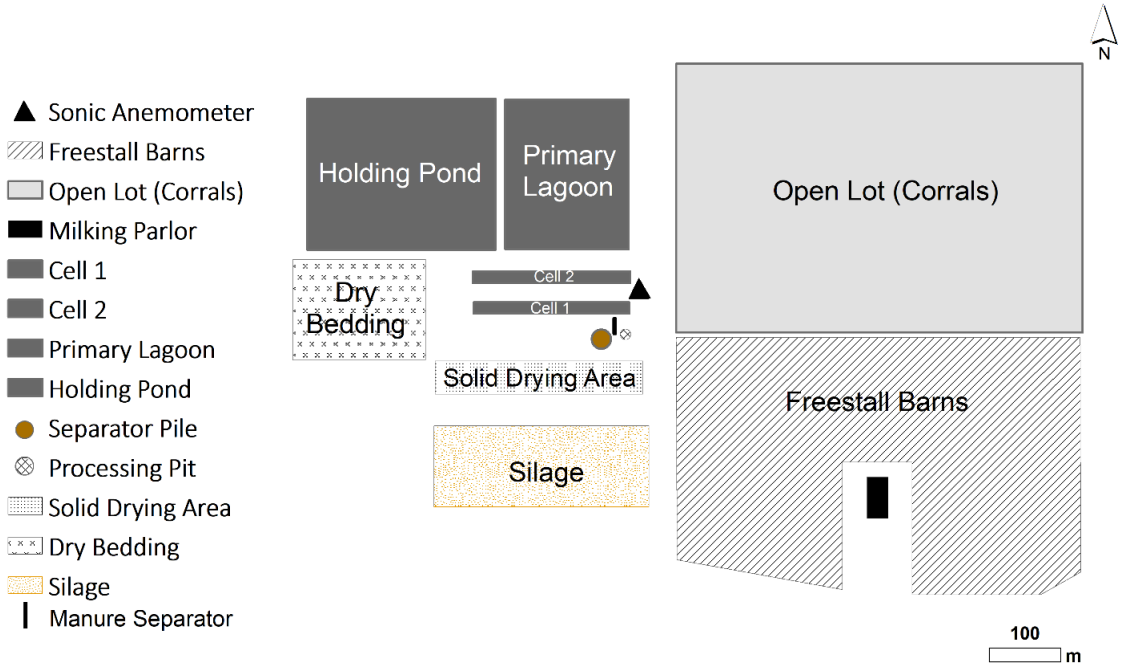

Figure 2.1. Facility layout and location of sonic anemometer on the reference test site of the San Joaquin Valley, California.

We also made measurements at other dairies within a 10 x 10 km region of agricultural land in the same county, which includes additional dairy farms, beef feedlots, poultry farms, and a landfill that are also emitting CH_4 (Figure 2.2). Other potential sources of emissions surround the region, including a wetland, plugged and abandoned oil and gas wells that are permanently sealed, and a wastewater treatment plant. Residential land is primarily located south of the region and contains an extensive natural gas pipeline

network. Globally, the $\delta^{13}C_{CH4}$ signatures from fossil fuel sources are typically around -44‰ (Schwietzke et al., 2016), with $\delta^{13}C_{CH4}$ signatures between −50‰ to −36‰ from fugitive natural gas in urban settings (Phillips et al., 2013; Xueref-Remy et al., 2020; Defratyka et al., 2021). Urban studies also use ethane (C_2H_6) to CH_4 ratios as a tracer to distinguish between sources in mixed source regions (e.g., thermogenic sources >0.01 and biogenic <0.005) (Hopkins et al., 2016b; Wennberg et al., 2012; McKain et al., 2015; Lopez et al., 2017; Plant et al., 2019; Lowry et al., 2020; Sargent et al., 2021).

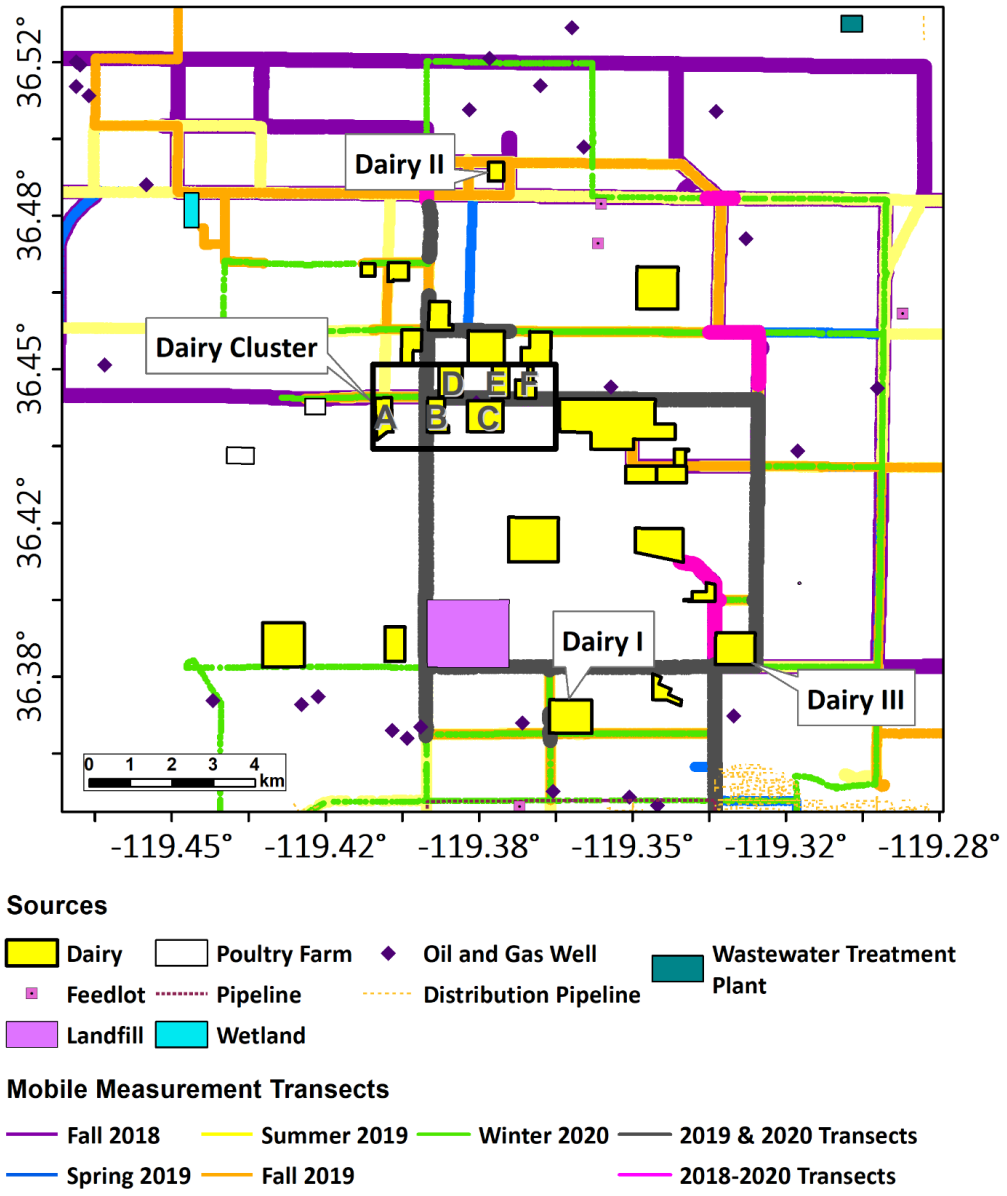

Figure 2.2. Mobile measurements routes in Tulare County region of the San Joaquin Valley, California. The symbols indicate the major known CH_4 sources in this agricultural region. The location of dairies sampled across multiple seasons are specified as Dairy I, Dairy II, Dairy III, and Dairy Cluster (A-F). Mobile measurement routes are colored by different seasonal campaigns. The pink lines show routes that were sampled in all 2018-2020 transects and the black lines show routes that were sampled in all 2019 and 2020 transects.

2.3.2 Mobile Platform and Micrometeorological Measurements

Continuous measurements of greenhouse gases and pollutants were collected using a mobile platform (Thiruvenkatachari et al., 2020), consisting of analyzers using the Cavity Ring-Down Spectroscopy (CRDS) technique (Picarro G2210-*i* and Picarro G2401, Picarro, Inc., Santa Clara, CA, USA), global satellite positioning unit (GPS 16X, Garmin Ltd., Olathe, KS, USA) to record geolocation and vehicle speed, 2-D sonic anemometer (METSENS500, Campbell Scientific, Inc., Logan, UT, USA) to measure wind direction, wind speed, air temperature and relative humidity, and calibration tanks. The following trace gas species were continuously measured from air drawn in at an inlet with a height of 2.87 m: CH_4, $\delta^{13}C_{CH4}$, carbon dioxide (CO_2), carbon monoxide (CO), C_2H_6. Reported trace gas mole fractions and isotope ratios were corrected using low and high custom gas mixtures that were measured before and after each measurement period. The isotopic values of the gas mixtures were -39.5‰ (Fall 2018, Spring 2019, Summer 2019), -40.7‰ (Fall 2019), and -38.5‰ (Winter 2020). These gas mixtures contained all the species of interest and were tied to the scale set by the NOAA Global Monitoring Division (GMD) by measurement against NOAA certified tanks. Isotopic standards were tied to the Vienna Pee Dee Belemnite (VPDB) scale and further calibrated by measuring two standards ranging from -23.9‰ to -68.6‰ with the Picarro 2210-*i* in the laboratory before the field campaign.

Micrometeorological measurements were collected at the reference test site each season, with a 3-D sonic anemometer (CSAT3, Campbell Scientific, Inc.) mounted on a stationary tower near the manure lagoons (Figure 2.1). Measurements were made at two

heights, 2.4 m and 11 m, at a frequency of 20 Hz. For the purposes of our analysis, we only used meteorological data from the 2.4 m tower.

On January 15th, 2020, we used a cuboid chamber (17.8 cm height and 28.0 cm width) made of clear PVC to isolate and measure $\delta^{13}C_{CH4}$ from freestall barns and static manure piles from the solid drying area (Litvak et al., 2014). The chamber was placed on the freestall barn or manure pile surface and connected to the gas analysis system of the mobile platform with Synflex tubing. For each sample, we collected measurements for ten minutes. We also measured $\delta^{13}C_{CH4}$ from the breath of milking cows, dry cows, heifers, bull calves, and calves in hutches by holding Synflex tubing connected to the mobile platform gas analysis system near the mouths of cows (Townsend-Small et al., 2012). We measured within 16 cm of milking and dry cows, ~1 m from heifers and bull calves, and ~10 m from calves in hutches.

2.3.3 Data Processing

Several corrections to observations were applied for each measurement period. First, observations collected from different instruments were cross-correlated and synchronized to local time (Hopkins et al., 2016b). Offsets were recorded between local time and each instrument's internal clock, which were then used to correct data prior to performing the cross-correlation method. Picarro raw mixing ratio measurements were time synchronized to collocated GPS measurements based on time stamp. Second, a correction was applied based on the lag time between the inlet and instrument reading.

Third, trace gas mole fraction and $\delta^{13}C_{CH4}$ observations were corrected by applying a correction factor from calibrations performed before and after each measurement period.

2.3.4 Whole Air Samples and Continuous Mobile Laboratory Measurements

We compared measurements of $\delta^{13}C_{CH4}$ using our mobile laboratory sampling technique using CRDS with analysis of whole-air samples collected at the same time and then analyzed with standard Isotope Ratio Mass Spectrometry (IRMS). Five whole-air samples of atmospheric CH_4 were collected in preconditioned and evacuated 2-L stainless steel canisters with bellow valves, over a period of about one minute (Blake et al., 1994; Colman et al., 2001). Whole-air samples were collected at the same height of the mobile laboratory inlet. The canisters were first processed by University of California, Irvine for chemical analysis, and a subsample was then sent to the University of Cincinnati for isotopic analysis with IRMS using a method described in detail by Yarnes (2013). Over the course of the same time intervals, the mobile laboratory continuously measured $\delta^{13}C_{CH4}$ with the CRDS instrument. The differences between $\delta^{13}C$ measured by IRMS and CRDS were within the uncertainties of each respective technique (Table 2.1). These findings suggest that $\delta^{13}C_{CH4}$ measurements by the mobile laboratory CRDS technique is comparable to the standard IRMS method.

We conducted a dilution experiment to analyze the precision of $\delta^{13}C_{CH4}$ sampled with the CRDS instrument at varying CH_4 levels similar to what we observed during downwind plume sampling of other dairies in the region. Following a similar method by Miles et al. (2018), a high gas standard with 20.1 ppm CH_4 and $\delta^{13}C$-CH_4 of -44.35‰

(traceable to the scale set by the NOAA GMD by measurement against NOAA certified tanks) was mixed with zero air using a mass flow controller (MC-20SLPM-D-SV and MCS-100SCCM-D-PCV03, Alicat Scientific, Inc.). The mass flow controllers were used to direct isotopic calibration standard tank into a mixing volume at 20 sccm (standard cubic centimeter per minute) and mixed with zero CH_4 air at 203.3, 181.0, 140.0, 114.00, 20.2 and 13.5 sccm to create target CH_4 mole fractions of 1.8, 2.0 , 2.5, 3.0, 10.0 and 12.0 ppm, respectively. To compare with the time interval used to average regional measurements, the final 15 seconds of data for each dilution were averaged to evaluate the precision of the instrument. The standard error of the $\delta^{13}C$-CH_4 collected during these tests increased with decreasing CH_4 mole fractions (Appendix A1, Figure S1). The $\delta^{13}C$ end-member (-43.52‰) from the data collected was within 0.83‰ of the isotopic value of calibration standard tank.

Table 2.1. Samples Collected by the Mobile Platform Using the CRDS and IRMS Technique.

Date	Local Time[a]	Source Type[b]	IRMS δ^2H-CH_4 (‰)[c]	IRMS δ^{13}C-CH_4 (‰)[c]	IRMS CH_4 (ppm)	Average CRDS δ^{13}C-CH_4 (‰)[d]	Average CRDS CH_4 (ppm)[d]	*n*[e]
March 25, 2019	13:37:50 - 13:38:50	Cell 1	-325.66 ± 4	-42.91 ± 0.23	56.7	-43.3 ± 0.1	40.5 ± 0.4	34
March 25, 2019	18:37:30 - 18:38:30	Primary lagoon	-262.58 ± 4	-50.13 ± 0.23	17.1	-49.9 ± 0.1	14.6 ± 0.2	44
March 26, 2019	7:52:05 - 7:53:05	Freestall barns	-279.53 ± 4	-54.16 ± 0.23	11.2	-54.2 ± 0.2	11.1 ± 0.5	46
March 26, 2019	8:12:30 - 8:13:30	Corrals	-276.62 ± 4	-52.07 ± 0.23	10.1	-52.0 ± 0.1	10.2 ± 0.1	45
March 26, 2019	9:12:30 - 9:13:30	Landfill	-245.33 ± 4	-49.21 ± 0.23	5.4	-49.0 ± 0.2	5.5 ± 0.0	47

[a] One-minute time interval for CRDS measurements. Flask samples for IRMS were also instantaneously collected within this time interval.
[b] All source types were at reference test site except the landfill (Figure 2.2).
[c] Precision of the IRMS technique is reported.
[d] Standard error of the average CRDS measurements is reported. Note these are all the values measured.
[e] Sample size of CRDS observations that were averaged.

2.3.5 Farm-scale Analysis

Sources of CH_4 emissions at the reference test site farm were identified by categorizing atmospheric observations based on proximity to the emission source and wind direction. To evaluate $\delta^{13}C_{CH4}$ from biogenic sources at the farm scale, observations with $CH_4 \leq 30$ ppm (Picarro G2210-*i* dynamic range) were selected and averaged by 1-min intervals to minimize uncertainty according to the performance standards of the instrument. For each source, $\delta^{13}C_{CH4}$ and the corresponding standard errors were estimated as the y-intercept from a weighted linear regression of the inverse of the atmospheric CH_4 mole fraction and $\delta^{13}C_{CH4}$ (i.e., Keeling plot) (Keeling, 1958; Pataki et al., 2003). Keeling plots were generated for each dairy farm source (i.e., manure lagoons, corrals, and freestall barns) by applying a weighted linear regression with errors in both the independent and dependent variables (i.e., *x*-data: CH_4^{-1} and *y*-data: $\delta^{13}C_{CH4}$) based on the York et al. (2004) method (Thirumalai et al., 2011). To exclude CH_4 emissions from fossil-fuel sources, such as from vehicles, which have $\delta^{13}C_{CH4}$ signatures between -46‰ to -30‰ (Townsend-Small et al., 2012), we omitted CH_4 observations that had corresponding excess C_2H_6 values > 0.1 ppm (0.02% of reference test site farm measurements) and excess CO values > 500 ppb, the 99th percentile from all regional transects (Miller et al., 2015). We define excess C_2H_6 and excess CO as mole fractions above the minimum C_2H_6 and CO observations for each dairy farm source. At the reference test site, no excess CO measurements above this threshold were detected. For the inverse of CH_4, the uncertainty was defined as the mean of the standard errors from the 1-min averaged observations in the weighted linear regression. For $\delta^{13}C_{CH4}$ observations, we first evaluated the mean of the standard errors from the 1-min averaged observations against the standard error from 1-min averages of

the standard gas run. Then, we selected the largest standard error of the two as the corresponding uncertainty. In this study, the $\delta^{13}C_{CH4}$ values reported hereafter are referring to the $\delta^{13}C_{CH4}$ end-members derived from Keeling plots.

2.3.6 Downwind Plume Sampling Analysis

Isotopic signatures of CH_4 were classified into the following two categories: Dairy Cluster (dairies A-F) or isolated dairy farms (Dairy I, Dairy II, Dairy III), where there were no major potential sources of CH_4 within at least 2 km from the dairy farm. We used 15-s averaged observations to detect CH_4 hotspots, defined as locations with CH_4 levels exceeding 350 ppb above local background. We exclude potential CH_4 emissions from fossil fuel sources using the same C_2H_6 and CO criteria as described above. For each season, we then identified hotspots of CH_4 downwind of dairy farms and derived the $\delta^{13}C$ end-members with a Keeling plot, using the method described in section 2.5. To ensure the method described in section 2.5 is appropriate for the lower mole fractions observed from downwind sampling of other dairies in the region, we compared the $\delta^{13}C$ end-members using the standard error from the CH_4 dilution experiment described in section 2.3.4. against the standard error selected using the method described in section 2.5. There was no statistically significant difference between $\delta^{13}C$ end-members using Welch's t-test. Thus, to be consistent with analysis at the farm-scale, the method described in section 2.5 was selected to obtain source $\delta^{13}C$ end-members from downwind plume sampling of other dairies.

Isotope mixing equations from Fry (2006) were used to estimate the fractional contribution of the two CH_4 sources, enteric fermentation source areas and manure lagoons,

from CH_4 hotspots. We averaged the isotopic signatures of cow breath measurements ($\delta_{enteric}$) from milking cows, dry cows, heifers, bull calves, and calves in hutches from the winter 2020 measurements from the reference test site (-61.1 ± 0.3‰). We also averaged the manure lagoon isotopic signatures, δ_{manure}, observed at the reference test site (-45.1 ± 0.4‰). The following equation was used to estimate the fraction of enteric methane emissions,

$$f_{enteric} = (\delta_{observation} - \delta_{manure}) / (\delta_{enteric} - \delta_{manure})$$

where $f_{enteric}$ is the fraction of enteric methane from the total sum of two sources and $\delta_{observation}$ is the isotopic signature of the CH_4 hotspot. Uncertainties were calculated by propagation of error.

To further characterize CH_4 hotspots, we used a Eulerian numerical (EN) dispersion model to identify the CH_4 flux footprint, which is the upwind area where CH_4 emissions measured by the mobile platform were generated (refer to details in Thiruvenkatachari et al., 2020). For this study, the EN model identified which dairy farm areas contributed the most to the atmospheric CH_4 observations. We applied a roughness length of 0.002 m in the EN model. The dairy farm areas were divided into smaller sources by a 5 m grid.

2.4 Results

2.4.1 Source-scale Isotopic Signatures of CH_4 Measured at a Single Farm

Different sources of CH_4 emissions of the dairy farm had distinct isotopic signatures of CH_4 that were comparable across seasons (

Figure **2.3**). The $\delta^{13}C_{CH4}$ signatures from enteric fermentation source areas were more depleted than CH_4 from manure lagoons. The $\delta^{13}C_{CH4}$ from animal housing areas ranged from -69.7 ± 0.6‰ to -51.6 ± 0.1‰, whereas the $\delta^{13}C_{CH4}$ from manure lagoons ranged from -49.5 ± 0.1‰ to -40.5 ± 0.2‰. Methane emissions from freestall barns had heavier $\delta^{13}C_{CH4}$, with values ranging from -59.9 ± 0.2‰ to -51.6 ± 0.1‰. Meanwhile, corrals exhibited the most depleted $\delta^{13}C_{CH4}$, ranging from -69.7 ± 0.6‰ to -55.5 ± 0.5‰. We observed some subtle seasonal differences in isotopic signatures from manure lagoons. The most enriched $\delta^{13}C_{CH4}$ from manure lagoons was observed in January 2020 (-40.5 ± 0.2‰) relative to other seasons, such as in June 2019 (-49.5 ± 0.1‰) and September 2019 (-46.69 ± 0.02‰). Freestall barns and corrals displayed a relatively larger range, impacted by differences in C3 and C4 feed composition, but, notably, the heaviest $\delta^{13}C_{CH4}$ was observed in September 2018 (freestall barns: -52.8 ± 0.1‰) and January (freestall barns: -51.6 ± 0.1‰), with the most depleted $\delta^{13}C_{CH4}$ observed in September 2018 (corrals: -69.7 ± 0.6‰). Methane observations varied drastically between corrals, freestall barns, and manure lagoons. Across all seasons, the average CH_4 mole fractions at corrals and freestall barns were 5.4 ± 3.4 ppm and 8.5 ± 6.3 ppm, respectively. Manure lagoons had on average the highest CH_4 mole fraction of 18.4 ± 18.2 ppm.

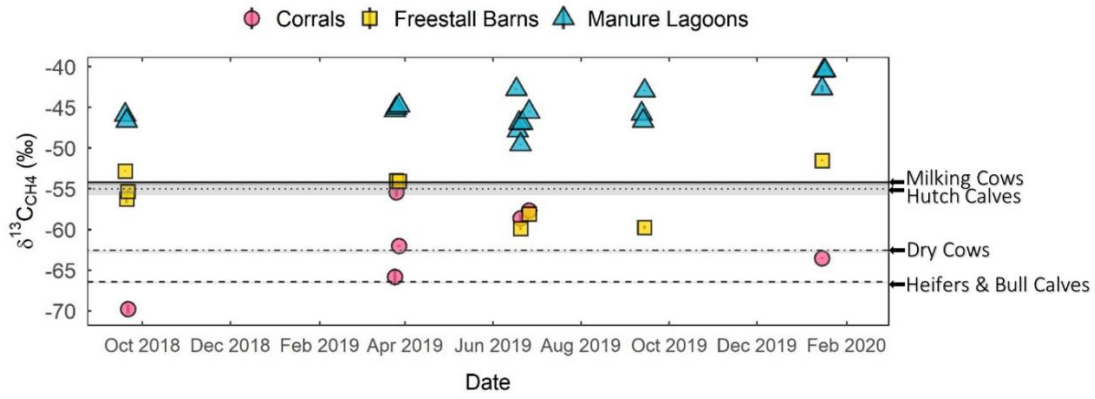

Figure 2.3. Seasonal $\delta^{13}C_{CH4}$ isotopic signatures from different CH_4 source areas on the reference test site farm (corrals, freestall barns, and manure lagoons). Each symbol represents the $\delta^{13}C_{CH4}$ isotopic signature derived from Keeling plots. The lines and shaded regions represent the $\delta^{13}C_{CH4}$ isotopic signatures (lines) and associated standard errors (shaded regions) of cow breath by cattle type during the winter 2020 campaign (Figure 2.4).

Table 2.2. Seasonal $\delta^{13}C_{CH4}$ Isotopic Signatures at a Dairy Farm (i.e., Reference Test Site).

Season	Date	Source	$\delta^{13}C_{CH4}$ (‰)[a]
Fall	September 19, 2018	Freestall Barns	-52.8 ± 0.1
	September 20, 2018	Freestall Barns	-56.2 ± 0.5
	September 21, 2018	Freestall Barns	-55.4 ± 0.2
Spring	March 26, 2019	Freestall Barns	-54.1 ± 0.1
	March 28, 2019	Freestall Barns	-54.0 ± 0.1
Summer	June 20, 2019	Freestall Barns	-59.9 ± 0.2
	June 26, 2019	Freestall Barns	-58.2 ± 0.1
Fall	September 14, 2019	Freestall Barns	-59.8 ± 0.2
Winter	January 15, 2020	Freestall Barns	-51.6 ± 0.1
Fall	September 21, 2018	Corrals	-69.7 ± 0.6
Spring	March 25, 2019	Corrals	-65.7 ± 1.0
	March 26, 2019	Corrals	-55.5 ± 0.5
	March 28, 2019	Corrals	-62.1 ± 0.1
Summer	June 20, 2019	Corrals	-58.6 ± 0.5
	June 26, 2019	Corrals	-57.6 ± 0.2
Winter	January 15, 2020	Corrals	-63.5 ± 0.1
Fall	September 19, 2018	Manure Lagoons	-46.02 ± 0.03
	September 20, 2018	Manure Lagoons	-46.75 ± 0.04
Spring	March 25, 2019	Manure Lagoons	-45.48 ± 0.02
	March 26, 2019	Manure Lagoons	-45.2 ± 0.1
	March 28, 2019	Manure Lagoons	-44.9 ± 0.1
Summer	June 17, 2019	Manure Lagoons	-42.9 ± 0.1
	June 18, 2019	Manure Lagoons	-47.99 ± 0.03
	June 19, 2019	Manure Lagoons	-47.03 ± 0.01
	June 20, 2019	Manure Lagoons	-49.5 ± 0.1
	June 21, 2019	Manure Lagoons	-46.94 ± 0.03
	June 26, 2019	Manure Lagoons	-45.5 ± 0.1
Fall	September 12, 2019	Manure Lagoons	-45.80 ± 0.02
	September 13, 2019	Manure Lagoons	-46.69 ± 0.02
	September 14, 2019	Manure Lagoons	-43.0 ± 0.1
Winter	January 15, 2020	Manure Lagoons	-42.7 ± 0.4
	January 16, 2020	Manure Lagoons	-40.5 ± 0.2
	January 17, 2020	Manure Lagoons	-40.5 ± 0.1

[a] Standard errors are reported for $\delta^{13}C_{CH4}$ isotopic signatures derived from Keeling plot analyses. All *p* values are <0.001, except on September 14, 2019, for Freestall Barns (*p* value = 0.01) and January 15, 2020 for Manure Lagoons (*p* value = 0.85)

Differences in the isotopic signatures from CH_4 emissions generated from the freestall barns and corrals may be explained by the types of cattle housed in each area. To further explore this, we conducted isolated breath measurements of different cattle production groups during the winter season and evaluated their diet composition across seasons. Freestall barns only house milking cows and cows within a few days of parturition, while corrals house milk-fed calves in hutches (hereafter, hutch calves), heifers, bull calves, and dry cows (i.e., non-lactating cows). As shown from the Keeling plots in Figure 2.4, the breath of milking cows (-54.2 ± 0.2‰) and hutch calves (-55.0 ± 1.7‰) were more enriched in $\delta^{13}C_{CH4}$ relative to dry cows (-62.6 ± 0.3‰) and heifers and bull calves (-66.4 ± 0.2‰).

We used feed data collected at our reference test site farm to interpret the variations in $\delta^{13}C$ of CH_4 emited from cattle in corrals and freestall barns at the reference test site farm. We found that the types of cattle housed in each area were each fed a distinct type of feed, consisting of C3, C4, or distiller's dried grains of unknown composition (DDG) (Table 2.3). In all seasons, milking cows were fed a mixture consisting primarily of C3 (36-43%) and C4 feeds (50-58%), with a small percentage of DDG (5-8%). Hutch calves were milk-fed and also fed a mixture of C3, C4, and DDG feed, but with a larger percentage of DDG (27-45%)—the diet composition for hutch calves was more variable depending on the season. Bull calves were fed a wide range of C3 (12-45%), C4 (12-66%), and DDG (22-43%) feed depending on the month. In contrast, dry cows and heifers were predominately fed a C3 diet (85-100%) with a small percentage of DDG (0-15%). Given that isotopic measurements of substrates were outside the scope of this study, we assumed

that C4 feed had a $\delta^{13}C$ of -12.2 ± 0.3‰ and C3 feed had a $\delta^{13}C$ of -23.6‰ based on reported $\delta^{13}C$ of maize and wheat in Chang et al. (2019). For DDG, we assumed an equal mixture of C3 and C4 feed, resulting in a $\delta^{13}C$ of -17.9 ± 0.3‰. To estimate the expected $\delta^{13}C_{CH4}$ for different cattle production groups at the reference test site, we used the linear regression equation derived from the empirical relationship between $\delta^{13}C_{diet}$ and $\delta^{13}C_{CH4}$ from enteric fermentation of ruminants in Chang et al. (2019) ($\delta^{13}C_{CH4} = 0.91 \times \delta^{13}C_{diet} - 43.49‰$, with the standard errors of the intercept and slope being 2.86‰ and 0.12‰, respectively). Based on these assumptions, milking cows and hutch calves are projected to emit more enriched $\delta^{13}C_{CH4}$ values relative to other cattle production groups (Table 2.3). Although this pattern generally agrees with our study's $\delta^{13}C_{CH4}$ measurements from enteric fermentation source areas, our $\delta^{13}C_{CH4}$ measurements were often more enriched than expected. The $\delta^{13}C_{CH4}$ from animal housing is likely impacted by emissions of isotopically enriched CH_4 from manure deposited in corrals and freestall barns.

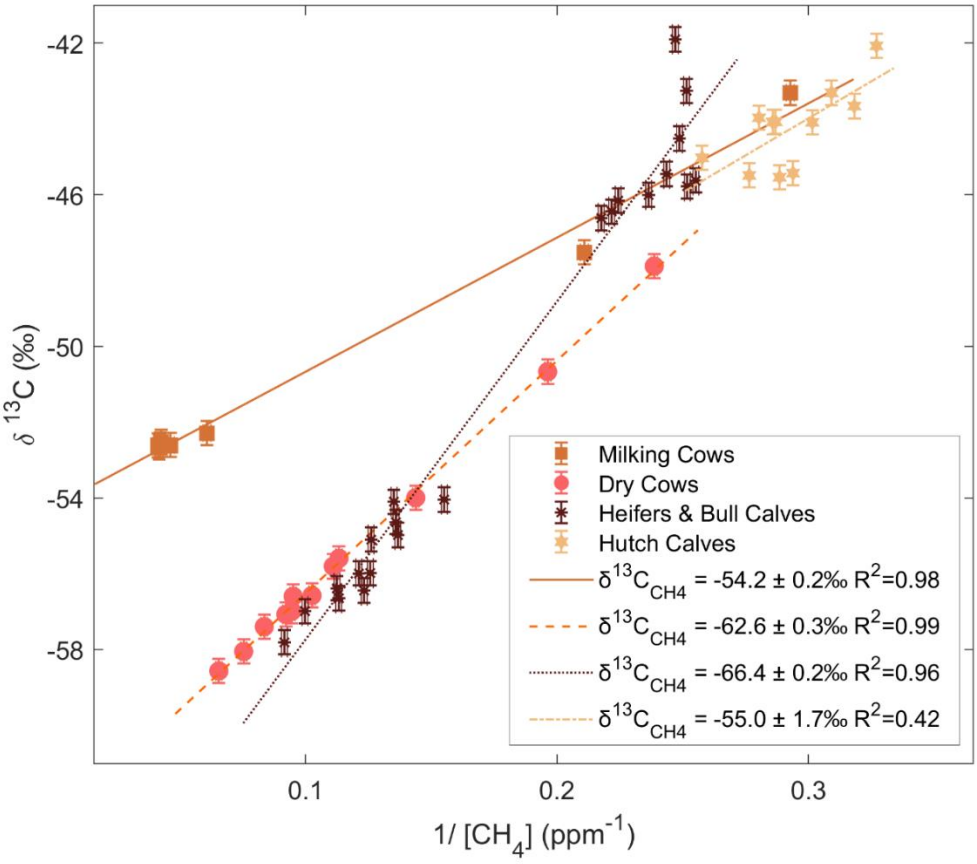

Figure 2.4. Keeling plot of $1/CH_4$ concentration versus $\delta^{13}C$ isotope measurements of CH_4 from cow breath on January 15th, 2020. Different cattle types and their Keeling intercepts are shown with different colors in the key.

Table 2.3. Feed Composition at Reference Test Site Farm.

Cow Type	Month	C4 (%)	C3 (%)	DDG (%)	Estimated $\delta^{13}C_{CH4}$ (‰)[a]
Milking Cows	Oct 2018	42	50	8	-60.2 ± 2.9
	Jan 2019	36	57	7	-60.9 ± 2.9
	Mar 2019	36	58	6	-60.9 ± 2.9
	Jun 2019	37	57	6	-60.8 ± 2.9
	Sep 2019	43	50	5	-60.2 ± 2.9
Dry Cows	Oct 2018	0	100	0	-65.0 ± 2.9
	Jan 2019	0	100	0	-65.0 ± 2.9
	Mar 2019	0	100	0	-65.0 ± 2.9
	Jun 2019	0	100	0	-65.0 ± 2.9
	Sep 2019	0	100	0	-65.0 ± 2.9
Heifers	Oct 2018	0	87	13	-64.3 ± 2.9
	Jan 2019	0	86	14	-64.3 ± 2.9
	Mar 2019	0	90	14	-64.3 ± 2.9
	Jun 2019	0	92	15	-64.3 ± 2.9
	Sep 2019	0	85	15	-64.2 ± 2.9
Bull Calves	Oct 2018	45	12	43	-58.1 ± 2.9
	Jan 2019	23	51	26	-61.3 ± 2.9
	Mar 2019	20	55	25	-61.6 ± 2.9
	Jun 2019	17	59	24	-62.0 ± 2.9
	Sep 2019	12	66	22	-62.6 ± 2.9
Hutch Calves	Oct 2018	49	6	45	-57.6 ± 2.9
	Jan 2019	25	48	27	-61.0 ± 2.9
	Mar 2019	25	48	27	-61.0 ± 2.9
	Jun 2019	25	48	27	-70.0 ± 2.9
	Sep 2019	25	48	27	-61.0 ± 2.9

[a] Estimated $\delta^{13}C_{CH4}$ using Chang et al. (2019) linear regression equation described in section 3.1.

The progression of manure from one component of the system to another also influenced the isotopic signature of CH_4 at the reference test site. Using a chamber to isolate sources of manure at different stages of the manure management on January 15th, 2020, we observed that a mixture of fresh volatile solids with urine on the floor of freestall barns yielded the most depleted $\delta^{13}C_{CH4}$ (-56.3 ± 0.4‰). Methane emitted from two separate manure piles at the solid drying area, however, had heavier $\delta^{13}C_{CH4}$ signatures (-46.0 ± 0.9‰ and -39.1 ± 0.5‰) (refer to Figure 2.1 for facility layout). The more depleted $\delta^{13}C_{CH4}$ observations were from a manure pile that was noticeably drier than the second sample. In comparison, measurements from manure lagoons using the mobile laboratory resulted in $\delta^{13}C_{CH4}$ of -43.4 ± 0.4‰. Based on our measurement of the oxidation reduction potential (ORP), the manure waste stream is anaerobic from cell 1 onward to the holding pond (ORP was ≤ -300 mV). Prior to that, we expect the waste stream to have varied conditions that include anaerobic and aerobic microsites. Presumably some of the manure on the floors of cattle housing areas is anaerobic, given the continuous presence of water on the floors of freestalls.

2.4.2 Downwind Plume Sampling of Other Dairies in the Region

Isotopic signatures from CH_4 hotspots observed from downwind plume sampling of other dairies in the region were consistent with on-farm isotopic signatures (Table 2.4). For example, downwind plume sampling at Dairy I resulted in a depleted $\delta^{13}C_{CH4}$ value of -57.1 ± 3.4‰, representative of enteric CH_4, with an estimated $f_{enteric}$ of 0.75 ± 0.21 (Figure 2.5a-b, Table 2.4). At Dairy III, we observed isotopic signatures ranging from -59.9 ± 2.0‰

to -43.9 ± 0.7‰. The estimated $f_{enteric}$ and CH_4 flux footprint revealed that the most enriched isotopic signatures corresponded to CH_4 emissions from manure lagoons, while the most depleted isotopic signatures were from emissions from the corrals and manure lagoon areas (Figure 2.5, Table 2.4, Appendix A1: Figures S3-S13). Within the same day, on June 25th, we observed two CH_4 hotspots with more enriched isotopic signatures, -44.5 ± 1.6‰ (Figure 2.5c-d) and -43.9 ± 0.7‰, which fall within the range of manure lagoon $\delta^{13}C_{CH4}$ observed at the reference test site, and a hotspot with a more depleted isotopic signature (-59.9 ± 2.0‰), similar to enteric fermentation sources observed at the reference test site. We observed a similar circumstance on March 24th—the flux footprint primarily captured the manure lagoon areas with a more enriched isotopic signature of -51.6 ± 1.2‰ in the early afternoon with predominantely southwesterly winds, but the flux footprints shifted to both corrals and lagoons in the late afternoon with predominantly northeasterly winds, resulting in a more depleted isotopic signature of -58.4 ± 2.9‰. The resulting $f_{enteric}$ of 0.41 ± 0.08 was estimated for the more enriched isotopic signature of -51.6 ± 1.2‰, meanwhile the more depleted isotopic signature of -58.4 ± 2.9‰ had a higher $f_{enteric}$ of 0.83 ± 0.19.

Isotopic signatures were also influenced by the distance between the location of measurements and dairy farm, as well as the proximity to other dairy farms. To illustrate this further, a CH_4 plume was observed approximately 140 m downwind of Dairy II, with a $\delta^{13}C_{CH4}$ value of -50.2 ± 1.5‰, a value that is representative of atmospheric mixing of CH_4 emissions from dairy manure lagoon and enteric fermentation sources. The largest contributing source to the CH_4 flux footprint was corrals and the corresponding $f_{enteric}$ was

0.32 ± 0.10, suggesting an additional source of CH_4 emissions with an enriched isotopic signature, such as manure piles in the corrals. We detected four CH_4 hotspots downwind of the Dairy Cluster with a narrow range of $\delta^{13}C_{CH4}$ values, -53.5 ± 2.3‰ to -50.4 ± 1.8‰. Different upwind areas of the dairy farms A-F were captured by the CH_4 flux footprint (Table 2.4, Figures S10-S13).

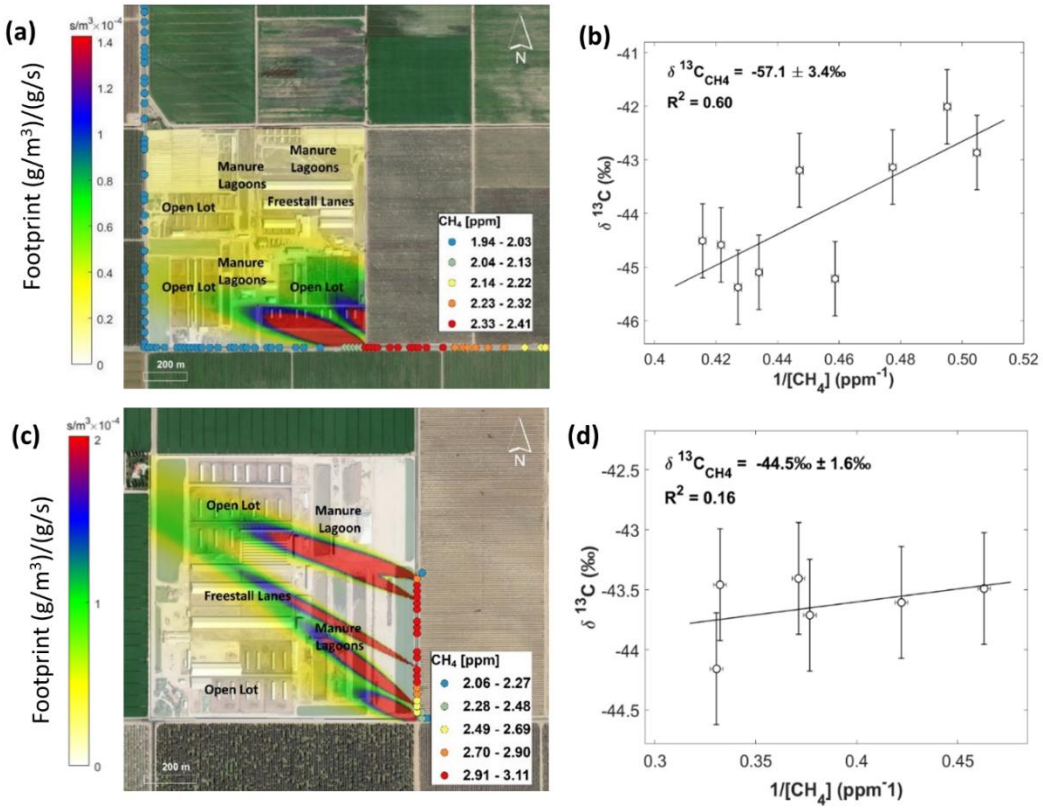

Figure 2.5. Examples of flux footprints from CH_4 hotspots downwind of other dairy farms. (a) Methane flux footprint of Dairy I on June 25th, 2019, using the mobile survey (colored points). The color gradient shows the relative contribution from the upwind areas where CH_4 was emitted. (b) Keeling plot using 15-second averages from the mobile survey shown in (a). (c) Methane flux footprint of Dairy III on June 25th, 2019, using the mobile survey. (d) Keeling plot using 15-second averages from the mobile survey shown in (c).

Table 2.4. Regional Isotopic Signatures of CH_4 Downwind from Dairy Farms.

Date[a]	Start	End	Dairy	$\delta^{13}C_{CH4}$	R^2	*p value*	Predominant Wind Direction	Measurement Location Relative to Dairy Farm	Largest Contributing Sources to the Methane Flux Footprint	Fraction of Enteric Methane Emissions[b]
6/25/2019	15:51:40	15:53:50	Dairy I	-57.1 ± 3.4	0.60	0.03	WNW	S	Corrals	0.75 ± 0.21
9/21/2018	18:05:01	18:09:30	Dairy II	-50.2 ± 1.5	0.18	0.01	W	E	Corrals	0.32 ± 0.10
3/24/2019	13:28:01	13:32:00	Dairy III	-51.6 ± 1.2	0.20	<.001	SW	E, S	Lagoons	0.41 ± 0.08
3/24/2019	17:53:01	17:55:13	Dairy III	-58.4 ± 2.9	0.33	0.01	NE	S	Corrals & Lagoons	0.83 ± 0.19
6/25/2019	14:02:00	14:05:30	Dairy III	-59.9 ± 2.0	0.23	<.001	NW	E, S, W	Corrals & Lagoons	0.93 ± 0.13
6/25/2019	15:17:00	15:18:28	Dairy III	-44.5 ± 1.6	0.16	0.62	WNW	E	Lagoons	-0.04 ± 0.10
6/25/2019	17:11:30	17:15:00	Dairy III	-43.9 ± 0.7	0.02	0.22	NW	S, E	Lagoons	-0.08 ± 0.05
9/21/2018	17:18:12	17:23:36	Dairy Cluster	-52.9 ± 1.6	0.13	<.001	WNW	In-between	Dairies D-F	0.49 ± 0.10
3/24/2019	14:16:59	14:23:34	Dairy Cluster	-53.5 ± 2.3	0.06	<.001	NNW	In-between	Dairies A-F	0.53 ± 0.15
6/24/2019	16:06:41	16:12:05	Dairy Cluster	-50.4 ± 1.8	0.02	0.06	NW	In-between	Dairies D-F	0.33 ± 0.12
6/25/2019	14:14:54	14:20:28	Dairy Cluster	-52.6 ± 2.6	0.05	0.04	WNW	In-between	Dairies C-F	0.47 ± 0.17

[a] Date format: M/DD/YYYY.

[b] Standard errors are reported for $\delta^{13}C_{CH4}$ isotopic signatures.

2.5 Discussion and Conclusion

Stable carbon isotope measurements of CH_4 can be a valuable source apportionment technique to distinguish between enteric and manure CH_4. At the reference test site farm, we found a clear separation of $\delta^{13}C_{CH4}$ signatures between enteric fermentation source areas (more depleted: -69.7 ± 0.6‰ to -51.6 ± 0.1‰) and manure lagoons (more enriched: -49.5 ± 0.05‰ to -40.5 ± 0.2‰). These source signatures were comparable across season, particularly from manure lagoons, and were always different from one another by at least ~8‰. Additionally, isotopic signatures from CH_4 hotspots observed from remote mobile surveys were consistent with on-farm isotopic signatures and captured CH_4 source areas. Our downwind observations revealed that enteric fermentation-derived CH_4 contributed from 0 to 93% of CH_4 in plumes that varied with the amount of animal housing and lagoon in the emission footprint (Table 2.4). Measurements of ^{13}C of CH_4 downwind of dairy farms may be a useful tool to monitor and quantify enteric:manure ratios with changes in mitigation (Marklein et al., 2021). As shown in this study, isotopic signatures of CH_4 downwind of dairy farms can be used to estimate the fraction of contributing sources, such as from manure lagoons and enteric fermentation source areas. We measured that the fraction of enteric CH_4 to total CH_4 from a mixed cluster of dairy farms ranged from 0.33 to 0.53 similar to model predictions of 0.5 for this region (Table 2.4; Marklein et al., 2021). Most CH_4 mitigation strategies separately address CH_4 emitted from enteric fermentation, such as through feed additives (Honan et al., 2021), or manure emissions by changing management techniques (Joshi, 2020). As governing bodies undertake mitigation strategies to reduce CH_4 emissions from enteric fermentation or dairy

manure management, it is essential to verify mitigation effectiveness. In California, for example, numerous dairy farms have recently adopted or plan to install digesters in the near future to capture and convert CH_4 from manure lagoons into fuel. Although digesters are designed to capture most CH_4 emissions, studies have detected notable CH_4 leaks from biogas plants (Bakkaloglu et al., 2021). An important area of future research is to quantify the effect of mitigation strategies by comparing $\delta^{13}C_{CH4}$ downwind of dairy farms before and after installation of digesters.

Isotopic signatures in this study agree with previous research showing that manure CH_4 is more enriched in ^{13}C than enteric CH_4. Our on-farm measurements, however, show that manure lagoon CH_4 is relatively more enriched in ^{13}C than previously reported in Southern California (Table 2.5). Townsend-Small et al. (2012) reported a $^{13}C_{CH4}$ range of -52.4‰ to -50.3‰ from manure biofuel from a manure digester facility and Viatte et al. (2017) reported ^{13}C of CH_4 of about -57‰ near manure lagoons. This may be explained by differences in CH_4 generation processes and manure management differences between Southern California and San Joaquin Valley. Dairies in the San Joaquin Valley predominately use flush systems and store manure in lagoons, while Southern California dairies typically operate dry lots that forgo flushing manure from the feedlanes such that less manure is stored in anaerobic lagoons (Meyer et al., 2019; Marklein et al., 2021). Nevertheless, all California farms produce liquid manure from flushing solids in the milking parlor (Meyer et al., 2019). Although Viatte et al. (2017) reported a more depleted ^{13}C of CH_4 of about -57‰ near manure lagoons compared to this study, they also observed an ~8‰ fractionation between enteric CH_4 and manure CH_4, consistent with our findings

of isotopic fractionation between manure lagoons and enteric CH_4 from freestall barns. There may also be differences in the stable carbon isotope composition of feed and differences in biogeochemical factors that play a key role in determining which microbial communities and pathways promote or inhibit CH_4 generation from dairy manure management, and in turn affect the isotopic signature of CH_4 emissions. These include pH, dissolved oxygen level, temperature, volatile fatty acids, chemical composition of the substrate, total nitrogen, and nutrient composition (Amon et al., 2007; Weiland, 2010).

Table 2.5. Comparison of Isotopic Signatures from Relevant Studies in California.

Region	Enteric $\delta^{13}C$-CH_4 (‰)	Manure $\delta^{13}C$-CH_4 (‰)	Overall (‰)[b]	Reference
Los Angeles Basin	-64.6 to -60.2	-52.4 to -50.3[a]	-65.0 to -50.2	Townsend-Small et al. (2012)
Los Angeles Basin	-65	-57	-65 to -45	Viatte et al. (2017)
San Joaquin Valley	-69.7 ± 0.6 to -51.6 ± 0.1	-49.5 ± 0.1 to -40.5 ± 0.2	-69.7 ± 0.6 to -40.5 ± 0.2	This study

[a] Reported values from manure digester facility.

[b] Overall range from reported observations downwind from dairy facilities.

Future work is needed to explain the isotopic composition of CH_4 emissions from manure lagoons. This area of research can provide important information on the dominant microbial communities and biogeochemical processes, which can inform mitigation efforts to reduce CH_4 emissions from the dairy sector. In our study, whole air sample analysis using IRMS (Table 2.1) showed that CH_4 emissions from cell 1 were relatively more enriched in $\delta^{13}C$ (-42.91 ± 0.23‰) and more depleted in the hydrogen isotopic composition of CH_4 (δ^2H-CH_4 or δD-CH_4, -326 ± 4‰) than CH_4 from the primary lagoon ($\delta^{13}C$-CH_4 = -50.13 ± 0.23‰, δ^2H-CH_4 = -263 ± 4‰). The differences in the isotopic signatures of these samples indicate that CH_4 generated from cell 1 may be explained primarily by acetate

fermentation, but CH_4 generated from the primary lagoon may have undergone further processes such as partial oxidation or CO_2 reduction. Substrate depletion may also explain this variation, but additional measurements of $\delta^{13}C$ of volatile solids or CO_2 concentrations would be needed to confirm isotopically fractionated substrates. During acetate fermentation, CH_4 and CO_2 are commonly formed simultaneously. Reduction of CO_2 may further transform the generated CO_2 into CH_4. In the influential study conducted by Whiticar et al. (1986), CH_4 generated from pure acetate fermentation resulted in $\delta^{13}C$-CH_4 ranging from -60 to -33‰, whereas CH_4 from pure CO_2 reduction had $\delta^{13}C$-CH_4 values ranging from -110 to -60‰. However, bacterial oxidation in the substrate may affect these pathways before being emitted to the atmosphere, and consequently enrich ^{13}C values of CH_4. Measurements of $\delta^{2}H$-CH_4 can provide information about partial oxidation since this process enriches $\delta^{13}C$-CH_4 and $\delta^{2}H$-CH_4 values (Coleman et al., 1981). Possible explanations for the subtle differences of the manure isotopic signatures between seasons at the reference site may be influenced by changes in diet composition of the milking cows, substrate depletion, perterbations in the lagoon (e.g., high wind conditions, precipitation events, mechanical removal of solids), or a combination of these factors. A future study examining $\delta^{13}C$ and $\delta^{2}H$ of methane and $\delta^{13}C$-CO_2 from dairy manure lagoon waste is necessary to confirm the dominant processes contributing to the enriched $\delta^{13}C_{CH4}$ signatures from California dairy manure lagoons.

Isotopic signatures of CH_4 from enteric fermentation depend on the C isotopic ratio of foods, specifically with the proportion of plants with C3 and C4 photosynthetic pathways in cattle diets (Metges et al., 1990; Levin et al., 1993; Schulze et al., 1998; Bilek

et al., 2001). A diet consisting mostly of C3 plants (e.g., wheat) has been shown to generate more depleted $\delta^{13}C_{CH4}$ than a diet of C4 plants (e.g., maize) (Levin et al., 1993; Schwietzke et al., 2016). A database of studies found that ruminants fed a diet of more than 60% C4 plants emit CH_4 with $\delta^{13}C_{CH4}$ signatures of -54.6 ± 3.1‰, whereas ruminants fed a C3 diet emit CH_4 with $\delta^{13}C_{CH4}$ signatures of -69.4 ± 3.1‰ (Schwietzke et al., 2016). This ~15‰ difference is about the same difference between ^{13}C of C3 and C4 feeds. Furthermore, there is a ~41‰ difference between feed and CH_4 regardless of ruminant species and diet (Schaefer & Whiticar, 2008). Future studies could explore the relationship between diet and CH_4 isotope composition across seasons from different cattle production groups. To improve source apportionment of regional CH_4 emissions in top-down studies, it is important to consider direct measurements of $\delta^{13}C_{CH4}$ of enteric methane given that it varies depending on diet composition.

We have shown that $\delta^{13}C$ measurements of atmospheric CH_4 using a mobile platform can be used for source attribution of enteric and manure methane. Our findings show that CH_4 from manure lagoons is more enriched in $\delta^{13}C$ than CH_4 from enteric fermentation across seasons on average by 14 ± 2‰. This has implications to track the effectiveness of mitigation strategies by measuring $\delta^{13}C_{CH4}$ to quantify enteric:manure ratios over time. In addition, this study contributes to a body of knowledge dedicated to investigating the sources and processes responsible for the increasing global mole fraction of atmospheric methane. Future work could explore whether $\delta^{13}C_{CH4}$ signatures change with mitigation efforts. Additional measurements using $\delta^{13}C$ and $\delta^{2}H$ of CH_4 and $\delta^{13}C$-CO_2 could elucidate which methane generation processes drive manure lagoon emissions.

Major differences in $\delta^{13}C_{CH4}$ from dairy farms among regions underscore the importance of $\delta^{13}C_{CH4}$ measurements at local scales for global analyses.

2.6 Open Research

The dataset for this paper is available online at the Dryad Digital Repository: https://doi.org/10.6086/D1W10G.

2.7 References

Amon, T., Amon, B., Kryvoruchko, V., Zollitsch, W., Mayer, K., & Gruber, L. (2007). Biogas production from maize and dairy cattle manure-Influence of biomass composition on the methane yield. *Agriculture, Ecosystems and Environment*, *118*(1–4), 173–182. https://doi.org/10.1016/j.agee.2006.05.007

Bakkaloglu, S., Lowry, D., Fisher, R. E., France, J. L., Brunner, D., Chen, H., & Nisbet, E. G. (2021). Quantification of methane emissions from UK biogas plants. *Waste Management*, *124*, 82–93. https://doi.org/https://doi.org/10.1016/j.wasman.2021.01.011

Bilek, R. S., Tyler, S. C., Kurihara, M., & Yagi, K. (2001). Investigation of cattle methane production and emission over a 24-hour period using measurements of $\delta^{13}C$ and δD of emitted CH_4 and rumen water. *Journal of Geophysical Research: Atmospheres*, *106*(D14), 15405–15413. https://doi.org/10.1029/2001JD900177

Blake, D. R., Smith, T. W., Chen, T.-Y., Whipple, W. J., & Rowland, F. S. (1994). Effects of biomass burning on summertime nonmethane hydrocarbon concentrations in the Canadian wetlands. *Journal of Geophysical Research*, *99*(D1), 1699. https://doi.org/10.1029/93jd02598

Chang, J., Peng, S., Ciais, P., Saunois, M., Dangal, S. R. S., Herrero, M., Havlík, P., Tian, H., & Bousquet, P. (2019). Revisiting enteric methane emissions from domestic ruminants and their δ13CCH4 source signature. *Nature Communications*, *10*(1). https://doi.org/10.1038/s41467-019-11066-3

Coleman, D. D., Risatti, J. B., & Schoell, M. (1981). Fractionation of carbon and hydrogen isotopes by methane-oxidizing bacteria. *Geochimica et Cosmochimica Acta*, *45*(7), 1033–1037. https://doi.org/10.1016/0016-7037(81)90129-0

Colman, J. J., Swanson, A. L., Meinardi, S., Sive, B. C., Blake, D. R., & Rowland, F. S. (2001). Description of the analysis of a wide range of volatile organic compounds in whole air samples collected during PEM-Tropics A and B. *Analytical Chemistry*, *73*(15), 3723–3731. https://doi.org/10.1021/ac010027g

Cui, Y. Y., Brioude, J., Angevine, W. M., Peischl, J., McKeen, S. A., Kim, S. W., Andrew Neuman, J., Henze, D. K., Bousserez, N., Fischer, M. L., Jeong, S., Michelsen, H. A., Bambha, R. P., Liu, Z., Santoni, G. W., Daube, B. C., Kort, E. A., Frost, G. J., Ryerson, T. B., … Trainer, M. (2017). Top-down estimate of methane emissions in California using a mesoscale inverse modeling technique: The San Joaquin Valley. *Journal of Geophysical Research*, *122*(6), 3686–3699. https://doi.org/10.1002/2016JD026398

Defratyka, S. M., Paris, J. D., Yver-Kwok, C., Fernandez, J. M., Korben, P., & Bousquet, P. (2021). Mapping Urban Methane Sources in Paris, France. *Environmental Science and Technology*, *55*(13), 8583–8591. https://doi.org/https://doi.org/10.1021/acs.est.1c00859

Dlugokencky, E. J., Masarie, K. A., Lang, P. M., & Tans, P. P. (1998). Continuing decline in the growth rate of the atmospheric methane burden. *Nature*, *393*(6684), 447–450. https://doi.org/https://doi.org/10.1038/30934

Dlugokencky, E. J., Nisbet, E. G., Fisher, R., & Lowry, D. (2011). Global atmospheric methane: budget, changes and dangers. *Philosophical Transactions of the Royal Society A: Mathematical, Physical and Engineering Sciences*, *369*(1943), 2058–2072. https://doi.org/10.1098/rsta.2010.0341

Drouillard, J. S. (2018). Current situation and future trends for beef production in the United States of America — A review. *Asian-Australasian Journal of Animal Sciences*, *31*(7), 1007–1016. https://doi.org/10.5713/ajas.18.0428

Duren, R. M., Thorpe, A. K., Foster, K. T., Rafiq, T., Hopkins, F. M., Yadav, V., Bue, B. D., Thompson, D. R., Conley, S., Colombi, N. K., Frankenberg, C., McCubbin, I. B., Eastwood, M. L., Falk, M., Herner, J. D., Croes, B. E., Green, R. O., & Miller, C. E. (2019). California's methane super-emitters. *Nature*, *575*(7781), 180–184. https://doi.org/10.1038/s41586-019-1720-3

Fry, B. (2006). *Stable isotope ecology*. Springer.

Fujita, R., Morimoto, S., Maksyutov, S., Kim, H. S., Arshinov, M., Brailsford, G., Aoki, S., & Nakazawa, T. (2020). Global and Regional CH4 Emissions for 1995–2013 Derived From Atmospheric CH4, δ13C-CH4, and δD-CH4 Observations and a Chemical Transport Model. *Journal of Geophysical Research: Atmospheres*, *125*(14), e2020JD032903. https://doi.org/https://doi.org/ 10.1029/2020JD032903

Gromov, S., Brenninkmeijer, C. A. M., & Jöckel, P. (2018). A very limited role of tropospheric chlorine as a sink of the greenhouse gas methane. *Atmospheric Chemistry and Physics*, *18*(13), 9831–9843. https://doi.org/https://doi.org/10.5194/acp-18-9831-2018

Hoheisel, A., Yeman, C., Dinger, F., Eckhardt, H., & Schmidt, M. (2019). An improved method for mobile characterisation of δ 13 CH 4 source signatures and its application in Germany. *Atmospheric Measurement Techniques*, *12*(2), 1123–1139. https://doi.org/10.5194/amt-12-1123-2019

Honan, M., Feng, X., Tricarico, J. M., & Kebreab, E. (2021). Feed additives as a strategic approach to reduce enteric methane production in cattle: Modes of action, effectiveness and safety. *Animal Production Science*. https://doi.org/10.1071/AN20295

Hopkins, F. M., Ehleringer, J. R., Bush, S. E., Duren, R. M., Miller, C. E., Lai, C. T., Hsu, Y. K., Carranza, V., & Randerson, J. T. (2016). Mitigation of methane emissions in cities: How new measurements and partnerships can contribute to emissions reduction strategies. *Earth's Future*, *4*(9), 408–425. https://doi.org/10.1002/2016EF000381

Hopkins, F. M., Kort, E. A., Bush, S. E., Ehleringer, J. R., Lai, C.-T., Blake, D. R., & Randerson, J. T. (2016). Spatial patterns and source attribution of urban methane in the Los Angeles Basin. *Journal of Geophysical Research: Atmospheres*, *121*(5), 2490–2507. https://doi.org/10.1002/2015JD024429

Jeong, S., Hsu, Y. K., Andrews, A. E., Bianco, L., Vaca, P., Wilczak, J. M., & Fischer, M. L. (2013). A multitower measurement network estimate of California's methane emissions. *Journal of Geophysical Research Atmospheres*, *118*(19), 11,339-11,351. https://doi.org/10.1002/jgrd.50854

Jeong, S., Newman, S., Zhang, J., Andrews, A. E., Bianco, L., Bagley, J., Cui, X., Graven, H., Kim, J., Salameh, P., LaFranchi, B. W., Priest, C., Campos-Pineda, M., Novakovskaia, E., Sloop, C. D., Michelsen, H. A., Bambha, R. P., Weiss, R. F., Keeling, R., & Fischer, M. L. (2016). Estimating methane emissions in California's urban and rural regions using multitower observations. *Journal of Geophysical Research: Atmospheres*, *121*(21), 13,031-13,049. https://doi.org/10.1002/2016JD025404

Joshi, G. (2020, January). Less methane by 2030. *Journal of Nutrient Management*, 18–19. https://jofnm.com/article-37-Less-methane-by-2030.html

Keeling, C. D. (1958). The concentration and isotopic abundances of atmospheric carbon dioxide in rural areas. *Geochimica et Cosmochimica Acta*, *13*, 322–334. https://doi.org/https://doi.org/10.1016/0016-7037(58)90033-4

Lan, X., Basu, S., Schwietzke, S., Bruhwiler, L. M. P., Dlugokencky, E. J., Michel, S. E., Sherwood, O. A., Tans, P. P., Thoning, K., Etiope, G., Zhuang, Q., Liu, L., Oh, Y., Miller, J. B., Pétron, G., Vaughn, B. H., & Crippa, M. (2021). Improved Constraints on Global Methane Emissions and Sinks Using δ13C-CH4. *Global Biogeochemical Cycles*, *35*(6), e2021GB007000. https://doi.org/https://doi.org/10.1029/2021GB007000

Lan, X., Nisbet, E. G., Dlugokencky, E. J., & Michel, S. E. (2021). What do we know about the global methane budget? Results from four decades of atmospheric CH4 observations and the way forward. *Philosophical Transactions of the Royal Society A*, *379*(2210), 20200440. https://doi.org/https://doi.org/10.1098/rsta.2020.0440

Levin, I., Bergamaschi, P., Dörr, H., & Trapp, D. (1993). Stable isotopic signature of methane from major sources in Germany. *Chemosphere*, *26*(1–4), 161–177. https://doi.org/10.1016/0045-6535(93)90419-6

Litvak, E., Bijoor, N. S., & Pataki, D. E. (2014). Adding trees to irrigated turfgrass lawns may be a water-saving measure in semi-arid environments. *Ecohydrology*, *7*(5), 1314–1330. https://doi.org/10.1002/eco.1458

Lopez, M., Sherwood, O. A., Dlugokencky, E. J., Kessler, R., Giroux, L., & Worthy, D. E. J. (2017). Isotopic signatures of anthropogenic CH4 sources in Alberta, Canada. *Atmospheric Environment*, *164*, 280–288. https://doi.org/10.1016/j.atmosenv.2017.06.021

Lowry, D., Fisher, R. E., France, J. L., Coleman, M., Lanoisellé, M., Zazzeri, G., Nisbet, E. G., Shaw, J. T., Allen, G., Pitt, J., & Ward, R. S. (2020). Environmental baseline monitoring for shale gas development in the UK: Identification and geochemical characterisation of local source emissions of methane to atmosphere. *Science of the Total Environment*, *708*, 134600. https://doi.org/10.1016/j.scitotenv.2019.134600

Marklein, A. R., Meyer, D., Fischer, M. L., Jeong, S., Rafiq, T., Carr, M., & Hopkins, F. M. (2021). Facility-scale inventory of dairy methane emissions in California: implications for mitigation. *Earth System Science Data*, *13*(3), 1151–1166. https://doi.org/10.5194/essd-13-1151-2021

McKain, K., Down, A., Raciti, S. M., Budney, J., Hutyra, L. R., Floerchinger, C., Herndon, S. C., Nehrkorn, T., Zahniser, M. S., Jackson, R. B., Phillips, N., & Wofsy, S. C. (2015). Methane emissions from natural gas infrastructure and use in the urban region of Boston, Massachusetts. *Proceedings of the National Academy of Sciences*, *112*(7), 1941–1946. https://doi.org/10.1073/pnas.1416261112

Metges, C., Kempe, K., & Schmidt, H.-L. (1990). Dependence of the carbon-isotope contents of breath carbon dioxide, milk, serum and rumen fermentation products on the δ13C value of food in dairy cows. *British Journal of Nutrition*, *63*(2), 187–196. https://doi.org/10.1079/bjn19900106

Meyer, D., Heguy, J., Karle, B., & Robinson, P. (2019). *Characterize Physical and Chemical Properties of Manure in California Dairy Systems to Improve Greenhouse Gas Emission Estimates. Final Report: Contract No. 16RD002.* (pp. 1–70). California Air Resources Board and the California Environmental Protection Agency.

Miles, N. L., Martins, D. K., Richardson, S. J., Rella, C. W., Arata, C., Lauvaux, T., Davis, K. J., Barkley, Z. R., McKain, K., & Sweeney, C. (2018). Calibration and field testing of cavity ring-down laser spectrometers measuring CH4, CO2, and δ13CH4 deployed on towers in the Marcellus Shale region. *Atmospheric Measurement Techniques*, *11*(3), 1273–1295. https://doi.org/10.5194/amt-11-1273-2018

Miller, D. J., Sun, K., Tao, L., Pan, D., Zondlo, M. A., Nowak, J. B., Liu, Z., Diskin, G., Sachse, G., Beyersdorf, A., Ferrare, R., & Scarino, A. J. (2015). Ammonia and methane dairy emission plumes in the San Joaquin Valley of California from individual feedlot to regional scales. *Journal of Geophysical Research: Atmospheres*, *120*(18), 9718–9738. https://doi.org/10.1002/2015JD023241

Miller, S. M., Wofsy, S. C., Michalak, A. M., Kort, E. A., Andrews, A. E., Biraud, S. C., Dlugokencky, E. J., Eluszkiewicz, J., Fischer, M. L., Janssens-Maenhout, G., Miller, B. R., Miller, J. B., Montzka, S. A., Nehrkorn, T., & Sweeney, C. (2013). Anthropogenic emissions of methane in the United States. *Proceedings of the National Academy of Sciences*, *110*(50), 20018–20022. https://doi.org/10.1073/pnas.1314392110

Mullinax, D., Meyer, D., & Summer, D. (2020). *Small Dairy Climate Change Research: An economic evaluation of strategies for methane emission reduction effectiveness and appropriateness in small and large California dairies*. https://www.cdfa.ca.gov/oefi/research/docs/CDFA_SmallDairyResearch_Final_Report.pdf

Naus, S., Montzka, S. A., Pandey, S., Basu, S., Dlugokencky, E. J., & Krol, M. (2019). Constraints and biases in a tropospheric two-box model of OH. *Atmospheric Chemistry and Physics*, *19*(1), 407–424. https://doi.org/10.5194/acp-19-407-2019

Nicely, J. M., Canty, T. P., Manyin, M., Oman, L. D., Salawitch, R. J., Steenrod, S. D., Strahan, S. E., & Strode, S. A. (2018). Changes in Global Tropospheric OH Expected as a Result of Climate Change Over the Last Several Decades. *Journal of Geophysical Research: Atmospheres*, *123*(18), 10,774-10,795. https://doi.org/10.1029/2018JD028388

Nisbet, E. G., Dlugokencky, E. J., & Bousquet, P. (2014). Methane on the Rise—Again. *Science*, *343*(6170), 493–495. https://doi.org/10.1017/CBO9781107415324.004

Nisbet, E. G., Dlugokencky, E. J., Fisher, R. E., France, J. L., Lowry, D., Manning, M. R., Michel, S. E., & Warwick, N. J. (2021). Atmospheric methane and nitrous oxide: challenges along the path to Net Zero. *Philosophical Transactions of the Royal Society A: Mathematical, Physical and Engineering Sciences*, *379*(2210), 20200457. https://doi.org/10.1098/rsta.2020.0457

Nisbet, E. G., Fisher, R. E., Lowry, D., France, J. L., Allen, G., Bakkaloglu, S., Broderick, T. J., Cain, M., Coleman, M., Fernandez, J., Forster, G., Griffiths, P. T., Iverach, C. P., Kelly, B. F. J., Manning, M. R., Nisbet-Jones, P. B. R., Pyle, J. A., Townsend-Small, A., Al-Shalaan, A., … Zazzeri, G. (2020). Methane Mitigation: Methods to Reduce Emissions, on the Path to the Paris Agreement. *Reviews of Geophysics*, *58*(1), e2019RG000675. https://doi.org/https://doi.org/10.1029/2019RG000675

Nisbet, E. G., Manning, M. R., Dlugokencky, E. J., Fisher, R. E., Lowry, D., Michel, S. E., Myhre, C. L., Platt, S. M., Allen, G., Bousquet, P., Brownlow, R., Cain, M., France, J. L., Hermansen, O., Hossaini, R., Jones, A. E., Levin, I., Manning, A. C., Myhre, G., … White, J. W. C. (2019). Very Strong Atmospheric Methane Growth in the 4 Years 2014–2017: Implications for the Paris Agreement. *Global Biogeochemical Cycles*, *33*(3), 318–342. https://doi.org/https://doi.org/10.1029/2018GB006009

Owen, J. J., & Silver, W. L. (2015). Greenhouse gas emissions from dairy manure management: a review of field-based studies. *Global Change Biology*, *21*(2), 550–565. https://doi.org/10.1111/gcb.12687

Pataki, D. E., Ehleringer, J. R., Flanagan, L. B., Yakir, D., Bowling, D. R., Still, C. J., Buchmann, N., Kaplan, J. O., & Berry, J. A. (2003). The application and interpretation of Keeling plots in terrestrial carbon cycle research. *Global Biogeochemical Cycles*, *17*(1), 1022. https://doi.org/10.1029/2001GB001850

Phillips, N. G., Ackley, R., Crosson, E. R., Down, A., Hutyra, L. R., Brondfield, M., Karr, J. D., Zhao, K., & Jackson, R. B. (2013). Mapping urban pipeline leaks: Methane leaks across Boston. *Environmental Pollution*, *173*, 1–4. https://doi.org/10.1016/j.envpol.2012.11.003

Plant, G., Kort, E. A., Floerchinger, C., Gvakharia, A., Vimont, I., & Sweeney, C. (2019). Large Fugitive Methane Emissions From Urban Centers Along the U.S. East Coast. *Geophysical Research Letters*, *46*(14), 8500–8507. https://doi.org/https://doi.org/10.1029/2019GL082635

Rigby, M., Montzka, S. A., Prinn, R. G., C White, J. W., Young, D., Lunt, M. F., Ganesan, A. L., Manning, A. J., Simmonds, P. G., Salameh, P. K., Harth, C. M., Weiss, R. F., Fraser, P. J., Paul Steele, L., Krummel, P. B., McCulloch, A., & Park, S. (2017). Role of atmospheric oxidation in recent methane growth. *Proceedings of the National Academy of Sciences*, *114*(21), 5373–5377. https://doi.org/10.1073/pnas.1616426114

Sargent, M. R., Floerchinger, C., McKain, K., Budney, J., Gottlieb, E. W., Hutyra, L. R., Rudek, J., & Wofsy, S. C. (2021). Majority of US urban natural gas emissions unaccounted for in inventories. *Proceedings of the National Academy of Sciences*, *118*(44), e2105804118. https://doi.org/10.1073/pnas.2105804118

Schaefer, H., Fletcher, S. E. M., Veidt, C., Lassey, K. R., Brailsford, G. W., Bromley, T. M., Dlugokencky, E. J., Michel, S. E., Miller, J. B., Levin, I., Lowe, D. C., Martin, R. J., Vaughn, B. H., & White, J. W. C. (2016). A 21st-century shift from fossil-fuel to biogenic methane emissions indicated by 13CH4. *Science*, *352*(6281), 80–84. https://doi.org/10.1126/science.aad2705

Schaefer, H., & Whiticar, M. J. (2008). Potential glacial-interglacial changes in stable carbon isotope ratios of methane sources and sink fractionation. *Global Biogeochemical Cycles*, *22*(1). https://doi.org/10.1029/2006GB002889

Schulze, E., Lohmeyer, S., & Giese, W. (1998). Determination of13C/12C-ratios in rumen produced methane and CO2 of cows, sheep and camels. *Isotopes in Environmental and Health Studies*, *34*(1–2), 75–79. https://doi.org/10.1080/10256019708036334

Schwietzke, S., Sherwood, O. A., Bruhwiler, L. M. P., Miller, J. B., Etiope, G., Dlugokencky, E. J., Michel, S. E., Arling, V. A., Vaughn, B. H., White, J. W. C., & Tans, P. P. (2016). Upward revision of global fossil fuel methane emissions based on isotope database. *Nature*, *538*(7623), 88–91. https://doi.org/10.1038/nature19797

Thirumalai, K., Singh, A., & Ramesh, R. (2011). A MATLAB™ code to perform weighted linear regression with (correlated or uncorrelated) errors in bivariate data. *Journal of the Geological Society of India*, *77*(4), 377–380. https://doi.org/10.1007/s12594-011-0044-1

Thiruvenkatachari, R. R., Carranza, V., Ahangar, F., Marklein, A., Hopkins, F., & Venkatram, A. (2020). Uncertainty in using dispersion models to estimate methane emissions from manure lagoons in dairies. *Agricultural and Forest Meteorology*, *290*, 108011. https://doi.org/10.1016/j.agrformet.2020.108011

Townsend-Small, A., Botner, E. C., Jimenez, K. L., Schroeder, J. R., Blake, N. J., Meinardi, S., Blake, D. R., Sive, B. C., Bon, D., Crawford, J. H., Pfister, G., & Flocke, F. M. (2016). Using stable isotopes of hydrogen to quantify biogenic and thermogenic atmospheric methane sources: A case study from the Colorado Front Range. *Geophysical Research Letters*, *43*(21), 11,462-11,471. https://doi.org/10.1002/2016GL071438

Townsend-Small, A., Tyler, S. C., Pataki, D. E., Xu, X., & Christensen, L. E. (2012). Isotopic measurements of atmospheric methane in Los Angeles, California, USA: Influence of "fugitive" fossil fuel emissions. *Journal of Geophysical Research: Atmospheres*, *117*(D7). https://doi.org/10.1029/2011JD016826

Trousdell, J. F., Conley, S. A., Post, A., & Faloona, I. C. (2016). Observing entrainment mixing, photochemical ozone production, and regional methane emissions by aircraft using a simple mixed-layer framework. *Atmospheric Chemistry and Physics*, *16*(24), 15433–15450. https://doi.org/10.5194/acp-16-15433-2016

Turner, A. J., Frankenberg, C., Wennberg, P. O., & Jacob, D. J. (2017). Ambiguity in the causes for decadal trends in atmospheric methane and hydroxyl. *Proceedings of the National Academy of Sciences*, *114*(21), 5367–5372. https://doi.org/10.1073/pnas.1616020114

United Nations Environment Programme and Climate and Clean Air Coalition. (2021). *Global Methane Assessment: Benefits and Costs of Mitigating Methane Emissions. Nairobi: United Nations Environment Programme*. https://doi.org/978-92-807-3854-4

Viatte, C., Lauvaux, T., Hedelius, J. K., Parker, H., Chen, J., Jones, T., Franklin, J. E., Deng, A. J., Gaudet, B., Verhulst, K., Duren, R., Wunch, D., Roehl, C., Dubey, M. K., Wofsy, S., & Wennberg, P. O. (2017a). Methane emissions from dairies in the Los Angeles Basin. *Atmospheric Chemistry and Physics*, *17*(12), 7509–7528. https://doi.org/10.5194/acp-17-7509-2017

Viatte, C., Lauvaux, T., Hedelius, J. K., Parker, H., Chen, J., Jones, T., Franklin, J. E., Deng, A. J., Gaudet, B., Verhulst, K., Duren, R., Wunch, D., Roehl, C., Dubey, M. K., Wofsy, S., & Wennberg, P. O. (2017b). Methane emissions from dairies in the Los Angeles Basin. *Atmospheric Chemistry and Physics*, *17*(12), 7509–7528. https://doi.org/10.5194/acp-17-7509-2017

Wecht, K. J., Jacob, D. J., Sulprizio, M. P., Santoni, G. W., Wofsy, S. C., Parker, R., Bösch, H., & Worden, J. (2014). Spatially resolving methane emissions in California: constraints from the CalNex aircraft campaign and from present (GOSAT, TES) and future (TROPOMI, geostationary) satellite observations. *Atmospheric Chemistry and Physics*, *14*(15), 8173–8184. https://doi.org/10.5194/acp-14-8173-2014

Weiland, P. (2010). Biogas production: Current state and perspectives. *Applied Microbiology and Biotechnology*, *85*(4), 849–860. https://doi.org/10.1007/s00253-009-2246-7

Wennberg, P. O., Mui, W., Wunch, D., Kort, E. A., Blake, D. R., Atlas, E. L., Santoni, G. W., Wofsy, S. C., Diskin, G. S., Jeong, S., & Fischer, M. L. (2012). On the Sources of Methane to the Los Angeles Atmosphere. *Environmental Science and Technology*, *46*(17), 9282–9289. https://doi.org/10.1021/ES301138Y

Whiticar, M., Faber, E., Acta, M. S.-G. et C., & 1986, U. (1986). Biogenic methane formation in marine and freshwater environments: CO2 reduction vs. acetate fermentation—isotope evidence. *Geochimica et Cosmochimica Acta*, *50*(5), 693–709. https://doi.org/https://doi.org/10.1016/0016-7037(86)90346-7

Worden, J. R., Bloom, A. A., Pandey, S., Jiang, Z., Worden, H. M., Walker, T. W., Houweling, S., & Röckmann, T. (2017). Reduced biomass burning emissions reconcile conflicting estimates of the post-2006 atmospheric methane budget. *Nature Communications*, *8*(1), 1–11. https://doi.org/10.1038/s41467-017-02246-0

Xueref-Remy, I., Zazzeri, G., Bréon, F. M., Vogel, F., Ciais, P., Lowry, D., & Nisbet, E. G. (2020). Anthropogenic methane plume detection from point sources in the Paris megacity area and characterization of their δ13C signature. *Atmospheric Environment*, *222*, 117055. https://doi.org/10.1016/j.atmosenv.2019.117055

Yarnes, C. (2013). δ13C and δ2H measurement of methane from ecological and geological sources by gas chromatography/combustion/pyrolysis isotope-ratio mass spectrometry. *Rapid Communications in Mass Spectrometry*, *27*(9), 1036–1044. https://doi.org/10.1002/rcm.6549

York, D., Evensen, N. M., Martínez, M. L., & De Basabe Delgado, J. (2004). Unified equations for the slope, intercept, and standard errors of the best straight line. *American Journal of Physics*, *72*(3), 367–375. https://doi.org/10.1119/1.1632486

Zheng, W., Obrist, D., Weis, D., & Bergquist, B. A. (2016). Mercury isotope compositions across North American forests. *Global Biogeochemical Cycles*, *30*(10), 1475–1492. https://doi.org/10.1002/2015GB005323

3. Characterization of Ammonia, Nitrous Oxide, and Methane Emissions From California Dairy Farms Using Enhancement Ratios

3.0 Acknowledgement of Co-Authorship

This work was completed with contributions from Valerie Carranza, Michael Rodriguez, Ranga Rajan Thiruvenkatachari, Brenna Biggs, Donald R. Blake, and Francesca M. Hopkins

3.1 Abstract

Dairies are an important source of greenhouse gas (GHG) and ammonia (NH_3) emissions but remain highly uncertain across spatial and temporal scales. Quantifying and characterizing GHG and NH_3 enhancement ratios from dairy farms is essential for source apportionment and evaluation of emission control strategies. We characterize the spatiotemporal distribution of methane (CH_4), NH_3, and nitrous oxide (N_2O) dairy plumes with a mobile platform in the San Joaquin Valley (SJV) in California across 4 seasons in 2019 and 2020. We evaluate the statistical significance of enhancement ratios of NH_3, CH_4 and N_2O from downwind emission plumes of dairy farms and from different sources within a dairy facility, including livestock housing (e.g., corrals, freestall lanes), wet manure management (e.g., manure lagoons) and dry manure management (e.g., dry bedding), silage piles, and liquid manure-irrigated cropland. The average NH_3 to CH_4 enhancement ratio from freestall barns and corrals observed across all seasons is 0.58 ± 0.19 ppbv ppbv^{-1} and 0.48 ± 0.05 ppbv ppbv^{-1}, respectively. Whereas the average NH_3 to CH_4 enhancement ratio for wet manure management is 0.09 ± 0.01 ppbv ppbv^{-1} and dry manure management

is 2.71 ± 0.85 ppbv ppbv^{-1}. Enhancement ratios of N_2O to CH_4 also show distinct signatures between livestock housing, manure management, cropland, and silage, with the highest enhancement ratios observed in cropland (1.65 ± 0.17 ppbv ppbv^{-1}). Our analyses could improve spatial allocation of GHG and NH_3 emissions from dairy farms and constrain the relative contributions of these different sources of emissions to overall dairy farm emissions.

3.2 Introduction

Livestock agriculture is a major source of ammonia (NH_3) and greenhouse gas (GHG) emissions, such as methane (CH_4) and nitrous oxide (N_2O). In the United States, livestock contributes an estimated 66% of total agricultural GHG emissions (USDA, 2016). Methane is more efficient at trapping infrared radiation than carbon dioxide (CO_2), with a lifetime of about 10 years in the troposphere and a global warming potential (GWP) about 28 times that of CO_2 on a 100-year scale (IPCC, 2013). Nitrous oxide is even more effective at absorbing heat with a GWP 265 times that of CO_2. Ammonia is a gas-phase precursor to fine particulate matter, impacting human health and posing a threat to terrestrial and aquatic systems (Behera et al., 2013). As such, there is a need for accurate observations of GHG and NH_3 emissions from the agricultural sector are imperative to address poor air quality and climate change.

The San Joaquin Valley (SJV) of California is a region with significant CH_4, N_2O, and NH_3 emissions (Cassel et al., 2005; Jeong et al., 2013, 2020; Gentner et al., 2014; Wecht et al., 2014; Miller et al., 2015; Guha et al., 2015; Arndt et al., 2018; Amini et al.,

2022). Currently, there is disagreement whether state inventories accurately represent these gases across spatial and temporal scales. For example, atmospheric studies often report dairy CH_4 emissions in California up to two times higher than bottom-up inventories (Jeong et al., 2016; Trousdell et al., 2016; Cui et al., 2017). Meanwhile, other studies have reported that CH_4 observations were comparable to inventories during the summer but not winter seasons, or using ground observations but not airborne measurements (Arndt et al., 2018; Amini et al., 2022). A similar case is observed for NH_3 in the SJV, where chemical transport models substantially underestimate gas-phase NH_3 observations compared to airborne and satellite measurements (Heald et al., 2012; Schiferl et al., 2014; Kelly et al., 2014). These results suggest that inventories likely underestimate and misrepresent agricultural NH_3 emissions across spatial and temporal scales (Schiferl et al., 2014; Kelly et al., 2014). There are limited N_2O observations in the SJV of California, where most N_2O emissions is expected from the agriculture sector (Jeong et al., 2012, 2018; Xiang et al., 2013; Guha et al., 2015; Nevison et al., 2018; Herrera et al., 2021). These studies show that top-down observations of N_2O are at least two times higher than bottom-up inventories (Jeong et al., 2012, 2018; Xiang et al., 2013; Herrera et al., 2021). In addition, these studies use either short-term airborne or tower observations, which provide limited seasonal and spatial information on N_2O emission trends.

The dairy sector is an important source of GHG and NH_3 emissions in the SJV. Methane emissions from dairy farms is primarily emitted by enteric fermentation from ruminant gut microbes and anaerobic decomposition of dairy manure in storage ponds (Owen & Silver, 2015). Dairy manure management contributes a substantial fraction of

CH_4, N_2O, NH_3 emissions and the relative magnitudes depends on manure management practices (Leytem et al., 2011; Owen & Silver, 2015; Broucek, 2016). Solid manure management includes storing manure in piles, deep pits, open lots, and daily spreading of dairy waste. In contrast, in a liquid manure management system, waste from barns and other dairy infrastructure, such as milking parlors, are washed and collected in slurry ponds or anaerobic lagoons (Kaffka & Barzee, 2016). Anaerobic conditions, such as found in anaerobic manure lagoons, promote the production of CH_4, and to a lesser extent N_2O and NH_3 emissions (Owen & Silver, 2015; Broucek, 2016; Kupper et al., 2020). Solid manure storage systems have reportedly higher N_2O emissions than CH_4 and NH_3 emissions relative to manure lagoons. Nitrous oxide is generated from denitrification and nitrification reactions in manure-amended soils, manure storage, and direct N deposition by animals (He et al., 2001). In general, denitrification accounts for most of N_2O emissions under anaerobic conditions. Nitrous oxide, along with NH_3 and NO, is indirectly emitted through volatilization of manure N from nitrification and denitrification in soil after redeposition (Hristov et al., 2011; J. Li et al., 2015). Ammonia emissions, on the other hand, are primarily a byproduct of urea hydrolysis during the decomposition of urine and feces, which is mostly found in animal housing (Hristov et al., 2011). Ammonia volatilization at liquid-surface interface occurs under high pH conditions since the pKa of NH_4^+/NH_3 is 9.25 (Laubach et al., 2015). Storage of animal feed, such as silage piles, also emit NH_3 and N_2O (Kozloski et al., 2006; Borhan et al., 2011b) As California moves towards meeting GHG and air pollution reduction goals, it is critical to gain a better understanding of the magnitude, temporal patterns, and source of emissions from dairy farms in the SJV region.

Enhancement ratios between trace gas emissions can be used as a signature for source apportionment and evaluation of emission control strategies. Enhancement ratios are defined as ratios between enhancements of trace gas mole fractions—wherein an enhancement is calculated by subtracting a background mole fraction from the observed atmospheric mole fraction of a trace gas. Previous studies have used enhancement ratios of nitrogen gases to CH_4 (ΔNH_3:ΔCH_4; ΔN_2O:ΔCH_4) to distinguish between sources of co-located emissions at dairy farms (Miller et al., 2015; Eilerman et al., 2016). Enhancement ratios allows the identification of emission trends and characterization between sources. In this study, we characterize seasonal CH_4, N_2O, NH_3 emissions from a dairy farm in the SJV of California using enhancement ratios. We use enhancement ratios between NH_3 and CH_4 (ΔNH_3:ΔCH_4) and N_2O and CH_4 (ΔN_2O: ΔCH_4). We first characterize the spatial heterogeneity of NH_3, N_2O, and CH_4 mole fractions from a dairy farm. Then we quantify the enhancement ratios from different source areas at a dairy farm by season. We hypothesize that CH_4 is emitted primarily from manure lagoons and animal housing areas, whereas N_2O is emitted primarily from cropland and corrals. Additionally, we predict higher NH_3 from silage, cropland, and corrals. We also hypothesize that ΔNH_3:ΔCH_4 and ΔN_2O: ΔCH_4 will be highest during the summer, when temperatures are highest.

3.3 Methods

3.3.1 Study Site

Our study site was located at a dairy farm in Tulare County in the SJV of California. Figure 3.1 shows a schematic of the dairy farm with photographs representative of each source area. The dairy farm has on average 3,070 milking cows in freestall barns, with

approximately 400 dry cows and 3,000 heifers in open lots (corrals). Manure waste from the freestall barns is flushed and stored in manure lagoons (cell 1, cell 2, primary lagoon, and holding pond in Figure 3.1). Manure waste is flushed into a processing pit, where waste is diverted to a manure separator, which removes coarser solids from liquid effluent that flows into cell 1. The coarser solids are moved to a separator pile. Cropland is irrigated with water waste from the holding pond. Dry manure is spread out on the ground and sun dried in the solid drying area or separated into piles for dry bedding that is later used in freestall barns. The dairy farm is surrounded by cropland, primarily wheat or maize depending on the season, which is then preserved as silage piles after harvest and used as animal feed.

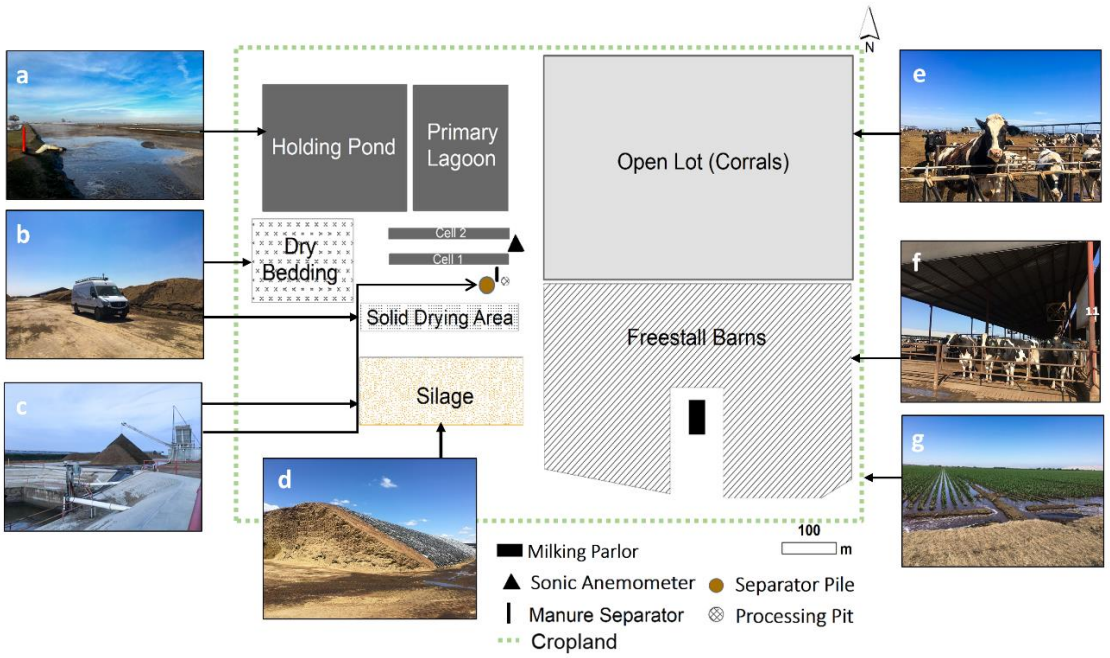

Figure 3.1. Dairy farm layout of the reference test site in the San Joaquin Valley. Photographs represent examples of the source areas. Photographs show dairy farm infrastructure including (a) manure lagoons, (b) solid manure storage as dry bedding and solid drying area, (c) manure separator pile, (d) feed stored as covered silage piles, (e) corrals, (f) freestall barns, and (g) cropland that surrounds the dairy farm.

3.3.2 Instrumentation

Ground-based mobile lab measurements were collected in autumn of 2018 (3 d), spring (4 d), summer (7 d), and autumn of 2019 (3 d), and winter of 2020 (4 d). Table 3.2 shows a summary of these measurements and associated environmental conditions. Atmospheric measurements were performed with a mobile platform outfitted with multiple trace gas analyzers (Thiruvenkatachari et al., 2020; Carranza et al., 2022; Yañez et al., 2022) based on cavity ringdown spectroscopy (Picarro G2401, Picarro G2210-*i*, Picarro G2308, Picarro G2123; Picarro, Inc.) and an isotopic N_2O analyzer based on off-axis integrated cavity output spectroscopy (Los Gatos Research, Inc.) (Table 3.1). In addition, a global satellite positioning unit (GPS 16X, Garmin Ltd.) recorded geolocation and vehicle speed and a weather station (METSENS500, Campbell Scientific, Inc.) measured wind direction, wind speed, air temperature and relative humidity. A stationary 3 m meteorological tower with a 3-D sonic anemometer (CSAT3, Campbell Scientific, Inc.) mounted was used to collect ambient temperature, wind speed, and wind direction. Atmospheric measurements of CH_4, NH_3, and N_2O were collected from an inlet height of 2.87 m above ground level. Greenhouse gas measurements were corrected using high and low gas mixtures before and after each measurement period. The gas mixtures were tied to the NOAA Global Monitoring Division (GMD) scale.

Table 3.1. Analyzers On Board the Mobile Platform and Corresponding Instrument Specifications.

Instrument	Trace Gases	Method	Time Resolution	Precision
Picarro G2401	CH_4, CO_2, CO, H_2O	cavity ringdown spectroscopy	2.5 s	CH_4: ± 20 ppbv CO_2: ± 2 ppmv CO: ± 7.6 ppbv H_2O: ± 0.02%
Picarro G2210-*i*	CH_4, CO_2, C_2H_6, $\delta^{13}C_{CH4}$	cavity ringdown spectroscopy	~1 -1.25 s.	CH_4: ± 8 ppbv CO_2: ± 2 ppmv C_2H_6: ± 8 ppbv $\delta^{13}C_{CH4}$: ± 1.7 ‰
Picarro G2308	CH_4, CO_2, N_2O, H_2O	cavity ringdown spectroscopy	<6 - 10 s	CH_4: ± 43 ppbv CO_2: ± 6 ppmv N_2O: ± 5 ppbv H_2O: ± 0.04 %
Picarro G2123	NH_3	cavity ringdown spectroscopy	1 s	NH_3: ± 0.5 ppbv
Los Gatos Research Isotopic N_2O Analyzer	N_2O, $\delta^{15}N^{\alpha}$, $\delta 15N^{\beta}$, δ15N, δ 18O	off-axis integrated cavity output spectroscopy	1 s	N_2O: ± 0.4 ppbv

Ammonia measurements were corrected using a stepwise dilution method, wherein an NH_3 Balance Standard (Airgas, Inc.) was mixed with Zero Grade Air (Airgas, Inc.) using mass flow controllers (MFC) (Zero Air: MC-20SLPM-D-SV and NH_3: MCS-100SCCM-D-PCV03, Alicat Scientific, Inc.). The dilution system, consisting of crack-resistant PFA clear tubing for chemicals (McMaster-Carr) and the MFC, was used to produce NH_3 mole fractions of 0, 104, 206, 306, 404, and 500 ppb.

Table 3.2. Summary of Mobile Lab Measurements at the Primary Dairy, Including Time of Observations, Trace Gases Measured, mean Air Temperature, Prevailing Wind Direction, Mean Wind Speed, Mean Relative Humidity and Number of Days After the Past Precipitation Event.

Season	Date	Local Time	Trace Gases Measured	Air Temperature (ºC)	Wind Direction	Wind Speed (m/s)	Relative Humidity (%)[a]	Number of Days After Last Precipitation Event [a]
Autumn	19-Sep-2018	12:25 - 17:23	CH_4, NH_3	25 - 31	WNW	2.8 ± 0.9	50	142
	20-Sep-2018	12:29 - 17:29	CH_4, NH_3	26 - 32	W	1.7 ± 0.7	46	143
	21-Sep-2018	5:32 - 7:40	CH_4, NH_3, N_2O	15 - 17	ENE	0.9 ± 0.3	43	144
Spring	25-Mar-2019	11:18 - 19:39	CH_4, NH_3, N_2O	18 - 24	W	1.9 ± 0.7	54	1
	26-Mar-2019	4:40 - 8:58	CH_4, NH_3, N_2O	7 - 12	SSE	1.3 ± 0.5	50	2
	28-Mar-2019	16:05 - 18:17	CH_4, NH_3	18 - 21	W	3.0 ± 0.8	59	0
Summer	17-Jun-2019	18:19 - 19:03	CH_4, NH_3, N_2O	33 - 34	NW	5.4 ± 0.6	46	21
	18-Jun-2019	14:52 - 18:50	CH_4, NH_3, N_2O	35 - 37	NW	3.2 ± 1.1	47	22
	19-Jun-2019	15:07 - 17:30	CH_4, NH_3, N_2O	36 - 39	NW	4.7 ± 1.3	45	23
	20-Jun-2019	11:07 - 17:38	CH_4, NH_3, N_2O	28 - 35	W	3.2 ± 1.4	45	24
	21-Jun-2019	9:41 - 12:07	CH_4, NH_3, N_2O	21 - 27	W	2.2 ± 1.1	49	25
	26-Jun-2019	12:41 - 16:08	CH_4, NH_3	26 - 32	WNW	4.1 ± 1.5	41	31
Autumn	10-Sep-2019	12:53 - 18:00	CH_4, NH_3, N_2O	23 - 28	NW	2.8 ± 1.0	45	108
	14-Sep-2019	5:38 - 8:42	CH_4, NH_3, N_2O	20 - 23	S	1.7 ± 0.3	39	112
Winter	14-Jan-2020	15:19 - 16:53	CH_4, NH_3, N_2O	10 - 12	WNW	12.7 ± 3.0	64	3
	16-Jan-2020	10:42 - 13:38	CH_4, NH_3, N_2O	13 - 16	S	3.4 ± 0.8	75	4
	17-Jan-2020	9:20 - 17:23	CH_4, NH_3, N_2O	6 - 12	W	1.6 ± 0.6	68	5

[a] Data collected from the Porterville weather station, provided from the California Irrigation Management Information System (CIMIS). All other meteorological data collected on site from the 3 m meteorological tower measurements.

3.3.3 Enhancement Ratios

Data streams between gas analyzers and GPS were synchronized using a cross-correlation method (crosscorrelation function in RStudio). Specifically, we cross-correlated the data streams between gas analyzer using the CO_2 channels from each instrument. Trace gas, location, and meteorological observations were then averaged across 5 s intervals. The observations were also categorized by each source at the dairy farm based on proximity to source location and prevailing wind direction. Enhancements for each gas species were estimated by subtracting the background mole fractions, defined as the minimum mole fractions observed upwind of each source during each measurement period (e.g., $\Delta CH_{4source} = CH_{4source\ measured} - CH_{4source\ background}$). Enhancement ratios (ERs) for NH_3 to CH_4 and N_2O to CH_4 were then estimated for each source. Enhancements for NH_3, N_2O, and CH_4 are represented as changes (Δ) in the component constituents ΔNH_3, ΔN_2O, and ΔCH_4, respectively, hereafter. ERs are calculated between NH_3 and CH_4 (ΔNH_3:ΔCH_4) and N_2O and CH_4 (ΔN_2O: ΔCH_4).

3.4 Results

3.4.1 Spatial Characterization of Methane, Ammonia, and Nitrous Oxide Observations at Dairy Farm

Spatial heterogeneity of CH_4, NH_3, and N_2O mole fractions was observed at the dairy farm (Figure 3.2). Across all measurement days, manure lagoons and the solid drying area piles had the highest mean ΔCH_4, with 16.1 ± 0.1 ppmv and 9.5 ± 0.3 ppmv, respectively (Table 3.3). Mean ΔNH_3 was highest for freestall barns (265 ± 4 ppbv) and corrals (231 ± 6 ppbv). In contrast, mean ΔN_2O were highest for silage (328 ± 25 ppbv) and cropland (215 ± 13 ppbv).

Table 3.3. Mean Enhancements of CH_4, N_2O, and NH_3 by Source Location from All Measurement Days. The Reported Uncertainty Corresponds to the Standard Error.

Source	ΔCH_4 (ppm)	ΔN_2O (ppb)	ΔNH_3 (ppb)
Freestall Barns	4.3 ± 0.1	54 ± 1	265 ± 4
Corrals	1.2 ± 0.0	26 ± 3	231 ± 6
Manure Lagoons	16.1 ± 0.1	17 ± 0	173 ± 2
Silage	1.7 ± 0.1	328 ± 25	73 ± 3
Crops	0.3 ± 0.0	215 ± 13	56 ± 3
Solid Drying Area	9.5 ± 0.3	12 ± 0	12 ± 0
Dry Bedding	1.7 ± 0.5	7 ± 0	36 ± 4

3.4.2 Temporal Variation of Methane, Ammonia, and Nitrous Oxide Observations at Dairy Farm

The relative contributions of CH_4 NH_3, and N_2O varied based on season. For example, spring and summer ΔNH_3 from corrals were relatively higher than ΔNH_3 from freestall barns. However, ΔNH_3 from freestall barns during autumn were relatively higher than corrals. Across all seasons, manure lagoons consistently had the highest ΔCH_4 relative to all other sources at the dairy farm (Figure 3.2). Freestall barns had relatively higher

ΔCH_4 than corrals. Silage had the highest ΔN_2O observations during autumn relative to other seasons and sources. Cropland ΔN_2O observations were only measured during the summer and autumn seasons. Cropland ΔN_2O was higher during the summer than during autumn measurements. Freestall barns and corrals had relatively higher ΔN_2O during the summer than during other seasons.

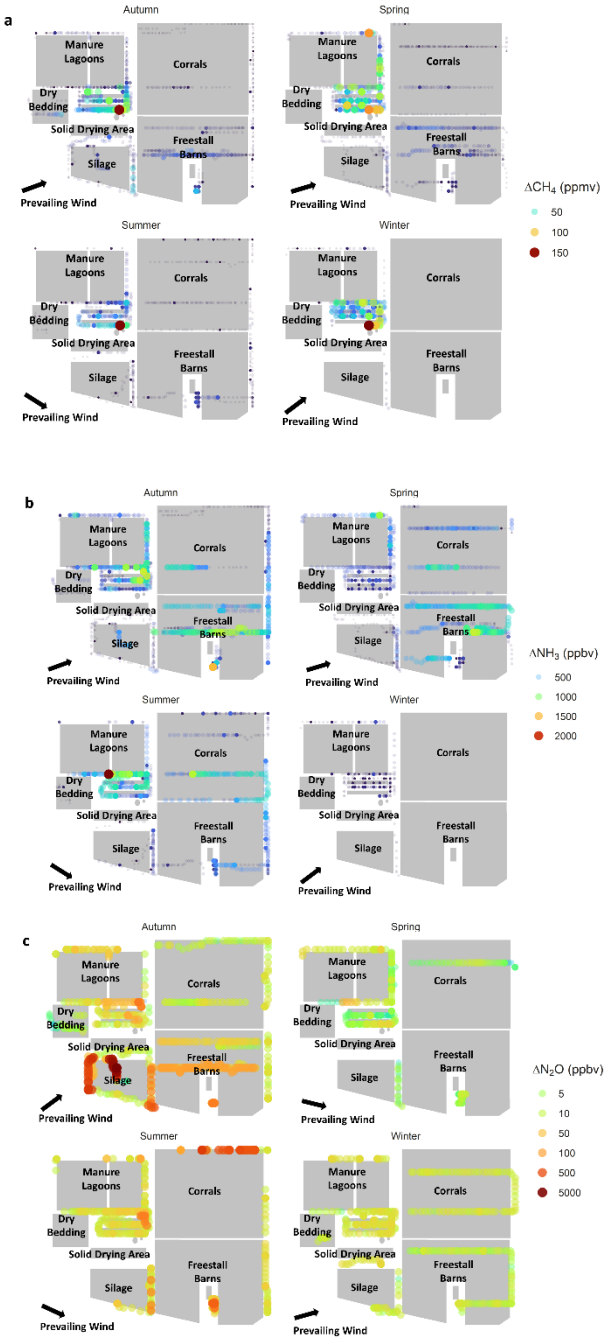

Figure 3.2. Mobile measurements of CH_4 (a), NH_3 (b), and N_2O (c) enhancements (5 s averages of 1 s data) at the primary dairy for each season. Note that cropland (not shown in schematic) surrounds the dairy farm.

3.4.3 Enhancement Ratios of Methane, Ammonia, and Nitrous Oxide from Dairy Source Areas

In general, source areas were characterized by distinct enhancement ratios (Table 3.4). On average, dry bedding piles had the highest ΔNH_3:ΔCH_4 (2.71 ± 0.85 ppbv/ppbv), followed by cropland (1.51 ± 0.41 ppbv/ppbv). Silage (0.65 ± 0.19 ppbv/ppbv), freestall barns, (0.58 ± 0.19 ppbv/ppbv), and corrals (0.48 ± 0.05 ppbv/ppbv) also had relatively high ΔNH_3: ΔCH_4. Manure lagoons (0.09 ± 0.01 ppbv/ppbv) and the solid drying area (0.00 ± 0.00 ppbv/ppbv) were characterized by negligible ΔNH_3:ΔCH_4. Cropland had the highest mean ΔN_2O:ΔCH_4 , with 1.65 ± 0.17 ppbv/ppbv. Silage had the next highest mean ΔN_2O:ΔCH_4, with 0.55 ± 0.09 ppbv/ppbv. Corrals (0.17 ± 0.03) and dry bedding piles (0.10 ± 0.03 ppbv/ppbv) also had relatively high mean ΔN_2O:ΔCH_4. Manure lagoons (0.05 ± 0.04 ppbv/ppbv), freestall barns (0.02 ± 0.00 ppbv/ppbv), and solid drying area piles (0.02 ± 0.00 ppbv/ppbv) had low ΔN_2O:ΔCH_4.

Table 3.4. Average Ammonia to Methane (ΔNH_3: ΔCH_4) and Nitrous Oxide to Methane (ΔN_2O:ΔCH_4) Enhancement Ratios from Each Source at the Dairy Farm. Standard Errors are Reported.

Source	ΔNH_3: ΔCH_4 (ppbv/ppbv)	ΔN_2O:ΔCH_4 (ppbv/ppbv)
Crops	1.51 ± 0.41	1.65 ± 0.17
Silage	0.65 ± 0.19	0.55 ± 0.09
Corrals	0.48 ± 0.05	0.17 ± 0.03
Freestall Barns	0.58 ± 0.19	0.02 ± 0.00
Dry Bedding	2.71 ± 0.85	0.10 ± 0.03
Manure Lagoons	0.09 ± 0.01	0.05 ± 0.04
Solid Drying Area	0.00 ± 0.00	0.02 ± 0.00

3.4.4 Seasonal Variation in Enhancement Ratios at Dairy Farm

Summer and autumn had the highest mean ΔNH_3:ΔCH_4 and ΔN_2O: ΔCH_4 (Table 3.5) from all sources at the dairy farm. The highest mean ΔNH_3:ΔCH_4 was observed in autumn, with 0.45 ± 0.10 ppbv/ppbv. Similarly, the highest mean ΔN_2O:ΔCH_4 was observed in autumn, with 0.30 ± 0.09 ppbv/ppbv. During the summer, the mean ΔNH_3:ΔCH_4 was 0.42 ± 0.09 ppbv/ppbv and the mean ΔN_2O:ΔCH_4 was 0.11 ± 0.01 ppbv/ppbv. Spring measurements had a low mean ΔNH_3:ΔCH_4 value of 0.05 ± 0.00 ppbv/ppbv and mean ΔN_2O:ΔCH_4 value of 0.00 ± 0.00 ppbv/ppbv. Winter measurements had the lowest ΔNH_3:ΔCH_4 value of 0.03 ± 0.00 ppbv/ppbv and ΔN_2O: ΔCH_4 of 0.04 ± 0.01 ppbv/ppbv.

Table 3.5. Air Temperature, Prevailing Wind Direction, Mean Wind Speed, and Mean Enhancement Ratios from All Sources at the Dairy Farm. Standard Deviation is Reported for Wind Speed and Standard Error is Reported for Enhancement Ratios.

Season	Air Temperature (ºC)	Wind Direction (º)	Wind Speed (m/s)	ΔNH_3:ΔCH_4 (ppbv/ppbv)	ΔN_2O: ΔCH_4 (ppbv/ppbv)
Winter	8 – 17	W	3 ± 1	0.03 ± 0.00	0.04 ± 0.01
Spring	18 – 25	W	2 ± 1	0.05 ± 0.00	0.00 ± 0.00
Summer	22 – 39	W	3 ± 2	0.42 ± 0.09	0.11 ± 0.01
Autumn	15 – 28	SW	2 ± 1	0.45 ± 0.10	0.30 ± 0.09

Enhancement ratios for individual sources at the dairy farm also had seasonal variability (Figure 3.3, Table 3.6). The highest ΔNH_3:ΔCH_4 maxima were observed during the summer and autumn seasons for freestall barns, corrals, manure lagoons, and silage. Significantly higher ΔNH_3:ΔCH_4 enhancement ratios were observed for crops in autumn

compared to summer measurements (Tukey test, P = 0.0001). Dry bedding, in contrast, had relatively high ΔNH_3:ΔCH_4 values in the summer compared to autumn measurements (P = 0.05). The solid drying area was characterized by the lowest ΔNH_3:ΔCH_4 values across seasons. Higher ΔNH_3:ΔCH_4 values for the solid drying area were observed in the winter and spring relative to summer and autumn. Corrals had significantly higher ΔNH_3:ΔCH_4 values during autumn measurements relative to spring (P < 0.001) and summer (P < 0.05). Manure lagoons had significantly higher ΔNH_3:ΔCH_4 during the autumn compared to winter, spring, and summer seasons. (P < 0.0001).

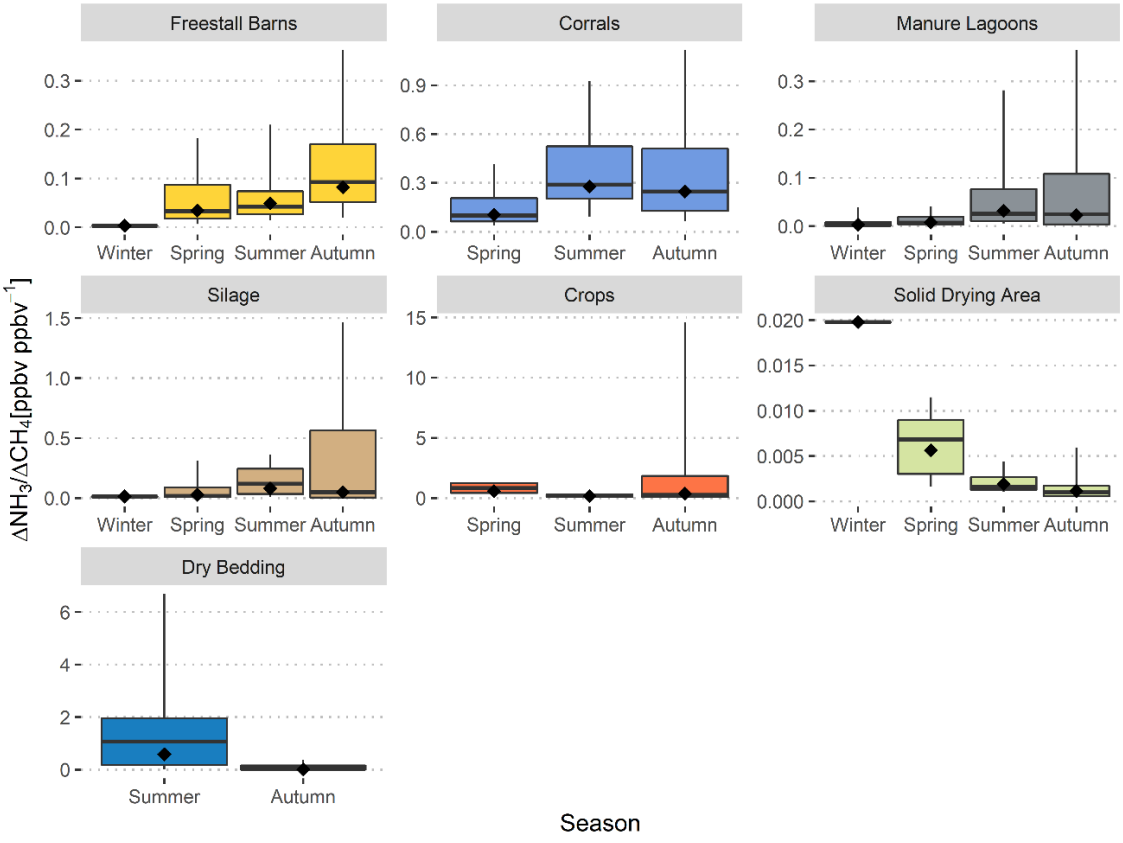

Figure 3.3 Seasonal ammonia to methane enhancement ratios (ΔNH_3: ΔCH_4) for each emission source at the primary dairy farm.

$\Delta N_2O:\Delta CH_4$ maxima were highest during the summer for freestall barns, corrals, and crops (Figure 3.4). Freestall barns had significantly higher $\Delta N_2O:\Delta CH_4$ values during the summer than during autumn (Tukey test, $P < 0.001$), spring ($P < 0.01$), and winter ($P < 0.001$) seasons (Table 3.6). In contrast, $\Delta N_2O:\Delta CH_4$ enhancement ratios were higher during the autumn for manure lagoons and silage. Manure lagoons were relatively higher in autumn compared to winter ($P = 0.01$) and summer ($P < 0.0001$). The solid drying area had a higher $\Delta N_2O:\Delta CH_4$ value in winter relative to autumn measurements ($P < 0.0001$). Similarly, dry bedding had a higher $\Delta N_2O:\Delta CH_4$ value in winter compared to autumn measurements ($P < 0.0001$).

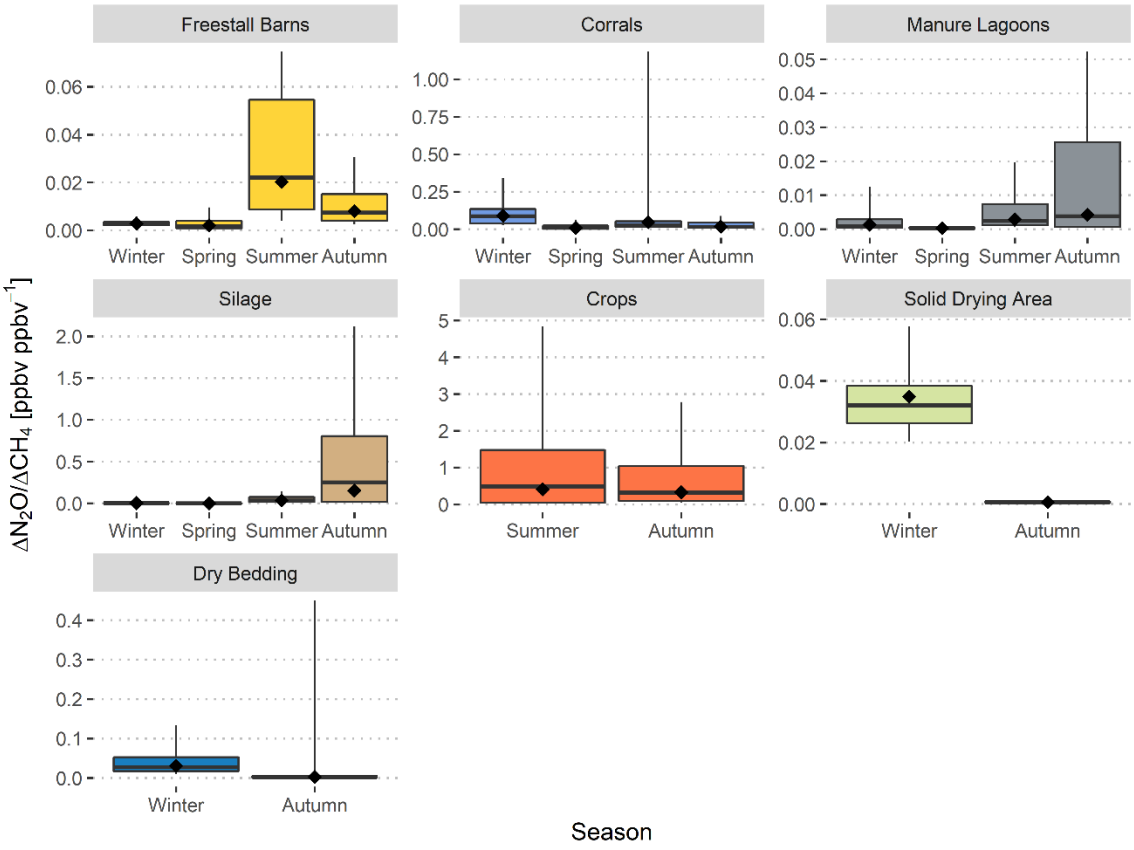

Figure 3.4. Seasonal nitrous oxide to methane enhancement ratios (ΔN_2O: ΔCH_4) for each emission source at the primary dairy farm.

Table 3.6. Seasonal Enhancement Ratios for Each Source at the Dairy Farm in the San Joaquin Valley. The Geometric Means and Standard Errors are Reported.

	Winter		Spring		Summer		Autumn	
Source	ΔNH_3:ΔCH_4	ΔN_2O:ΔCH_4	ΔNH_3:ΔCH_4	ΔN_2O:ΔCH_4	ΔNH_3:ΔCH_4	ΔN_2O:ΔCH_4	ΔNH_3:ΔCH_4	ΔN_2O:ΔCH_4
Freestall Barns	0.00 ± 0.00	0.00 ± 0.00	0.03 ± 0.03	0.00 ± 0.00	0.05 ± 0.05	0.02 ± 0.02	0.08 ± 0.08	0.01 ± 0.01
Corrals	n.m.	0.09 ± 0.09	0.10 ± 0.10	0.01 ± 0.01	0.28 ± 0.28	0.05 ± 0.05	0.25 ± 0.25	0.02 ± 0.02
Manure Lagoons	0.00 ± 0.00	0.00 ± 0.00	0.01 ± 0.01	0.00 ± 0.00	0.03 ± 0.03	0.00 ± 0.00	0.02 ± 0.02	0.00 ± 0.00
Silage	0.01 ± 0.01	0.00 ± 0.00	0.03 ± 0.03	0.00 ± 0.00	0.08 ± 0.08	0.04 ± 0.04	0.05 ± 0.05	0.15 ± 0.15
Crops	n.m.	n.m.	0.57 ± 0.57	n.m.	0.15 ± 0.15	0.41 ± 0.41	0.37 ± 0.37	0.33 ± 0.33
Solid Drying Area	0.02 ± 0.02	0.03 ± 0.03	0.01 ± 0.01	n.m.	0.00 ± 0.00	n.m.	0.00 ± 0.00	0.00 ± 0.00
Dry Bedding	n.m.	0.03 ± 0.03	n.m.	n.m.	0.59 ± 0.59	n.m.	0.01 ± 0.01	0.00 ± 0.00

[a] n.m. denotes sources that were not measured during that season.

3.5 Discussion & Conclusion

In this study, we demonstrated how enhancement ratios (ΔNH_3:ΔCH_4 and ΔN_2O:ΔCH_4) can be used as source signatures to characterize distinct areas of emissions from dairy farms in the SJV. Emission trends of NH_3,N_2O, and CH_4 from the dairy farm varied across space and time. The mean ΔNH_3:ΔCH_4 from freestall barns and corrals observed across all seasons is 0.58 ± 0.19 ppbv ppbv^{-1} and 0.48 ± 0.05 ppbv ppbv^{-1}, respectively, which were not statistically different (Tukey test, P=1). In comparison, the mean ΔNH_3:ΔCH_4 for manure lagoons is 0.09 ± 0.01 ppbv ppbv^{-1} , which was statistically different than the enhancement ratio of freestall barns (P < 0.001), silage (P = 0.05), cropland (P < 0.001), and dry bedding (P < 0.001). The mean enhancement of dry bedding is 2.71 ± 0.85 ppbv ppbv^{-1}, which is statistically different than the solid drying area (P < 0.01), corrals (P < 0.01), freestall barns (P = 0.01), and silage (P = 0.02) . The mean enhancement ratios between the solid drying area were also statistically different than cropland (P = 0.03). The ΔN_2O:ΔCH_4 trends also showed distinct signatures between livestock housing, manure management, cropland, and silage, with the highest enhancement ratios observed from cropland (1.65 ± 0.17 ppbv ppbv^{-1}). Cropland has a mean enhancement ratio that is statistically different than freestall barns (P < 0.0001), manure lagoons (P < 0.0001), corrals (P < 0.0001), solid drying area (P < 0.0001), silage (P < 0.0001), and dry bedding (P < 0.0001). Silage was also characterized by a high mean ΔN_2O:ΔCH_4 of 0.55 ± 0.09 ppbv ppbv^{-1}, which is statistically different than manure lagoons (P < 0.0001), freestall barns (P < 0.0001), and corrals (P = 0.05). Corrals (0.17 ±

0.03 ppbv ppbv^{-1}) and dry bedding piles (0.10 ± 0.03 ppbv ppbv^{-1}) also had relatively high mean ΔN_2O:ΔCH_4.

The highest ΔNH_3:ΔCH_4 maxima were observed during the summer and autumn seasons, when air temperatures were high, for freestall barns, corrals, manure lagoons, and silage. In animal housing, NH_3 emissions are a byproduct of urea hydrolysis from the decomposition of urine and feces. In general, NH_3 volatilization increases with higher concentrations of NH_4^+/NH_3, substrate temperature, pH, wind speed and turbulence (Olesen & Sommer, 1993; Teye & Hautala, 2008). When temperatures are high, this dairy farm increases the ventilation and moisture of freestall barns with ceiling fans and cools milking cows with periodic cooling water mist. Increased wind speed and ventilation rates tend to decrease CH_4 emissions in animal housing (Joo et al., 2015). Increased turbulence and moisture conditions during the summer months potentially promoted more NH_3 emissions in the freestall barns and decreased CH_4 emissions.

Methane emissions from animal housing are impacted by weather conditions and management practices. The quantity and quality of manure deposited onto the housing floor affects whether methanogenesis is promoted. In general, an influx and accumulation of fresh manure to a corral encourages methanogenesis and also enhances N_2O and NH_3 emissions with concentrated urine patches (Borhan et al., 2011; Leytem et al., 2011). In several studies, CH_4 uptake occurred in corrals, specifically in late summer when soil was dry and in winter when soil was frozen or cold, thereby inhibiting methanogenesis (Owen & Silver, 2015). On the barn floor, aerobic and anaerobic conditions may also lead to

relatively lower N_2O emissions (Eckard et al., 2003; Van Middelaar et al., 2013)**.** In addition**,** CH_4 emissions tend to be negatively correlated with heat stress (i.e., temperature and relative humidity) in naturally ventilated dairy barns because of decreased animal activity (Ngwa M. Ngwabie et al., 2014; Saha et al., 2014; Joo et al., 2015).

ΔN_2O:ΔCH_4 maxima were also highest during the summer for freestall barns, corrals, and crops. This may be explained by the higher air temperatures in animal housing areas and irrigation of croplands using the manure wastewater from the holding pond. Generally, the relative abundance of available N, whether as NH_4^+ or NO_3^-, soil oxidation-reduction potential, soil temperature, moisture, oxygen availability, pH, microbial communities, and degradable carbon sources impact N_2O emissions. Manure application to cropland promotes N_2O and NH_3 losses (Hristov et al., 2011; J. Li et al., 2015). Direct N_2O losses are generated from nitrification and denitrification reactions in the soil. NH_3 volatilization is an indirect source of N_2O when NH_3 is volatilized from manure, for example, and re-deposited onto soil, where it is converted into N_2O. Methane losses from manure application are relatively low because of carbon uptake by the soils under aerobic conditions (Goulding et al., 1996). Higher N_2O emissions generally occur in warmer and moist soils, which enhance denitrification and nitrification (Owen & Silver, 2015). Thus, during the summer, higher temperatures and moist conditions in the animal housing areas increased CH_4 emissions and, to an even larger extent, N_2O emissions. We also observed higher N_2O losses from manure effluent application during the summer, with relatively low CH_4 emissions.

Manure lagoons were characterized by considerably higher ΔN_2O:ΔCH_4 in autumn compared to winter and summer measurements. Aerobic conditions at the inlets of manure lagoons can lead to denitrification reactions performed by facultative anaerobes (Owen & Silver, 2015). Summer measurements are likely to have higher CH_4 emissions relative to N_2O emissions. Increasing air temperatures and wind speed commonly increase CH_4 emissions since they affect microbial activity, diffusion, and convection of liquid manure storage (Sommer et al., 2007; Leytem et al., 2017a). N_2O emissions from denitrification are also impacted by similar factors, including warm temperatures, labile C, and anaerobic conditions (Kebreab et al., 2006; Broucek, 2016). Other factors that influence N_2O emissions from manure include redox potential, pH, and substrate concentration. Winter measurements were conducted a few days after a rainfall event, which may have increased CH_4 emissions from the manure lagoons relative to N_2O emissions. Methane emissions may increase after a rainfall event, given that it agitates the surfaces and increases ebullition rates of CH_4 from super-saturated lagoon waters (Kaharabata & Schuepp, 1998; Minato et al., 2013; Baldé et al., 2016; A.B. Leytem et al., 2017b; Arndt et al., 2018; Kupper et al., 2020). Our study shows that manure lagoons had relatively higher CH_4 emissions than N_2O emissions during the summer, given warmer air temperatures, and winter months, following agitation of manure surface from rainfall events.

The solid drying area and dry bedding of manure had higher ΔN_2O:ΔCH_4 values in winter relative to autumn measurements. Winter measurements were conducted only a few days after a rainfall event, which may have produced higher N_2O emissions relative to CH_4 emissions in the dry manure storage piles. In contrast, dry bedding had relatively high

ΔNH_3:ΔCH_4 values in the summer compared to autumn measurements. Higher air temperatures during the summer may have volatilized more NH_3 relative to CH_4 emissions. The solid drying area had the lowest ΔNH_3:ΔCH_4 values among all sources across seasons. Higher ΔNH_3:ΔCH_4 values for the solid drying area were observed in the winter and spring relative to summer and autumn. Solid manure storage is heterogenous in aerobic and anaerobic composition depending on manure management practices. Nitrous oxide emissions from solid manure storage are positively related to total N content since it enhances nitrification and denitrification (He et al., 2001). N_2O production is also positively related to the total carbon content because denitrifiers strongly rely on carbohydrates for energy (Burford & Bremner, 1975; El Kader et al., 2007). The heterogeneity of solid manure storage also affects the relative abundance of methanogens and methanotrophs in the substrate (Sonoki et al., 2013; S. Li et al., 2017). Methane fluxes from solid manure systems are positively correlated with moisture, C/N ratio, NH_4^+-N, and total organic carbon (S. Li et al., 2017; Ba et al., 2020). High CH_4 and NH_3 emissions occur primarily at the early stage of decomposition of carbon and nitrogen sources from fresh manure (Martins & Dewes, 1992; Parkinson et al., 2004). Methane fluxes increase with higher NH_4^+ since it inhibits CH_4 oxidation via production of toxic hydroxylamine and nitrate from ammonium oxidation or competition for methane monooxygenase. Static solid manure piles are predominantly aerobic, but may form anaerobic areas if the proper moisture, density, and porosity is met. The anaerobic areas in the piles enhance CH_4 emissions (Pardo et al., 2015; Fournel et al., 2019). In our study, N_2O:CH_4 enhancement ratios from dry bedding were primarily influenced by rainfall events that enhanced N_2O

emissions during the winter measurements. In addition, NH_3:CH_4 enhancement ratios from dry bedding were primarily influenced by higher air temperatures that increased NH_3 emissions during the summer.

This study's enhancement ratios were consistent with previous relevant studies (Table 3.7) (Bjorneberg et al., 2009; Ngwabie et al., 2009; April B. Leytem et al., 2011, 2013; Miller et al., 2015; Eilerman et al., 2016). Our summer and autumn NH_3:CH_4 and N_2O:CH_4 enhancement ratios were higher than previously reported in literature and state inventories. Our winter NH_3:CH_4 enhancement ratios were lower compared to another California study conducted during the winter (Miller et al., 2015). This difference may be explained by the rainfall events presiding our measurements, which enhanced CH_4 emissions more than NH_3 emissions. Our work underscores the importance of seasonal measurements as enhancement ratios are greatly influenced by changes in environmental factors, such as temperature, rainfall, and wind speed.

Enhancement ratios may be a useful tool to characterize and identify emission sources from dairy farms. As shown in this study, animal housing (e.g., freestall barns, corrals), wet manure management (e.g., manure lagoons), dry manure management (e.g., dry bedding), silage piles, and cropland had distinct enhancement ratios. This tool could be particularly useful for source attribution of an emission plume in a region with multiple sources of CH_4, NH_3, and N_2O emissions. Seasonal information about enhancement ratios is also important as shown by the seasonal variability in enhancement ratios for different sources of emissions. Dairy management practices (e.g., ventilation of animal housing

irrigation of cropland using manure wastewater during the summer) and physicochemical and meteorological factors (e.g., air temperature, rainfall) greatly influenced the relative contributions of CH_4, NH_3, and N_2O emissions.

Table 3.7. Comparison of Enhancement Ratios From Relevant Published Studies.

Study	NH_3:CH_4 (mol/mol)	N_2O:CH_4 (mol/mol)	Dairy Farm Type/Location/Season
This study	0.03 ± 0.00	0.04 ± 0.01	Winter
	0.05 ± 0.00	0.00 ± 0.00	Spring
	0.42 ± 0.09	0.11 ± 0.01	Summer
	0.45 ± 0.10	0.30 ± 0.09	Autumn
Miller 2015	0.15 ± 0.03	---	California dairies (winter)
State inventories	0.36	0.006	EIA 2017 (livestock waste), CARB 2020 (enteric fermentation and manure management)
Eilerman 2016	0.17 (+0.13/–0.08)	0.006 (+0.005/–0.003)	Colorado dairy, beef, and sheep CAFOs (winter, spring, summer, autumn)
	0.14 (+0.13/–0.07)	0.004 (+0.002/–0.001)	Dairy (site 3) (winter, spring, summer, fall)
	0.17 (+0.08/–0.05)	0.006 (+0.002/–0.002)	Dairy (site 4) (winter, spring, summer, autumn)
Leytem 2011	0.1	0.005	Idaho open-lot dairy (site total) (winter, spring, summer, autumn)
	0.24	0.007	Open lots (winter, spring, summer, autumn)
	0.018	0.002	Wastewater ponds (spring, summer, autumn)
	0.11	0.002	Compost facility (spring, summer, autumn)
Leytem 2013	0.25	---	Idaho freestall dairy (site total) (winter, spring, summer, autumn)
	0.18	0.018	Open freestall (winter, spring, summer, autumn)
	0.29	0.003	Wastewater ponds (winter, spring, summer, autumn)
Ngwabie 2009	0.08	---	Sweden, inside a naturally ventilated dairy barn (winter, spring)
Bjorneberg 2009	0.45	---	Idaho dairy (winter, spring, summer, autumn)

3.6 References

Amini, S., Kuwayama, T., Gong, L., Falk, M., Chen, Y., Mitloehner, Q., Weller, S., Mitloehner, F. M., Patteson, D., Conley, S. A., Scheehle, E., & FitzGibbon, M. (2022). Evaluating California dairy methane emission factors using short-term ground-level and airborne measurements. *Atmospheric Environment: X*, *14*(November 2021), 100171. https://doi.org/10.1016/j.aeaoa.2022.100171

Arndt, C., Leytem, A. B., Hristov, A. N., Zavala-Araiza, D., Cativiela, J. P., Conley, S., Daube, C., Faloona, I., & Herndon, S. C. (2018). Short-term methane emissions from 2 dairy farms in California estimated by different measurement techniques and US Environmental Protection Agency inventory methodology: A case study. *Journal of Dairy Science*, *101*(12), 11461–11479. https://doi.org/10.3168/jds.2017-13881

Ba, S., Qu, Q., Zhang, K., & Groot, J. C. J. (2020). Meta-analysis of greenhouse gas and ammonia emissions from dairy manure composting. *Biosystems Engineering*, *193*, 126–137. https://doi.org/10.1016/j.biosystemseng.2020.02.015

Baldé, H., VanderZaag, A. C., Burtt, S., Evans, L., Wagner-Riddle, C., Desjardins, R. L., & MacDonald, J. D. (2016). Measured versus modeled methane emissions from separated liquid dairy manure show large model underestimates. *Agriculture, Ecosystems and Environment*, *230*, 261–270. https://doi.org/10.1016/j.agee.2016.06.016

Behera, S. N., Sharma, M., Aneja, V. P., & Balasubramanian, R. (2013). Ammonia in the atmosphere: A review on emission sources, atmospheric chemistry and deposition on terrestrial bodies. In *Environmental Science and Pollution Research* (Vol. 20, Issue 11, pp. 8092–8131). https://doi.org/10.1007/s11356-013-2051-9

Bjorneberg, D. L., Leytem, A. B., Westermann, D. T., Griffiths, P. R., Shao, L., & Pollard, M. J. (2009). Measurement of atmospheric ammonia, methane, and nitrous oxide at a concentrated dairy production facility in southern idaho using open-path FTIR spectrometry. *Transactions of the ASABE*, *52*(5), 1749–1756.

Borhan, M. S., Capareda, S. C., Mukhtar, S., Faulkner, W. B., McGee, R., & Parnell, C. B. (2011a). Greenhouse Gas Emissions from Ground Level Area Sources in Dairy and Cattle Feedyard Operations. *Atmosphere*, *2*(3), 303–329. https://doi.org/10.3390/atmos2030303

Borhan, M. S., Capareda, S., Mukhtar, S., Faulkner, W. B., McGee, R., & Parnell, C. B. (2011b). Determining Seasonal Greenhouse Gas Emissions from Ground-Level Area Sources in a Dairy Operation in Central Texas. *Journal of the Air & Waste Management Association*, *61*(7), 786–795. https://doi.org/10.3155/1047-3289.61.7.786

Broucek, J. (2016). Nitrous Oxide Production from Cattle and Swine Manure. *Journal of Animal Behaviour and Biometeorology*, *5*(1), 13–19. https://doi.org/10.14269/2318-1265/jabb.v5n1p13-19

Burford, J. R., & Bremner, J. M. (1975). Relationships between the denitrification capacities of soils and total, water-soluble and readily decomposable soil organic matter. *Soil Biology and Biochemistry*, *7*(6), 389–394. https://doi.org/10.1016/0038-0717(75)90055-3

Carranza, V., Biggs, B., Meyer, D., Townsend-Small, A., Thiruvenkatachari, R. R., Venkatram, A., Fischer, M. L., & Hopkins, F. M. (2022). Isotopic Signatures of Methane Emissions From Dairy Farms in California's San Joaquin Valley. *Journal of Geophysical Research: Biogeosciences*, *127*(1), 1–15. https://doi.org/10.1029/2021JG006675

Cassel, T., Ashbaugh, L., Flocchini, R., & Meyer, D. (2005). Ammonia emission factors for open-lot dairies: Direct measurements and estimation by nitrogen intake. *Journal of the Air and Waste Management Association*, *55*(6), 826–833. https://doi.org/10.1080/10473289.2005.10464660

Cui, Y. Y., Brioude, J., Angevine, W. M., Peischl, J., McKeen, S. A., Kim, S. W., Andrew Neuman, J., Henze, D. K., Bousserez, N., Fischer, M. L., Jeong, S., Michelsen, H. A., Bambha, R. P., Liu, Z., Santoni, G. W., Daube, B. C., Kort, E. A., Frost, G. J., Ryerson, T. B., … Trainer, M. (2017). Top-down estimate of methane emissions in California using a mesoscale inverse modeling technique: The San Joaquin Valley. *Journal of Geophysical Research*, *122*(6), 3686–3699. https://doi.org/10.1002/2016JD026398

Eckard, R. J., Chen, D., White, R. E., & Chapman, D. F. (2003). Gaseous nitrogen loss from temperate perennial grass and clover dairy pastures in south-eastern Australia. *Australian Journal of Agricultural Research*, *54*(6), 561–570. https://doi.org/10.1071/AR02100

Eilerman, S. J., Peischl, J., Neuman, J. A., Ryerson, T. B., Aikin, K. C., Holloway, M. W., Zondlo, M. A., Golston, L. M., Pan, D., Floerchinger, C., & Herndon, S. (2016). Characterization of Ammonia, Methane, and Nitrous Oxide Emissions from Concentrated Animal Feeding Operations in Northeastern Colorado. *Environmental Science and Technology*, *50*(20), 10885–10893. https://doi.org/10.1021/acs.est.6b02851

El Kader, N. A., Robin, P., Paillat, J. M., & Leterme, P. (2007). Turning, compacting and the addition of water as factors affecting gaseous emissions in farm manure composting. *Bioresource Technology*, *98*(14), 2619–2628. https://doi.org/10.1016/j.biortech.2006.07.035

Fournel, S., Godbout, S., Ruel, P., Fortin, A., Duquette-Lozeau, K., Létourneau, V., Généreux, M., Lemieux, J., Potvin, D., Côté, C., Duchaine, C., & Pellerin, D. (2019). Production of recycled manure solids for use as bedding in Canadian dairy farms: II. Composting methods. *Journal of Dairy Science*, *102*(2), 1847–1865. https://doi.org/10.3168/jds.2018-14967

Gentner, D. R., Ford, T. B., Guha, A., Boulanger, K., Brioude, J., Angevine, W. M., De Gouw, J. A., Warneke, C., Gilman, J. B., Ryerson, T. B., Peischl, J., Meinardi, S., Blake, D. R., Atlas, E., Lonneman, W. A., Kleindienst, T. E., Beaver, M. R., St. Clair, J. M., Wennberg, P. O., … Goldstein, A. H. (2014). Emissions of organic carbon and methane from petroleum and dairy operations in California's San Joaquin Valley. *Atmospheric Chemistry and Physics*, *14*(10), 4955–4978. https://doi.org/10.5194/acp-14-4955-2014

Goulding, K. W. T., Willison, T. W., Webster, C. P., & Powlson, D. S. (1996). Methane fluxes in aerobic soils. *Environmental Monitoring and Assessment*, *42*(1–2), 175–187. https://doi.org/10.1007/BF00394049

Guha, A., Gentner, D. R., Weber, R. J., Provencal, R., & Goldstein, A. H. (2015). Source apportionment of methane and nitrous oxide in California's San Joaquin Valley at CalNex 2010 via positive matrix factorization. *Atmospheric Chemistry and Physics*, *15*(20), 12043–12063. https://doi.org/10.5194/acp-15-12043-2015

He, Y., Inamori, Y., Mizuochi, M., Kong, H., Iwami, N., & Sun, T. (2001). Nitrous oxide emissions from aerated composting of organic waste. *Environmental Science and Technology*, *35*(11), 2347–2351. https://doi.org/10.1021/es0011616

Heald, C. L., Collett, J. L., Lee, T., Benedict, K. B., Schwandner, F. M., Li, Y., Clarisse, L., Hurtmans, D. R., Van Damme, M., Clerbaux, C., Coheur, P. F., Philip, S., Martin, R. V., & Pye, H. O. T. (2012). Atmospheric ammonia and particulate inorganic nitrogen over the United States. *Atmospheric Chemistry and Physics*, *12*(21), 10295–10312. https://doi.org/10.5194/acp-12-10295-2012

Herrera, S. A., Diskin, G. S., Harward, C., Sachse, G., De Wekker, S. F. J., Yang, M., Choi, Y., Wisthaler, A., Mallia, D. V., & Pusede, S. E. (2021). Wintertime Nitrous Oxide Emissions in the San Joaquin Valley of California Estimated from Aircraft Observations. *Environmental Science & Technology*, *55*(8), 4462–4473. https://doi.org/10.1021/acs.est.0c08418

Hristov, A. N., Hanigan, M., Cole, A., Todd, R., McAllister, T. A., Ndegwa, P. M., & Rotz, A. (2011). Review: Ammonia emissions from dairy farms and beef feedlots. In *Canadian Journal of Animal Science* (Vol. 91, Issue 1, pp. 1–35). Agricultural Institute of Canada. https://doi.org/10.4141/CJAS10034

IPCC. (2013). Carbon and Other Biogeochemical Cycles. In: Climate Change 2013: The Physical Science Basis. Contribution of Working Group I to the Fifth Assessment Report of the Intergovernmental Panel on Climate Change. *Cambridge University Press*, *9781107057*, 465–570. https://doi.org/10.1017/CBO9781107415324.015

Jeong, S., Hsu, Y. K., Andrews, A. E., Bianco, L., Vaca, P., Wilczak, J. M., & Fischer, M. L. (2013). A multitower measurement network estimate of California's methane emissions. *Journal of Geophysical Research Atmospheres*, *118*(19), 11,339-11,351. https://doi.org/10.1002/jgrd.50854

Jeong, S., Newman, S., Zhang, J., Andrews, A. E., Bianco, L., Bagley, J., Cui, X., Graven, H., Kim, J., Salameh, P., LaFranchi, B. W., Priest, C., Campos-Pineda, M., Novakovskaia, E., Sloop, C. D., Michelsen, H. A., Bambha, R. P., Weiss, R. F., Keeling, R., & Fischer, M. L. (2016). Estimating methane emissions in California's urban and rural regions using multitower observations. *Journal of Geophysical Research: Atmospheres*, *121*(21), 13,031-13,049. https://doi.org/10.1002/2016JD025404

Jeong, S., Newman, S., Zhang, J., Andrews, A. E., Bianco, L., Dlugokencky, E., Bagley, J., Cui, X., Priest, C., Campos-Pineda, M., & Fischer, M. L. (2018). Inverse Estimation of an Annual Cycle of California's Nitrous Oxide Emissions. *Journal of Geophysical Research: Atmospheres*, *123*(9), 4758–4771. https://doi.org/10.1029/2017JD028166

Jeong, S., Newman, S., Zhang, J., Andrews, A. E., Dlugokencky, E., Bagley, J., Cui, X., & Priest, C. (2020). *Inverse Estimation of an Annual Cycle of California ' s Nitrous Oxide Emissions*. *2030*, 4758–4771. https://doi.org/10.1029/2017JD028166

Jeong, S., Zhao, C., Andrews, A. E., Dlugokencky, E. J., Sweeney, C., Bianco, L., Wilczak, J. M., & Fischer, M. L. (2012). Seasonal variations in N2O emissions from central California. *Geophysical Research Letters*, *39*(16), n/a-n/a. https://doi.org/10.1029/2012GL052307

Joo, H. S., Ndegwa, P. M., Heber, A. J., Ni, J. Q., Bogan, B. W., Ramirez-Dorronsoro, J. C., & Cortus, E. (2015). Greenhouse gas emissions from naturally ventilated freestall dairy barns. *Atmospheric Environment*, *102*, 384–392. https://doi.org/10.1016/j.atmosenv.2014.11.067

Kaffka, S., & Barzee, T. (2016). *Evaluation of Dairy Manure Management Practices for Greenhouse Gas Emissions Mitigation in California*.

Kaharabata, S. K., & Schuepp, P. H. (1998). Methane emissions from aboveground open manure slurry tanks oxygen demand z 218. *Global Biogeochemical Cycles*, *12*(3), 545–554.

Kebreab, E., Clark, K., Wagner-Riddle, C., & France, J. (2006). Methane and nitrous oxide emissions from Canadian animal agriculture: A review. *Canadian Journal of Animal Science*, *86*(2), 135–157. https://doi.org/10.4141/A05-010

Kelly, J. T., Baker, K. R., Nowak, J. B., Murphy, J. G., Markovic, M. Z., VandenBoer, T. C., Ellis, R. A., Neuman, J. A., Weber, R. J., Roberts, J. M., Veres, P. R., de Gouw, J. A., Beaver, M. R., Newman, S., & Misenis, C. (2014). Fine-scale simulation of ammonium and nitrate over the South Coast Air Basin and San Joaquin Valley of California during CalNex-2010. *Journal of Geophysical Research: Atmospheres*, *119*(6), 3600–3614. https://doi.org/10.1002/2013JD021290

Kozloski, G. V., Senger, C. C. D., Perottoni, J., & Sanchez, L. M. B. (2006). Evaluation of two methods for ammonia extraction and analysis in silage samples. *Animal Feed Science and Technology*, *127*(3–4), 336–342. https://doi.org/10.1016/j.anifeedsci.2005.08.014

Kupper, T., Häni, C., Neftel, A., Kincaid, C., Bühler, M., Amon, B., & VanderZaag, A. (2020). Ammonia and greenhouse gas emissions from slurry storage - A review. *Agriculture, Ecosystems & Environment*, *300*, 106963. https://doi.org/10.1016/j.agee.2020.106963

Laubach, J., Heubeck, S., Pratt, C., Woodward, K., Guieysse, B., van der Weerden, T., Chung, M., Shilton, A., & Craggs, R. (2015). Review of greenhouse gas emissions from the storage and land application of farm dairy effluent. *New Zealand Journal of Agricultural Research*, *58*(2), 203–233. https://doi.org/10.1080/00288233.2015.1011284

Leytem, A.B., Bjorneberg, D. L., Koehn, A. C., Moraes, L. E., Kebreab, E., & Dungan, R. S. (2017a). Methane emissions from dairy lagoons in the western United States. *Journal of Dairy Science*, *100*(8), 6785–6803. https://doi.org/10.3168/jds.2017-12777

Leytem, A.B., Bjorneberg, D. L., Koehn, A. C., Moraes, L. E., Kebreab, E., & Dungan, R. S. (2017b). Methane emissions from dairy lagoons in the western United States. *Journal of Dairy Science*, *100*(8), 6785–6803. https://doi.org/10.3168/jds.2017-12777

Leytem, April B., Dungan, R. S., Bjorneberg, D. L., & Koehn, A. C. (2011). Emissions of Ammonia, Methane, Carbon Dioxide, and Nitrous Oxide from Dairy Cattle Housing and Manure Management Systems. *Journal of Environmental Quality*, *40*(5), 1383–1394. https://doi.org/10.2134/jeq2009.0515

Leytem, April B., Dungan, R. S., Bjorneberg, D. L., & Koehn, A. C. (2013). Greenhouse Gas and Ammonia Emissions from an Open-Freestall Dairy in Southern Idaho. *Journal of Environmental Quality*, *42*(1), 10–20. https://doi.org/10.2134/jeq2012.0106

Leytem, April B, Dungan, R. S., Bjorneberg, D. L., & Koehn, A. C. (2011). Emissions of Ammonia, Methane, Carbon Dioxide, and Nitrous Oxide from Dairy Cattle Housing and Manure Management Systems. *Journal of Environmental Quality*, *40*(5), 1383–1394. https://doi.org/10.2134/jeq2009.0515

Li, J., Luo, J., Shi, Y., Houlbrooke, D., Wang, L., Lindsey, S., & Li, Y. (2015). Nitrogen gaseous emissions from farm effluent application to pastures and mitigation measures to reduce the emissions: a review. *New Zealand Journal of Agricultural Research*, *58*(3), 339–353. https://doi.org/10.1080/00288233.2015.1028651

Li, S., Song, L., Gao, X., Jin, Y., Liu, S., Shen, Q., & Zou, J. (2017). Microbial Abundances Predict Methane and Nitrous Oxide Fluxes from a Windrow Composting System. *Frontiers in Microbiology*, *8*(MAR). https://doi.org/10.3389/fmicb.2017.00409

Martins, O., & Dewes, T. (1992). Loss of nitrogenous compounds during composting of animal wastes. *Bioresource Technology*, *42*(2), 103–111. https://doi.org/10.1016/0960-8524(92)90068-9

Miller, D. J., Sun, K., Tao, L., Pan, D., Zondlo, M. A., Nowak, J. B., Liu, Z., Diskin, G., Sachse, G., Beyersdorf, A., Ferrare, R., & Scarino, A. J. (2015). Ammonia and methane dairy emission plumes in the San Joaquin Valley of California from individual feedlot to regional scales. *Journal of Geophysical Research: Atmospheres*, *120*(18), 9718–9738. https://doi.org/10.1002/2015JD023241

Minato, K., Kouda, Y., Yamakawa, M., Hara, S., Tamura, T., & Osada, T. (2013). Determination of GHG and ammonia emissions from stored dairy cattle slurry by using a floating dynamic chamber. *Animal Science Journal*, *84*(2), 165–177. https://doi.org/10.1111/j.1740-0929.2012.01053.x

Nevison, C., Andrews, A., Thoning, K., Dlugokencky, E., Sweeney, C., Miller, S., Saikawa, E., Benmergui, J., Fischer, M., Mountain, M., & Nehrkorn, T. (2018). Nitrous Oxide Emissions Estimated With the CarbonTracker-Lagrange North American Regional Inversion Framework. *Global Biogeochemical Cycles*, *32*(3), 463–485. https://doi.org/10.1002/2017GB005759

Ngwabie, N.M., Jeppsson, K.-H., Nimmermark, S., Swensson, C., & Gustafsson, G. (2009). Multi-location measurements of greenhouse gases and emission rates of methane and ammonia from a naturally-ventilated barn for dairy cows. *Biosystems Engineering*, *103*(1), 68–77. https://doi.org/10.1016/j.biosystemseng.2009.02.004

Ngwabie, Ngwa M., Vanderzaag, A., Jayasundara, S., & Wagner-Riddle, C. (2014). Measurements of emission factors from a naturally ventilated commercial barn for dairy cows in a cold climate. *Biosystems Engineering*, *127*, 103–114. https://doi.org/10.1016/j.biosystemseng.2014.08.016

Olesen, J. E., & Sommer, S. G. (1993). Modelling effects of wind speed and surface cover on ammonia volatilization from stored pig slurry. *Atmospheric Environment Part A, General Topics*, *27*(16), 2567–2574. https://doi.org/10.1016/0960-1686(93)90030-3

Owen, J. J., & Silver, W. L. (2015). Greenhouse gas emissions from dairy manure management: a review of field-based studies. *Global Change Biology*, *21*(2), 550–565. https://doi.org/10.1111/gcb.12687

Pardo, G., Moral, R., Aguilera, E., & Del Prado, A. (2015). Gaseous emissions from management of solid waste: a systematic review. *Global Change Biology*, *21*, 1313–1327. https://doi.org/10.1111/gcb.12806

Parkinson, R., Gibbs, P., Burchett, S., & Misselbrook, T. (2004). Effect of turning regime and seasonal weather conditions on nitrogen and phosphorus losses during aerobic composting of cattle manure. *Bioresource Technology*, *91*(2), 171–178. https://doi.org/10.1016/S0960-8524(03)00174-3

Saha, C. K., Ammon, C., Berg, W., Fiedler, M., Loebsin, C., Sanftleben, P., Brunsch, R., & Amon, T. (2014). Seasonal and diel variations of ammonia and methane emissions from a naturally ventilated dairy building and the associated factors influencing emissions. *Science of the Total Environment*, *468–469*, 53–62. https://doi.org/10.1016/j.scitotenv.2013.08.015

Schiferl, L. D., Heald, C. L., Nowak, J. B., Holloway, J. S., Neuman, J. A., Bahreini, R., Pollack, I. B., Ryerson, T. B., Wiedinmyer, C., & Murphy, J. G. (2014). An investigation of ammonia and inorganic particulate matter in california during the calnex campaign. *Journal of Geophysical Research*, *119*(4), 1883–1902. https://doi.org/10.1002/2013JD020765

Sommer, S. G., Petersen, S. O., Sørensen, P., Poulsen, H. D., & Møller, H. B. (2007). Methane and carbon dioxide emissions and nitrogen turnover during liquid manure storage. *Nutrient Cycling in Agroecosystems*, *78*(1), 27–36. https://doi.org/10.1007/s10705-006-9072-4

Sonoki, T., Furukawa, T., Jindo, K., Suto, K., Aoyama, M., & Sánchez-Monedero, M. Á. (2013). Influence of biochar addition on methane metabolism during thermophilic phase of composting. *Journal of Basic Microbiology*, *53*(7), 617–621. https://doi.org/10.1002/jobm.201200096

Teye, F. K., & Hautala, M. (2008). Adaptation of an ammonia volatilization model for a naturally ventilated dairy building. *Atmospheric Environment*, *42*(18), 4345–4354. https://doi.org/10.1016/j.atmosenv.2008.01.019

Thiruvenkatachari, R. R., Carranza, V., Ahangar, F., Marklein, A., Hopkins, F., & Venkatram, A. (2020). Uncertainty in using dispersion models to estimate methane emissions from manure lagoons in dairies. *Agricultural and Forest Meteorology*, *290*, 108011. https://doi.org/10.1016/j.agrformet.2020.108011

Trousdell, J. F., Conley, S. A., Post, A., & Faloona, I. C. (2016). Observing entrainment mixing, photochemical ozone production, and regional methane emissions by aircraft using a simple mixed-layer framework. *Atmospheric Chemistry and Physics*, *16*(24), 15433–15450. https://doi.org/10.5194/acp-16-15433-2016

USDA. (2016). U . S . Agriculture and Forestry Greenhouse Gas Inventory 1990–2013. In *United States Department of Agriculture, Office of the Chief Economist, Climate Change Program Office*.

Van Middelaar, C. E., Berentsen, P. B. M., Dijkstra, J., & De Boer, I. J. M. (2013). Evaluation of a feeding strategy to reduce greenhouse gas emissions from dairy farming: The level of analysis matters. *Agricultural Systems*, *121*, 9–22. https://doi.org/10.1016/j.agsy.2013.05.009

Wecht, K. J., Jacob, D. J., Sulprizio, M. P., Santoni, G. W., Wofsy, S. C., Parker, R., Bösch, H., & Worden, J. (2014). Spatially resolving methane emissions in California: constraints from the CalNex aircraft campaign and from present (GOSAT, TES) and future (TROPOMI, geostationary) satellite observations. *Atmospheric Chemistry and Physics*, *14*(15), 8173–8184. https://doi.org/10.5194/acp-14-8173-2014

Xiang, B., Miller, S. M., Kort, E. A., Santoni, G. W., Daube, B. C., Commane, R., Angevine, W. M., Ryerson, T. B., Trainer, M. K., Andrews, A. E., Nehrkorn, T., Tian, H., & Wofsy, S. C. (2013). Nitrous oxide (N2O) emissions from California based on 2010 CalNex airborne measurements. *Journal of Geophysical Research: Atmospheres*, *118*(7), 2809–2820. https://doi.org/10.1002/jgrd.50189

Yañez, C. C., Hopkins, F. M., Xu, X., Tavares, J. F., Welch, A., & Czimczik, C. I. (2022). Reductions in California's Urban Fossil Fuel CO2 Emissions During the COVID-19 Pandemic. *AGU Advances*, *3*(6), 1–15. https://doi.org/10.1029/2022AV000732

Amini, S., Kuwayama, T., Gong, L., Falk, M., Chen, Y., Mitloehner, Q., Weller, S., Mitloehner, F. M., Patteson, D., Conley, S. A., Scheehle, E., & FitzGibbon, M. (2022). Evaluating California dairy methane emission factors using short-term ground-level and airborne measurements. *Atmospheric Environment: X*, *14*(November 2021), 100171. https://doi.org/10.1016/j.aeaoa.2022.100171

Arndt, C., Leytem, A. B., Hristov, A. N., Zavala-Araiza, D., Cativiela, J. P., Conley, S., Daube, C., Faloona, I., & Herndon, S. C. (2018). Short-term methane emissions from 2 dairy farms in California estimated by different measurement techniques and US Environmental Protection Agency inventory methodology: A case study. *Journal of Dairy Science*, *101*(12), 11461–11479. https://doi.org/10.3168/jds.2017-13881

Ba, S., Qu, Q., Zhang, K., & Groot, J. C. J. (2020). Meta-analysis of greenhouse gas and ammonia emissions from dairy manure composting. *Biosystems Engineering*, *193*, 126–137. https://doi.org/10.1016/j.biosystemseng.2020.02.015

Baldé, H., VanderZaag, A. C., Burtt, S., Evans, L., Wagner-Riddle, C., Desjardins, R. L., & MacDonald, J. D. (2016). Measured versus modeled methane emissions from separated liquid dairy manure show large model underestimates. *Agriculture, Ecosystems and Environment*, *230*, 261–270. https://doi.org/10.1016/j.agee.2016.06.016

Behera, S. N., Sharma, M., Aneja, V. P., & Balasubramanian, R. (2013). Ammonia in the atmosphere: A review on emission sources, atmospheric chemistry and deposition on terrestrial bodies. In *Environmental Science and Pollution Research* (Vol. 20, Issue 11, pp. 8092–8131). https://doi.org/10.1007/s11356-013-2051-9

Bjorneberg, D. L., Leytem, A. B., Westermann, D. T., Griffiths, P. R., Shao, L., & Pollard, M. J. (2009). Measurement of atmospheric ammonia, methane, and nitrous oxide at a concentrated dairy production facility in southern idaho using open-path FTIR spectrometry. *Transactions of the ASABE*, *52*(5), 1749–1756.

Borhan, M. S., Capareda, S. C., Mukhtar, S., Faulkner, W. B., McGee, R., & Parnell, C. B. (2011a). Greenhouse Gas Emissions from Ground Level Area Sources in Dairy and Cattle Feedyard Operations. *Atmosphere*, *2*(3), 303–329. https://doi.org/10.3390/atmos2030303

Borhan, M. S., Capareda, S., Mukhtar, S., Faulkner, W. B., McGee, R., & Parnell, C. B. (2011b). Determining Seasonal Greenhouse Gas Emissions from Ground-Level Area Sources in a Dairy Operation in Central Texas. *Journal of the Air & Waste Management Association*, *61*(7), 786–795. https://doi.org/10.3155/1047-3289.61.7.786

Broucek, J. (2016). Nitrous Oxide Production from Cattle and Swine Manure. *Journal of Animal Behaviour and Biometeorology*, *5*(1), 13–19. https://doi.org/10.14269/2318-1265/jabb.v5n1p13-19

Burford, J. R., & Bremner, J. M. (1975). Relationships between the denitrification capacities of soils and total, water-soluble and readily decomposable soil organic matter. *Soil Biology and Biochemistry*, *7*(6), 389–394. https://doi.org/10.1016/0038-0717(75)90055-3

Carranza, V., Biggs, B., Meyer, D., Townsend-Small, A., Thiruvenkatachari, R. R., Venkatram, A., Fischer, M. L., & Hopkins, F. M. (2022). Isotopic Signatures of Methane Emissions From Dairy Farms in California's San Joaquin Valley. *Journal of Geophysical Research: Biogeosciences*, *127*(1), 1–15. https://doi.org/10.1029/2021JG006675

Cassel, T., Ashbaugh, L., Flocchini, R., & Meyer, D. (2005). Ammonia emission factors for open-lot dairies: Direct measurements and estimation by nitrogen intake. *Journal of the Air and Waste Management Association*, *55*(6), 826–833. https://doi.org/10.1080/10473289.2005.10464660

Cui, Y. Y., Brioude, J., Angevine, W. M., Peischl, J., McKeen, S. A., Kim, S. W., Andrew Neuman, J., Henze, D. K., Bousserez, N., Fischer, M. L., Jeong, S., Michelsen, H. A., Bambha, R. P., Liu, Z., Santoni, G. W., Daube, B. C., Kort, E. A., Frost, G. J., Ryerson, T. B., … Trainer, M. (2017). Top-down estimate of methane emissions in California using a mesoscale inverse modeling technique: The San Joaquin Valley. *Journal of Geophysical Research*, *122*(6), 3686–3699. https://doi.org/10.1002/2016JD026398

Eckard, R. J., Chen, D., White, R. E., & Chapman, D. F. (2003). Gaseous nitrogen loss from temperate perennial grass and clover dairy pastures in south-eastern Australia. *Australian Journal of Agricultural Research*, *54*(6), 561–570. https://doi.org/10.1071/AR02100

Eilerman, S. J., Peischl, J., Neuman, J. A., Ryerson, T. B., Aikin, K. C., Holloway, M. W., Zondlo, M. A., Golston, L. M., Pan, D., Floerchinger, C., & Herndon, S. (2016). Characterization of Ammonia, Methane, and Nitrous Oxide Emissions from Concentrated Animal Feeding Operations in Northeastern Colorado. *Environmental Science and Technology*, *50*(20), 10885–10893. https://doi.org/10.1021/acs.est.6b02851

El Kader, N. A., Robin, P., Paillat, J. M., & Leterme, P. (2007). Turning, compacting and the addition of water as factors affecting gaseous emissions in farm manure composting. *Bioresource Technology*, *98*(14), 2619–2628. https://doi.org/10.1016/j.biortech.2006.07.035

Fournel, S., Godbout, S., Ruel, P., Fortin, A., Duquette-Lozeau, K., Létourneau, V., Généreux, M., Lemieux, J., Potvin, D., Côté, C., Duchaine, C., & Pellerin, D. (2019). Production of recycled manure solids for use as bedding in Canadian dairy farms: II. Composting methods. *Journal of Dairy Science*, *102*(2), 1847–1865. https://doi.org/10.3168/jds.2018-14967

Gentner, D. R., Ford, T. B., Guha, A., Boulanger, K., Brioude, J., Angevine, W. M., De Gouw, J. A., Warneke, C., Gilman, J. B., Ryerson, T. B., Peischl, J., Meinardi, S., Blake, D. R., Atlas, E., Lonneman, W. A., Kleindienst, T. E., Beaver, M. R., St. Clair, J. M., Wennberg, P. O., … Goldstein, A. H. (2014). Emissions of organic carbon and methane from petroleum and dairy operations in California's San Joaquin Valley. *Atmospheric Chemistry and Physics*, *14*(10), 4955–4978. https://doi.org/10.5194/acp-14-4955-2014

Goulding, K. W. T., Willison, T. W., Webster, C. P., & Powlson, D. S. (1996). Methane fluxes in aerobic soils. *Environmental Monitoring and Assessment*, *42*(1–2), 175–187. https://doi.org/10.1007/BF00394049

Guha, A., Gentner, D. R., Weber, R. J., Provencal, R., & Goldstein, A. H. (2015). Source apportionment of methane and nitrous oxide in California's San Joaquin Valley at CalNex 2010 via positive matrix factorization. *Atmospheric Chemistry and Physics*, *15*(20), 12043–12063. https://doi.org/10.5194/acp-15-12043-2015

He, Y., Inamori, Y., Mizuochi, M., Kong, H., Iwami, N., & Sun, T. (2001). Nitrous oxide emissions from aerated composting of organic waste. *Environmental Science and Technology*, *35*(11), 2347–2351. https://doi.org/10.1021/es0011616

Heald, C. L., Collett, J. L., Lee, T., Benedict, K. B., Schwandner, F. M., Li, Y., Clarisse, L., Hurtmans, D. R., Van Damme, M., Clerbaux, C., Coheur, P. F., Philip, S., Martin, R. V., & Pye, H. O. T. (2012). Atmospheric ammonia and particulate inorganic nitrogen over the United States. *Atmospheric Chemistry and Physics*, *12*(21), 10295–10312. https://doi.org/10.5194/acp-12-10295-2012

Herrera, S. A., Diskin, G. S., Harward, C., Sachse, G., De Wekker, S. F. J., Yang, M., Choi, Y., Wisthaler, A., Mallia, D. V., & Pusede, S. E. (2021). Wintertime Nitrous Oxide Emissions in the San Joaquin Valley of California Estimated from Aircraft Observations. *Environmental Science & Technology*, *55*(8), 4462–4473. https://doi.org/10.1021/acs.est.0c08418

Hristov, A. N., Hanigan, M., Cole, A., Todd, R., McAllister, T. A., Ndegwa, P. M., & Rotz, A. (2011). Review: Ammonia emissions from dairy farms and beef feedlots. In *Canadian Journal of Animal Science* (Vol. 91, Issue 1, pp. 1–35). Agricultural Institute of Canada. https://doi.org/10.4141/CJAS10034

IPCC. (2013). Carbon and Other Biogeochemical Cycles. In: Climate Change 2013: The Physical Science Basis. Contribution of Working Group I to the Fifth Assessment Report of the Intergovernmental Panel on Climate Change. *Cambridge University Press*, *9781107057*, 465–570. https://doi.org/10.1017/CBO9781107415324.015

Jeong, S., Hsu, Y. K., Andrews, A. E., Bianco, L., Vaca, P., Wilczak, J. M., & Fischer, M. L. (2013). A multitower measurement network estimate of California's methane emissions. *Journal of Geophysical Research Atmospheres*, *118*(19), 11,339-11,351. https://doi.org/10.1002/jgrd.50854

Jeong, S., Newman, S., Zhang, J., Andrews, A. E., Bianco, L., Bagley, J., Cui, X., Graven, H., Kim, J., Salameh, P., LaFranchi, B. W., Priest, C., Campos-Pineda, M., Novakovskaia, E., Sloop, C. D., Michelsen, H. A., Bambha, R. P., Weiss, R. F., Keeling, R., & Fischer, M. L. (2016). Estimating methane emissions in California's urban and rural regions using multitower observations. *Journal of Geophysical Research: Atmospheres*, *121*(21), 13,031-13,049. https://doi.org/10.1002/2016JD025404

Jeong, S., Newman, S., Zhang, J., Andrews, A. E., Bianco, L., Dlugokencky, E., Bagley, J., Cui, X., Priest, C., Campos-Pineda, M., & Fischer, M. L. (2018). Inverse Estimation of an Annual Cycle of California's Nitrous Oxide Emissions. *Journal of Geophysical Research: Atmospheres*, *123*(9), 4758–4771. https://doi.org/10.1029/2017JD028166

Jeong, S., Newman, S., Zhang, J., Andrews, A. E., Dlugokencky, E., Bagley, J., Cui, X., & Priest, C. (2020). *Inverse Estimation of an Annual Cycle of California ' s Nitrous Oxide Emissions*. *2030*, 4758–4771. https://doi.org/10.1029/2017JD028166

Jeong, S., Zhao, C., Andrews, A. E., Dlugokencky, E. J., Sweeney, C., Bianco, L., Wilczak, J. M., & Fischer, M. L. (2012). Seasonal variations in N2O emissions from central California. *Geophysical Research Letters*, *39*(16), n/a-n/a. https://doi.org/10.1029/2012GL052307

Joo, H. S., Ndegwa, P. M., Heber, A. J., Ni, J. Q., Bogan, B. W., Ramirez-Dorronsoro, J. C., & Cortus, E. (2015). Greenhouse gas emissions from naturally ventilated freestall dairy barns. *Atmospheric Environment*, *102*, 384–392. https://doi.org/10.1016/j.atmosenv.2014.11.067

Kaffka, S., & Barzee, T. (2016). *Evaluation of Dairy Manure Management Practices for Greenhouse Gas Emissions Mitigation in California*.

Kaharabata, S. K., & Schuepp, P. H. (1998). Methane emissions from aboveground open manure slurry tanks oxygen demand z 218. *Global Biogeochemical Cycles*, *12*(3), 545–554.

Kebreab, E., Clark, K., Wagner-Riddle, C., & France, J. (2006). Methane and nitrous oxide emissions from Canadian animal agriculture: A review. *Canadian Journal of Animal Science*, *86*(2), 135–157. https://doi.org/10.4141/A05-010

Kelly, J. T., Baker, K. R., Nowak, J. B., Murphy, J. G., Markovic, M. Z., VandenBoer, T. C., Ellis, R. A., Neuman, J. A., Weber, R. J., Roberts, J. M., Veres, P. R., de Gouw, J. A., Beaver, M. R., Newman, S., & Misenis, C. (2014). Fine-scale simulation of ammonium and nitrate over the South Coast Air Basin and San Joaquin Valley of California during CalNex-2010. *Journal of Geophysical Research: Atmospheres*, *119*(6), 3600–3614. https://doi.org/10.1002/2013JD021290

Kozloski, G. V., Senger, C. C. D., Perottoni, J., & Sanchez, L. M. B. (2006). Evaluation of two methods for ammonia extraction and analysis in silage samples. *Animal Feed Science and Technology*, *127*(3–4), 336–342. https://doi.org/10.1016/j.anifeedsci.2005.08.014

Kupper, T., Häni, C., Neftel, A., Kincaid, C., Bühler, M., Amon, B., & VanderZaag, A. (2020). Ammonia and greenhouse gas emissions from slurry storage - A review. *Agriculture, Ecosystems & Environment*, *300*, 106963. https://doi.org/10.1016/j.agee.2020.106963

Laubach, J., Heubeck, S., Pratt, C., Woodward, K., Guieysse, B., van der Weerden, T., Chung, M., Shilton, A., & Craggs, R. (2015). Review of greenhouse gas emissions from the storage and land application of farm dairy effluent. *New Zealand Journal of Agricultural Research*, *58*(2), 203–233. https://doi.org/10.1080/00288233.2015.1011284

Leytem, A.B., Bjorneberg, D. L., Koehn, A. C., Moraes, L. E., Kebreab, E., & Dungan, R. S. (2017a). Methane emissions from dairy lagoons in the western United States. *Journal of Dairy Science*, *100*(8), 6785–6803. https://doi.org/10.3168/jds.2017-12777

Leytem, A.B., Bjorneberg, D. L., Koehn, A. C., Moraes, L. E., Kebreab, E., & Dungan, R. S. (2017b). Methane emissions from dairy lagoons in the western United States. *Journal of Dairy Science*, *100*(8), 6785–6803. https://doi.org/10.3168/jds.2017-12777

Leytem, April B., Dungan, R. S., Bjorneberg, D. L., & Koehn, A. C. (2011). Emissions of Ammonia, Methane, Carbon Dioxide, and Nitrous Oxide from Dairy Cattle Housing and Manure Management Systems. *Journal of Environmental Quality*, *40*(5), 1383–1394. https://doi.org/10.2134/jeq2009.0515

Leytem, April B., Dungan, R. S., Bjorneberg, D. L., & Koehn, A. C. (2013). Greenhouse Gas and Ammonia Emissions from an Open-Freestall Dairy in Southern Idaho. *Journal of Environmental Quality*, *42*(1), 10–20. https://doi.org/10.2134/jeq2012.0106

Leytem, April B, Dungan, R. S., Bjorneberg, D. L., & Koehn, A. C. (2011). Emissions of Ammonia, Methane, Carbon Dioxide, and Nitrous Oxide from Dairy Cattle Housing and Manure Management Systems. *Journal of Environmental Quality*, *40*(5), 1383–1394. https://doi.org/10.2134/jeq2009.0515

Li, J., Luo, J., Shi, Y., Houlbrooke, D., Wang, L., Lindsey, S., & Li, Y. (2015). Nitrogen gaseous emissions from farm effluent application to pastures and mitigation measures to reduce the emissions: a review. *New Zealand Journal of Agricultural Research*, *58*(3), 339–353. https://doi.org/10.1080/00288233.2015.1028651

Li, S., Song, L., Gao, X., Jin, Y., Liu, S., Shen, Q., & Zou, J. (2017). Microbial Abundances Predict Methane and Nitrous Oxide Fluxes from a Windrow Composting System. *Frontiers in Microbiology*, *8*(MAR). https://doi.org/10.3389/fmicb.2017.00409

Martins, O., & Dewes, T. (1992). Loss of nitrogenous compounds during composting of animal wastes. *Bioresource Technology*, *42*(2), 103–111. https://doi.org/10.1016/0960-8524(92)90068-9

Miller, D. J., Sun, K., Tao, L., Pan, D., Zondlo, M. A., Nowak, J. B., Liu, Z., Diskin, G., Sachse, G., Beyersdorf, A., Ferrare, R., & Scarino, A. J. (2015). Ammonia and methane dairy emission plumes in the San Joaquin Valley of California from individual feedlot to regional scales. *Journal of Geophysical Research: Atmospheres*, *120*(18), 9718–9738. https://doi.org/10.1002/2015JD023241

Minato, K., Kouda, Y., Yamakawa, M., Hara, S., Tamura, T., & Osada, T. (2013). Determination of GHG and ammonia emissions from stored dairy cattle slurry by using a floating dynamic chamber. *Animal Science Journal*, *84*(2), 165–177. https://doi.org/10.1111/j.1740-0929.2012.01053.x

Nevison, C., Andrews, A., Thoning, K., Dlugokencky, E., Sweeney, C., Miller, S., Saikawa, E., Benmergui, J., Fischer, M., Mountain, M., & Nehrkorn, T. (2018). Nitrous Oxide Emissions Estimated With the CarbonTracker-Lagrange North American Regional Inversion Framework. *Global Biogeochemical Cycles*, *32*(3), 463–485. https://doi.org/10.1002/2017GB005759

Ngwabie, N.M., Jeppsson, K.-H., Nimmermark, S., Swensson, C., & Gustafsson, G. (2009). Multi-location measurements of greenhouse gases and emission rates of methane and ammonia from a naturally-ventilated barn for dairy cows. *Biosystems Engineering*, *103*(1), 68–77. https://doi.org/10.1016/j.biosystemseng.2009.02.004

Ngwabie, Ngwa M., Vanderzaag, A., Jayasundara, S., & Wagner-Riddle, C. (2014). Measurements of emission factors from a naturally ventilated commercial barn for dairy cows in a cold climate. *Biosystems Engineering*, *127*, 103–114. https://doi.org/10.1016/j.biosystemseng.2014.08.016

Olesen, J. E., & Sommer, S. G. (1993). Modelling effects of wind speed and surface cover on ammonia volatilization from stored pig slurry. *Atmospheric Environment Part A, General Topics*, *27*(16), 2567–2574. https://doi.org/10.1016/0960-1686(93)90030-3

Owen, J. J., & Silver, W. L. (2015). Greenhouse gas emissions from dairy manure management: a review of field-based studies. *Global Change Biology*, *21*(2), 550–565. https://doi.org/10.1111/gcb.12687

Pardo, G., Moral, R., Aguilera, E., & Del Prado, A. (2015). Gaseous emissions from management of solid waste: a systematic review. *Global Change Biology*, *21*, 1313–1327. https://doi.org/10.1111/gcb.12806

Parkinson, R., Gibbs, P., Burchett, S., & Misselbrook, T. (2004). Effect of turning regime and seasonal weather conditions on nitrogen and phosphorus losses during aerobic composting of cattle manure. *Bioresource Technology*, *91*(2), 171–178. https://doi.org/10.1016/S0960-8524(03)00174-3

Saha, C. K., Ammon, C., Berg, W., Fiedler, M., Loebsin, C., Sanftleben, P., Brunsch, R., & Amon, T. (2014). Seasonal and diel variations of ammonia and methane emissions from a naturally ventilated dairy building and the associated factors influencing emissions. *Science of the Total Environment*, *468–469*, 53–62. https://doi.org/10.1016/j.scitotenv.2013.08.015

Schiferl, L. D., Heald, C. L., Nowak, J. B., Holloway, J. S., Neuman, J. A., Bahreini, R., Pollack, I. B., Ryerson, T. B., Wiedinmyer, C., & Murphy, J. G. (2014). An investigation of ammonia and inorganic particulate matter in california during the calnex campaign. *Journal of Geophysical Research*, *119*(4), 1883–1902. https://doi.org/10.1002/2013JD020765

Sommer, S. G., Petersen, S. O., Sørensen, P., Poulsen, H. D., & Møller, H. B. (2007). Methane and carbon dioxide emissions and nitrogen turnover during liquid manure storage. *Nutrient Cycling in Agroecosystems*, *78*(1), 27–36. https://doi.org/10.1007/s10705-006-9072-4

Sonoki, T., Furukawa, T., Jindo, K., Suto, K., Aoyama, M., & Sánchez-Monedero, M. Á. (2013). Influence of biochar addition on methane metabolism during thermophilic phase of composting. *Journal of Basic Microbiology*, *53*(7), 617–621. https://doi.org/10.1002/jobm.201200096

Teye, F. K., & Hautala, M. (2008). Adaptation of an ammonia volatilization model for a naturally ventilated dairy building. *Atmospheric Environment*, *42*(18), 4345–4354. https://doi.org/10.1016/j.atmosenv.2008.01.019

Thiruvenkatachari, R. R., Carranza, V., Ahangar, F., Marklein, A., Hopkins, F., & Venkatram, A. (2020). Uncertainty in using dispersion models to estimate methane emissions from manure lagoons in dairies. *Agricultural and Forest Meteorology*, *290*, 108011. https://doi.org/10.1016/j.agrformet.2020.108011

Trousdell, J. F., Conley, S. A., Post, A., & Faloona, I. C. (2016). Observing entrainment mixing, photochemical ozone production, and regional methane emissions by aircraft using a simple mixed-layer framework. *Atmospheric Chemistry and Physics*, *16*(24), 15433–15450. https://doi.org/10.5194/acp-16-15433-2016

USDA. (2016). U . S . Agriculture and Forestry Greenhouse Gas Inventory 1990–2013. In *United States Department of Agriculture, Office of the Chief Economist, Climate Change Program Office*.

Van Middelaar, C. E., Berentsen, P. B. M., Dijkstra, J., & De Boer, I. J. M. (2013). Evaluation of a feeding strategy to reduce greenhouse gas emissions from dairy farming: The level of analysis matters. *Agricultural Systems*, *121*, 9–22. https://doi.org/10.1016/j.agsy.2013.05.009

Wecht, K. J., Jacob, D. J., Sulprizio, M. P., Santoni, G. W., Wofsy, S. C., Parker, R., Bösch, H., & Worden, J. (2014). Spatially resolving methane emissions in California: constraints from the CalNex aircraft campaign and from present (GOSAT, TES) and future (TROPOMI, geostationary) satellite observations. *Atmospheric Chemistry and Physics*, *14*(15), 8173–8184. https://doi.org/10.5194/acp-14-8173-2014

Xiang, B., Miller, S. M., Kort, E. A., Santoni, G. W., Daube, B. C., Commane, R., Angevine, W. M., Ryerson, T. B., Trainer, M. K., Andrews, A. E., Nehrkorn, T., Tian, H., & Wofsy, S. C. (2013). Nitrous oxide (N2O) emissions from California based on 2010 CalNex airborne measurements. *Journal of Geophysical Research: Atmospheres*, *118*(7), 2809–2820. https://doi.org/10.1002/jgrd.50189

Yañez, C. C., Hopkins, F. M., Xu, X., Tavares, J. F., Welch, A., & Czimczik, C. I. (2022). Reductions in California's Urban Fossil Fuel CO2 Emissions During the COVID-19 Pandemic. *AGU Advances*, *3*(6), 1–15. https://doi.org/10.1029/2022AV000732

4. Seasonality of Methane Fluxes from Dairy Manure Lagoons: A Case Study From a Southern California Dairy

4.0 Acknowledgement of Co-Authorship

This work was completed with contributions from Valerie Carranza, Ray G. Anderson, Dennise L. Jenkins, Deanne Meyer, Celia Limón , and Francesca M. Hopkins

4.1 Abstract

Methane (CH_4) is a potent greenhouse gas that is targeted in emissions mitigation policies by the State of California. Dairies are an important source in the statewide CH_4 budget, contributing over half of the statewide emissions, of which roughly half come from CH_4 produced from manure management. However, current CH_4 emission estimates from manure lagoons indicate a high level of uncertainty given the lack of high-frequency, long-term measurements from Californian dairy lagoons. In particular, the impacts of temporal variability of lagoon emissions are poorly understood or quantified. Here we use the eddy covariance technique to estimate seasonal and diurnal CH_4 fluxes from manure lagoons at a dairy in southern California for over a year. In addition, we measured meteorological and lagoon physicochemical characteristics that could influence emissions. We found that diurnal CH_4 observations are closely correlated with latent heat fluxes and show a peak in CH_4 emissions in the early afternoon when lagoon surface temperatures are high; however, the temperature relationship differs at seasonal timescales. Overall, CH_4 fluxes decreased over the course of the study, with the highest CH_4 fluxes observed during the spring of 2020 (6.89 μmol $m^{-2}s^{-1}$; 95% CI: 6.41 - 7.45 μmol $m^{-2}s^{-1}$), following precipitation events. At diurnal scales, a positive relationship is observed between CH_4 fluxes and lagoon

temperatures and wind speed. Findings from this study can help inform methane reduction policies by providing a better understanding of temporal variability of methane fluxes and determining which factors have the greatest impact on emissions.

4.2 Introduction

Manure lagoons contribute about 35% of California dairy farm CH_4 emissions statewide (Marklein et al., 2020). In these lagoons, organic-rich manure waste is stored as a liquid, creating anaerobic conditions that produce CH_4 that is subsequently emitted to the atmosphere, much of it from the lagoon surface. However, our understanding of manure lagoon CH_4 emissions is far from complete, complicating mitigation strategies for reducing or capturing CH_4 (Owen & Silver, 2015; Baldé et al., 2016; Leytem et al., 2017; Arndt et al., 2018; Thiruvenkatachari et al., 2020; Amini et al., 2022). In addition, temporal and spatial variability complicate emission estimates, which depend on physicochemical and micrometeorological predictors. Physicochemical predictors include organic substrate availability, pH, oxidation-reduction potential (ORP), nutrients, electron acceptors, chemical oxygen demand (COD). Micrometeorological factors include air and pond temperature, friction velocity, wind speed, and precipitation (Leytem et al., 2017). As such, it is essential to quantify the magnitude and uncertainty associated with CH_4 emissions from dairy manure lagoons specific to the location of interest.

The processes that impact CH_4 fluxes from manure lagoons are production, transport, and consumption. The large amounts of organic substrates found in liquid dairy manure under anaerobic conditions provide a conducive environment for methanogenesis and CH_4 production. Acetoclastic methanogens and acetogenic and hydrolyzing

microorganisms drive this methane fermentation process. Methanogenic substrates, such as H_2, CO_2, formate, and acetate, are generated as by-products by microorganisms in the dissolved and suspended solids found in the stored liquid manure (slurry) (Liu & Whitman, 2008; Habtewold et al., 2017). Total solids (TS) content in dairy slurry is an indicator of the volatile solids (VS) content, the biodegradable organic matter that may produce CH_4 (J.D. Wood et al., 2012). Dairy slurry with high VS content tend to have higher CH_4 production rates (Sommer et al., 2004; J.D. Wood et al., 2012; Habtewold et al., 2017). Favorable conditions for methanogenesis include neutral pH, ORP below -200 mV, nutrients (N, P, K, S) and depletion of electron acceptors such as NO_3^- (Conrad, 1989; Saggar et al., 2004; Kebreab et al., 2006). The fraction of degradable organic matter greatly determines the amount of CH_4 production in liquid manure and is expressed as biochemical or chemical oxygen demand (BOD or COD). Higher BOD or COD tends to produce more CH_4 (Saggar et al., 2004; Leytem et al., 2017). Methane oxidation can occur when there are low CH_4 production rates under high oxygen conditions and a slow diffusion process (Kebreab et al., 2006). Slurry may form crusts as it contains more solids that can float to the lagoon's surface. The crust layer may slow the diffusion of gases and provide a conducive environment for CH_4 oxidation under aerobic conditions (Petersen et al., 2005; Petersen & Ambus, 2006; Nielsen et al., 2010).

The primary transport pathways for CH_4 to reach the surface of manure lagoons are through diffusion, ebullition (i.e., irregular bubbling), and agitation events (Kaharabata et al., 1998; Whalen, 2005; Kebreab et al., 2006; Jeffrey D. Wood et al., 2013; Minato et al., 2013; Leytem et al., 2017). Diffusion of CH_4 occurs within the aqueous boundary layer or

plant-mediated transport via aerenchymatous vegetation. Transport of dissolved gases through the aqueous boundary layer is generally a slow process that is dependent on the concentration gradient (VanderZaag et al., 2010). Albeit uncommon in dairy manure lagoons, another potential CH_4 pathway is through aerenchymatous vegetation, as is commonly found in wetlands and lakes (Laanbroek, 2010; Iwata et al., 2018; Knox et al., 2021). Methane may also escape through ebullition when CH_4 is produced at such a fast rate that it forms bubbles and passes through the substrate layer (Whalen, 2005).

Mechanical agitation, from such events as rainfall and high wind speed, may also release CH_4 trapped in manure lagoons to the atmosphere (Kaharabata et al., 1998; Leytem et al., 2017; Arndt et al., 2018). Wind speed and friction velocity (u*) affects near-surface turbulence, and subsequently influences ebullition and diffusion of gases (Ro & Hunt, 2006; Koebsch et al., 2015; Knox et al., 2021). Increased turbulence of the lagoon surface emits more CH_4 to the atmosphere (Leytem et al., 2017).

Temperature can influence diffusion and ebullition of CH_4 fluxes from the lagoon surface at short time scales through changes in CH_4 solubility, transfer of gas across the air–water interface, and thermal contraction and expansion of free-phase gas (Barber et al., 1988; Chanton et al., 1989; Knox et al., 2021). Latent heat flux at diel scales (e.g., synchronous, hourly) serves as a proxy for CH_4 volatilization as evaporation of water and CH_4 emissions are driven by similar physical mechanisms and tend to positively covary (Morin et al., 2014; Knox et al., 2021). Methane production and oxidation rates are also impacted by the temperature effect on microbial metabolism and enzyme kinetics, with higher temperatures generally associated with higher CH_4 production or oxidation rates

(Kaharabata et al., 1998; Saggar et al., 2004; Sommer et al., 2007). Furthermore, CH_4 production is influenced indirectly by temperature through seasonal changes in substrate availability (Chang et al., 2021).

Several techniques are used to estimate CH_4 emissions from large area sources. These methods can be broadly separated into two categories: floating chambers (e.g., closed static chambers, open or closed dynamic chambers) and micrometeorological methods (e.g., inverse dispersion modeling, mass-balance approach, eddy covariance). Each of these approaches has its benefits and disadvantages. One of the main advantages of the eddy covariance method is its ability to measure long-term diurnal and temporal CH_4 fluxes. It is relatively low-maintenance and time-efficient compared to other techniques. Like other micrometeorological methods, the eddy covariance technique also measures across large spatial scales without disturbing the ecosystem. However, there is an inherent uncertainty with CH_4 emission estimates using micrometeorological methods since they are each based on unique assumptions about the micrometeorological transport of mass and energy and surface homogeneity (Harper et al., 2011; Mcginn, 2013). Another disadvantage of using the eddy covariance method is the inability to separate CH_4 fluxes between different areas of the manure lagoon. Other micrometeorological methods, such as presented in Thiruvenkatachari et al., (2020), where mobile atmospheric measurements were coupled with a dispersion model, and floating chambers could apportion CH_4 emissions to different areas of the manure lagoon. Floating chambers are a cost-effective method to measure accurate direct CH_4 emission rates from different regions of the manure lagoon. Some of the disadvantages of floating chambers include: (1) it is labor-intensive;

(2) there is a risk of disturbing the observational environment; (3) chambers capture only a snapshot of CH_4 fluxes at a given point in time; and (4) the sampling protocol needs to be carefully designed to avoid inaccurate estimates, such as large pressure differences between the inside of the chamber and ambient levels (Gerardo-Nieto et al., 2019; Lorke et al., 2015; Martinsen, Kragh, & Sand-jensen, 2018). In addition, floating chambers run the risk of overaccumulation of CH_4 within the chamber. This is especially a risk in manure lagoons where CH_4 can reach high concentrations at fast rates.

In California, there are 1,750,329 milk cows, of which 93% are in the Central Valley, wherein the predominant manure management includes storage of manure in lagoons (Marklein et al., 2021). The California GHG inventory currently quantifies CH_4 emissions from dairy manure management practices with emission factors based on several parameters, including cow population and demographics, average statewide manure management practices, and climate (CARB, 2020). However, these estimates are based on emission factors derived from few pilot and lab-scale studies outside of California (Owen & Silver, 2015). Consequently, current GHG inventory estimates are likely not representative of California's climate and unique biogeography. In addition, the current inventory includes no temporal information on emissions at timescales shorter than 1 year. So far, there is not a clear consensus whether inventories are representative of emissions given a dearth of measurements. As such, a major obstacle to assessing emissions through field measurements and comparing them to inventories are the different timescales (e.g., snapshot vs. annual average). The eddy covariance method provides valuable information

to better understand temporal variability and estimates an annual CH_4 emission average that can be compared to inventories.

Only a select number of studies have conducted in situ field measurements of CH_4 from California dairy manure lagoons. The magnitude and temporal patterns of CH_4 emissions from manure lagoons often vary depending on the method used to estimate emissions. There is also an important role of seasonality of CH_4 emissions that might confound comparison of atmosphere-based estimates with inventory. For example, Arndt et al. (2018) showed that summer CH_4 emissions were comparable to inventory estimates, but not during winter measurements. In addition, emissions from manure liquid storage were 3 to 6 times higher during the summer measurements than during the winter measurements using three different techniques (i.e., open-path measurements with inverse dispersion modeling, mobile laboratory measurements with tracer flux ratio method, and airborne measurements with the closed-path technique) (Arndt et al., 2018). In a recent study, statewide emission factors were comparable to ground-level measurements during the summer and fall seasons, but airborne measurements were 8% higher than the statewide inventories (Amini et al., 2022). Methane emissions from dairy manure lagoons may also differ by as much as a factor of two using different dispersion models (Thiruvenkatachari et al., 2020). Other important gaseous emissions are also co-emitted with CH_4 at dairy farms, but have different spatial patterns because they are coming from different sources (Miller et al., 2015).

Additional observations at the seasonal and diel scales are needed to address uncertainties in CH_4 emissions from dairy manure lagoons in California. In this study, we

investigate seasonal and diurnal CH_4 fluxes from manure lagoons at a dairy farm in Southern California using the eddy covariance technique. We pair our CH_4 fluxes with micrometeorological measurements, including wind speed, surface pond temperature, air temperature, among other parameters. We then discuss the impact of lagoon agitation events, such as precipitation and manure management practices, on CH_4 fluxes. Finally, we compare our CH_4 flux estimates using the eddy covariance technique with other methods deployed at the same location. We hypothesized that manure lagoon CH_4 emissions would follow seasonal patterns, with higher fluxes in spring and summer when manure substrate availability and temperature are higher. We also surmised that higher wind speeds would increase CH_4 fluxes through increased turbulence and mixing of the lagoon surface. Finally, we hypothesized that manure management practices would have a measurable impact on measured CH_4 emissions.

4.3 Methods

4.3.1 Description of the Study Area

Our study site is a manure storage lagoon on a typical dairy in southern California, located near 33.8º, -117.0º (Figure 4.1). The site has a semi-arid climate, with a mean annual temperature of 19ºC and mean annual precipitation of 0.5 ± 2.6 mm that mostly falls between November and March. It is an open dry lot dairy—meaning that milk cows are housed in open corrals with dirt surfaces, and manure deposited in feed lanes is primarily scraped off the lot rather than flushed with water. The manure that is scraped from the corrals is stored as dry manure piles south of the dry lot. Water is used to flush out manure deposited in the milking parlor into manure ponds via the subsurface and aboveground channels (Figure 4.1). Corral runoff flows to the channels via drainage pits,

with four weeping walls present to retain solids. Approximately 227,100 L of storm water runoff from corrals and feedlanes (when precipitation is present), milk parlor washdown water, and wash pen water enters the manure pond system daily. Manure ponds receive about 38,000 L of fresh dairy flush manure daily. From December 2016 to June 2018, 56,775 L per day of green waste digestate was also introduced to the manure lagoons for testing their Ag Waste Solutions (AWS) system that converts cow manure into biofuel, primarily diesel fuel, and biochar (Bagtang et al., 2020). Occasionally, solids are removed from the aboveground channels and stored as dry manure storage piles (Figure 4.1).

The dairy farm's population consist exclusively of Holstein cows. Demographics are relatively stable between seasons since it is a closed herd—births are on site and cows only leave once they retire or pass away. There are approximately 1066 milking cows, 200 dry cows, 685 heifers, and 370 calves. The dairy manure flush system only receives input from the milking cows and calves. The total annual manure produced from dry corral production is 6300 tons.

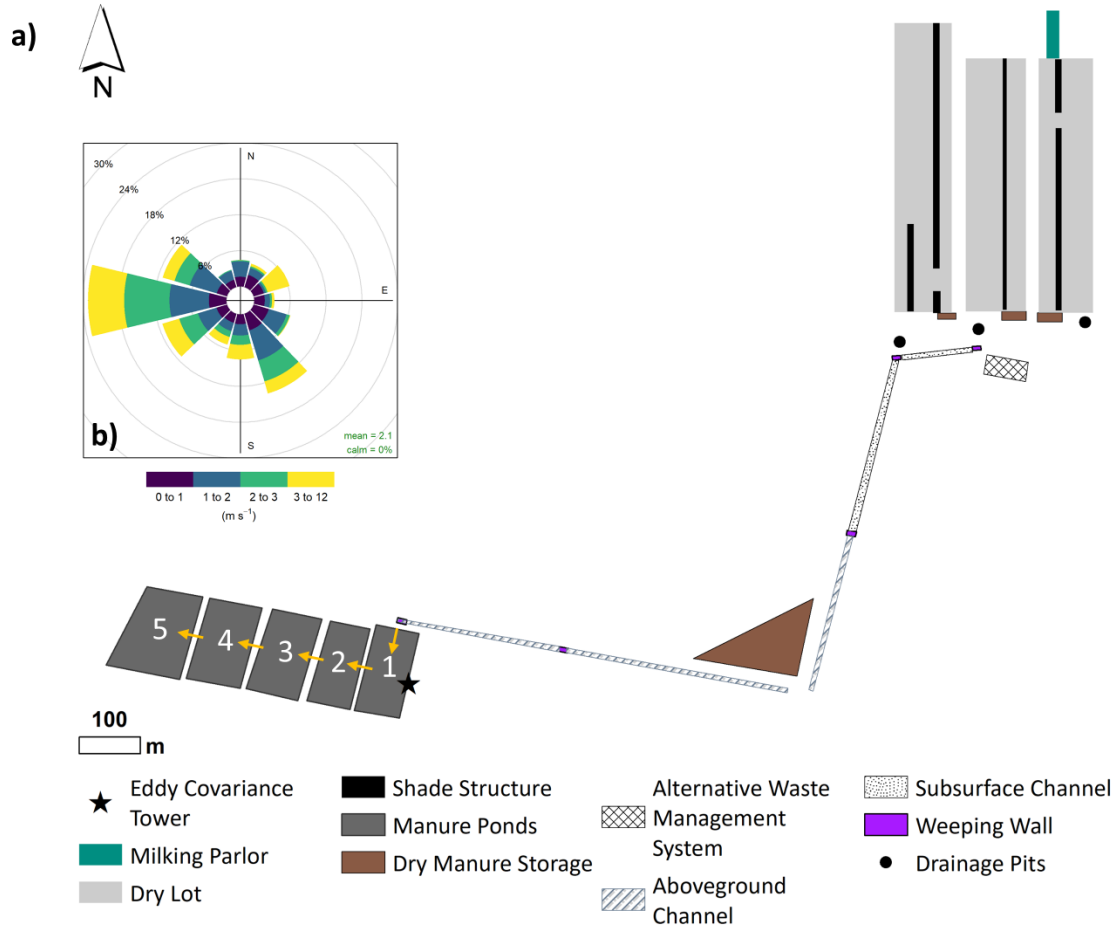

Figure 4.1 Southern California Dairy Farm. a) Layout of the dairy farm site and manure pond complex. Orange arrows indicate the inlet and flow of the manure via gravitational separation. b) Wind rose shows prevailing half-hourly wind speed and wind direction (at the eddy covariance tower from June 14, 2018 to June 17, 2021.

The manure pond system consists of five manure ponds (Figure 4.1), wherein the liquid manure navigates from manure pond 1 to manure pond 5 via gravity, decreasing the content of suspended volatile solids through anaerobic decomposition and settling as it navigates from one manure pond to the next. Throughout the study period (June 14, 2019 to June 17, 2021), the surface of manure pond 1 underwent a drastic change in vegetation and surface variation (Figure 4.2). To quantify the percentage change in crust/vegetation,

we calculated the change in vegetation/crust area using Google Earth satellite imagery between 2019 and 2021. There was a 147% increase in area covered by the crust layer and vegetation on manure pond 1 from June 2019 to June 2021. Peak vegetation growth occurred during the summer months (June-August), followed by a dry period. We define the pre-sedimentation stage occurring from June 2019 to May 2020 and the post-sedimentation stage occurring from June 2020 and June 2021 when a substantial crust and sediment layer formed on the surface of manure pond 1. A common practice is to dredge dairy manure ponds periodically. However, the Southern California dairy farm has not dredged their manure ponds since it was constructed in 2006, thus solids also accumulated throughout this study period. The solids in the channel leading to the manure pond system were dredged in March 2020 following rain events and December 1, 2020 (correspondence with Michael Bagtang, engineer at the dairy farm). Typically, the channels are dredged twice a year.

Figure 4.2. Photographs taken between 2019 to 2021 showing the surface variation of manure pond 1.

4.3.2 Instrumentation

We installed an eddy covariance flux tower at a height of 4 m on the southeastern edge of Lagoon 1 (Figure 4.1). The eddy covariance flux tower consisted of an open-path CH_4 analyzer (LI-7700, LI-COR, Inc.), integrated CO_2 and H_2O Open-Path Gas Analyzer and 3-D Sonic Anemometer (IRGASON, Campbell Scientific, Inc.). The analyzers measured at a rate of 10 Hz. They were calibrated before and after the field measurements using zero air and custom gas mixtures that were tied to the scale set by the NOAA Global Monitoring Division by measurement against NOAA certified tanks. We also measured air temperature and relative humidity (HMP45C-L, Campbell Scientific, Inc.), the surface temperature of the pond with an infrared radiometer (Apogee Instruments, Inc.), and precipitation with a rain gauge. The data were recorded using a CR3000 datalogger

(Campbell Scientific, Inc.). Instruments were powered using three solar panels, seven deep-cycle. Dust was removed using an automatic cleaning system.

4.3.3 Flux Calculations and Data Quality Control

In the eddy covariance method, fluxes (F_c) are calculated by averaging the product of the deviations of a mole fraction (c) and vertical wind component (w) from their means (Aubinet et al., 2012; You et al., 2021). That is,

$$F_c = \overline{c'w'}\,, \tag{1}$$

The mole fraction $c = \bar{c} + c'$ and $w = \bar{w} + w'$, where the overbar represents the mean quantity during the flux averaging periods and prime is the instantaneous deviation from the mean. Raw turbulence and gas concentration observations were processed into half-hourly fluxes using EddyPro (Version 7.0.9, LI-COR Inc.). The main processing included application of the Webb-Penman-Leuning correction to correct for density fluctuations (Webb et al., 1980), axis rotation (double rotation) (Wilczak et al., 2001), raw data detrending using block averaging, time lag compensation using the covariance maximation method using the default options (Fan et al., 1990), and spectral corrections for low- and high-pass filtering effects (Moncrieff et al., 1997, 2004). Raw CO_2 and CH_4 data were automatically removed when signal strengths were below 70% and 10%, respectively, as per LI-COR's recommendation. About 1.4% of raw data was removed after applying these corrections. Half-hour fluxes underwent quality control based on the Foken et al. (2004) and Mauder and Foken (2006) methods. Steady-state conditions and turbulence characteristics were categorized into three classes: 0 (best quality), 1 (good quality), and 2 (poor quality); only half-hourly fluxes categorized as 0 and 1 were included

in this study. To capture only the CH_4 fluxes from the manure lagoons, we selected half-hourly fluxes with wind direction between 270º and 340º (Figure 4.1), friction velocity (u*) greater than 0.1 ms^{-1}, and wind speed greater than 0.2 m s^{-1}. Additionally, a combination of technical difficulties and dust accumulation on the gas analyzers prevented measurements for periods of time throughout the study period. We captured 23% of the 2019-2021 measurement period after accounting for outages (20% of total) and data eliminated by QC procedures (3% of total).

Linear models were used to evaluate the relationships between CH_4 fluxes and physicochemical and meteorological measurements. Linear regression analysis between variables was performed in R using package 'stats' (RStudio version 2022.02.3.+492). A stepwise selection process was used to select the best predictors for a multiple regression model for CH_4 fluxes. We selected the best predictors in a stepwise selection process in R using package 'MASS' and function 'stepAIC' (Ripley, 2002).

4.3.4 Footprint of Flux Measurements

The footprint of an eddy covariance flux measurements represents the upwind area that contributes to the fluxes at the location of measurements. The extent of the footprint depends on the micrometeorological conditions such as stability of the boundary layer and wind speed. A flux footprint model by Kljun et al. (2015) was used to estimate the footprint of the eddy covariance flux measurements. The algorithm uses the following inputs to calculate the footprint: mean wind speed, wind direction, standard deviation of the horizontal wind speed, friction velocity, planetary boundary layer height, and Obukhov length. Figure 4.3 shows the upwind area that contributes to the flux observations with

friction velocity greater than 0.1 m s^{-1}, wind direction between 270º and 340º, and wind speed greater than 0.2 m s^{-1}. The distance of footprint contributions were calculated for each half-hour flux using the EddyPro software. The extent of the footprint captures manure pond 1, manure pond 2, and a portion of manure pond 3. As shown in Figure 4.3, 70% of the footprint primarily covers less than 50% of the area of manure pond 1.

Figure 4.3. Flux tower area with footprint raster and contour lines from 10 to 90%, in 10% steps. Location of eddy covariance tower is indicated by the green symbol.

4.3.5 Manure Lagoon Sampling

On August 28, 2019, we sampled the manure lagoon complex for various biophysical parameters using a boat at three different locations and depths. We sampled at three locations (L1, L2, L3) shown in Figure 4.4 and Figure 4.10. L1 and L2 were sampled at 0 and 0.3 m and L3 was sampled at surface level, 0.3, and 0.8 m. L1 and L2 were only sampled at the surface level and 0.3 depth since the high volatile content limited the instrumentation's reach. We measured pH and temperature with an Oakton PCTS 50, PCSTestr 35 or pHTestr 30. Oxidation-reduction potential (ORP) was measured with an

Oakton ORP Testr 10 that was calibrated with Zobell's solution from VWR Scientific in the lab 24 hours prior to field work. Electrical conductivity was measured on each liquid sample in the laboratory using an Oakton Con 100 series meter and conductivity probe. The probe was calibrated according to manufacturer's recommendations with 1413 uS standard solution from Fisher Scientific. Samples were removed from the 4 °C cold room and each was inverted gently 2-3 times to mix contents just prior to measurement. The probe was calibrated after every 10-15 readings to reduce drift. Total solids (TS) concentration (%), which is the solid concentration of biomass, was determined by weighing and drying 15-25 ml aliquots of each sample in triplicate in a 120 °C oven for 4-16 hours, weighing the residual, then dividing by the wet weight. Aliquots were made using the shake and pour method (Meyer et al. 2004). Fixed solids (FS) concentration (% DM basis), which is the inorganic fraction of total solids, was determined by further combustion of the dried samples in a muffle oven at 540 °C for 4 hours, weighing the residual, then dividing by the dry weight (Holstege et al.,2010). Volatile solids concentration (% as-is basis), which is the organic fraction of total solids, is the difference between TS and FS divided by wet weight.

4.3.6 Short-term Sampling of Manure Lagoons Using Other Techniques

Two short-term studies estimated CH_4 emissions from manure pond 1 with different methods. On August 14, 2018, stationary measurements of CH_4 mole fractions downwind of manure pond 1 were collected with a cavity-ringdown spectrometer (CRDS) (Thiruvenkatachari et al., 2020). Dispersion models were then used to estimate CH_4 emissions and showed that CH_4 emissions were heterogenous, with higher CH_4 emissions

near the manure stream inlet (Source Area 1, Figure 4.4). In a pilot study on August 27, 2019, CH_4 emissions were estimated using an auto-ventilated floating chamber connected to a CRDS (Carranza & Caruso, unpublished data). Figure 4.5 shows the timeline of measurements conducted at manure pond 1.

Figure 4.4. Manure Pond 1 source areas (1-4) and biogeochemical sampling locations (L1,L2,L3). The star indicates the location of the eddy covariance tower.

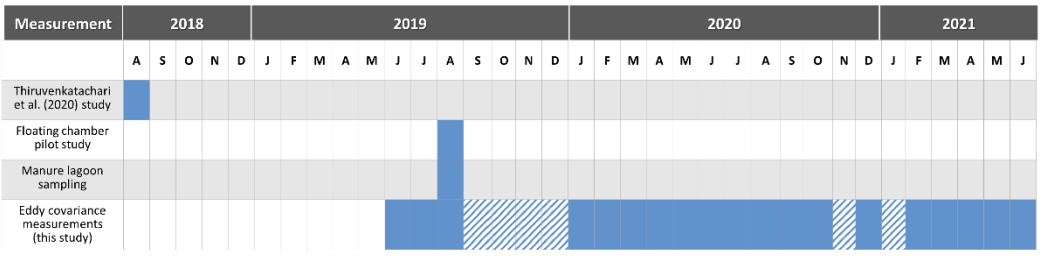

Figure 4.5. Timeline of measurements conducted on manure pond 1. Striped patterns indicate power outages of the eddy covariance tower.

4.4 Results

4.4.1 Meteorological Conditions

During the study period, observed air temperatures were on average 19 ºC, with the highest temperatures measured during the summer (June-August: 24 ºC) (Table 4.1, Figure 4.6). Sensible heat flux was on average 41 W m^{-2} (Table 4.1). Mean surface pond temperatures were comparable to mean air temperatures with 20 ºC. Friction velocity (u*) was on average 0.2 ± 0.1 ms^{-1} (Table 4.1). Lastly, incoming shortwave radiation near the manure ponds was 75±71 Wm^{-2}, on average (Table 4.1).

In our study site, precipitation events were highest during the winter and spring seasons. The highest precipitation events occurred during March and April in the year 2020. Daily CH_4 fluxes were also highest during this time (Figure 4.6). Surface and pond temperatures were on average highest during the summer months of August and September. Similarly, incoming shortwave radiation was strongest during the summer months of August and September in the year 2020. There were no overall seasonal patterns observed for friction velocity and wind speed.

Table 4.1. Summary Statistics of the Meteorological Parameters at the Study Site.

Parameter	**Mean**	**10^{th} percentile**	**90^{th} percentile**
Friction Velocity, u* (m s^{-1})	0.2	0.1	0.4
Air Temperature (ºC)	19	8	31
Pond Temperature (ºC)	20	8	34
Incoming Shortwave Radiation (W m^{-2})	75	1	177
Sensible Heat Flux (W m^{-2})	41	-25	143

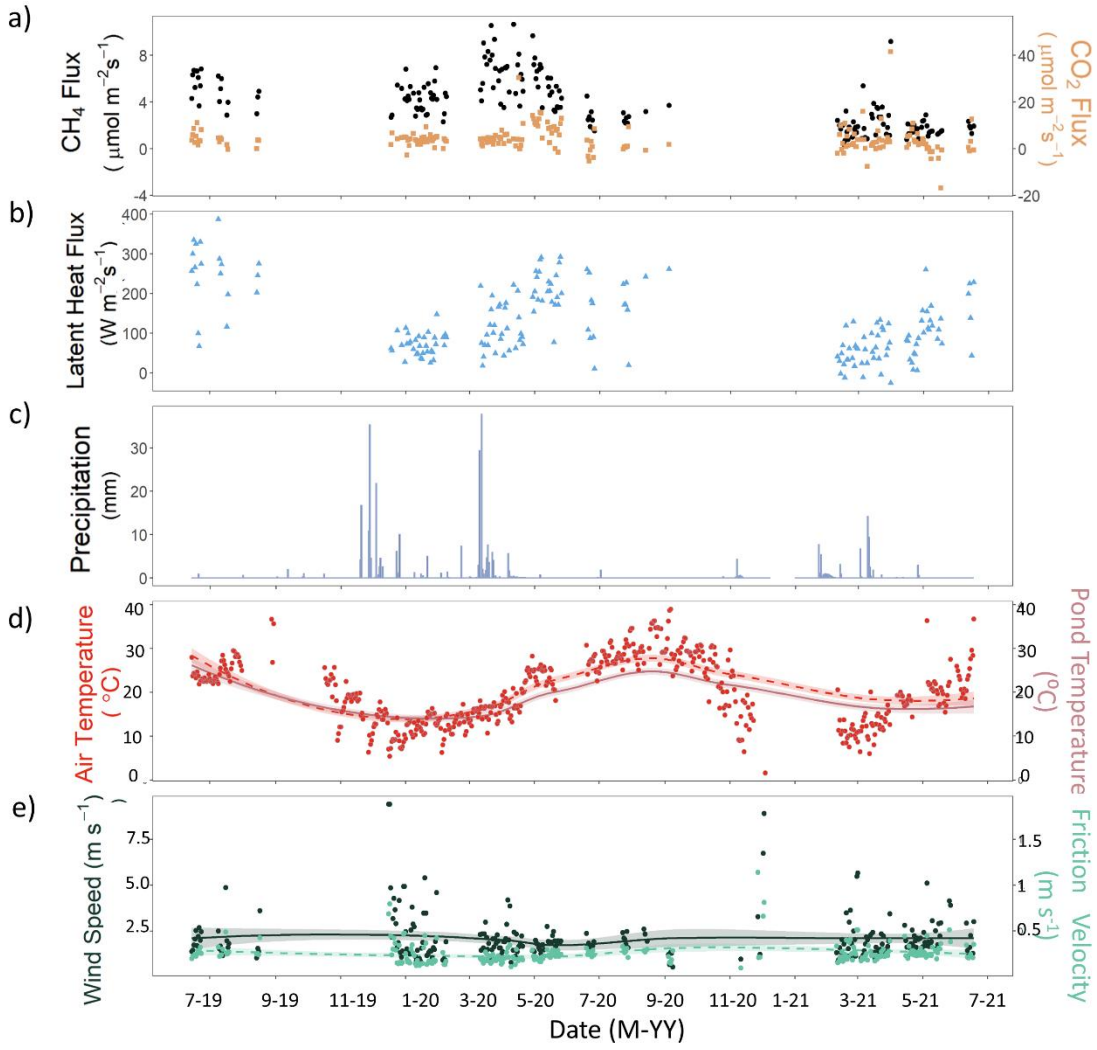

Figure 4.6. Time series of average daily methane fluxes and carbon dioxide fluxes (a), latent heat fluxes (b), precipitation events (c), air and pond temperature (d), wind speed and friction velocity (e). Solid lines show the mean and shaded regions indicate the 95% confidence intervals.

Diurnal patterns show that air and pond temperatures increased during the day, reaching peak temperatures in the early afternoon (Figure 4.7). In general, air temperatures were high from noon to 4 p.m., followed by a gradual decrease in the late afternoon. Meanwhile, pond temperatures steadily increased from dawn until around 1 p.m., then declined slowly thereafter. Incoming shortwave radiation and sensible heat flux gradually

increased during the day, peaking between noon and 2 p.m., followed by a gradual decrease in the afternoon. Friction velocity also increased during the day, reaching peak velocities after 2 p.m., then gradually decreasing after 4 p.m.

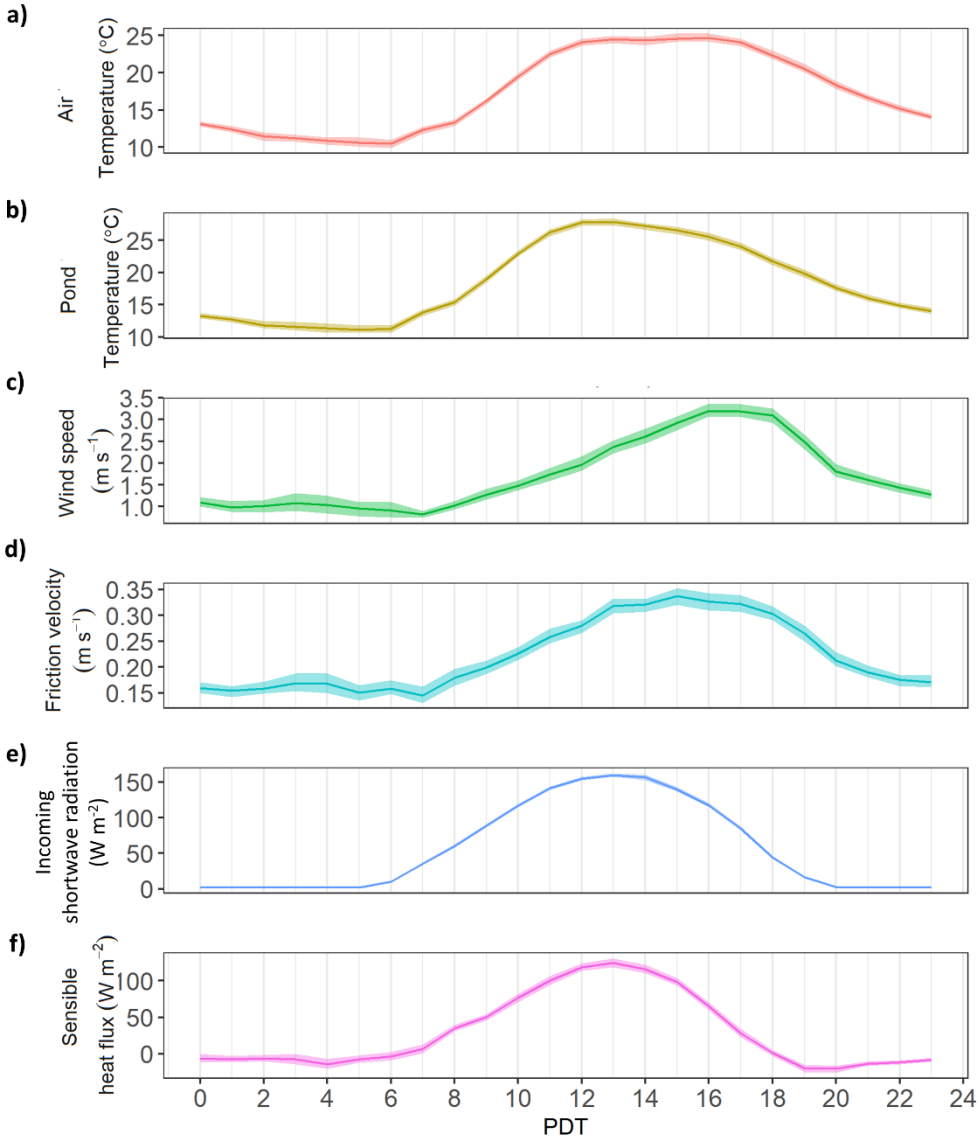

Figure 4.7. Diurnal variations of air temperature (a), surface pond temperature (b), wind speed (c), friction velocity (d), incoming shortwave radiation (e), and sensible heat flux (f). Solid lines show the hourly mean, and shaded regions indicate the 95% confidence intervals.

4.4.2 Temporal Variation in Fluxes

Average CH_4 fluxes (30-min averages) were 4.0 ± 2.6 µmol $m^{-2}s^{-1}$, and average CO_2 fluxes (30-min averages) were 4.6 ± 7.8 µmol $m^{-2}s^{-1}$. Average latent heat fluxes (30-min averages) were 139 ± 104 W $m^{-2}s^{-1}$. The 10th percentile of CH_4 flux observations was 1.13 µmol $m^{-2}s^{-1}$, whereas the 90th percentile of CH_4 flux observations was 7.65 µmol $m^{-2}s^{-1}$. In terms of CO_2 fluxes, the 10th percentile was -2.05 µmol $m^{-2}s^{-1}$, whereas the 90th percentile was 13.65 µmol $m^{-2}s^{-1}$.

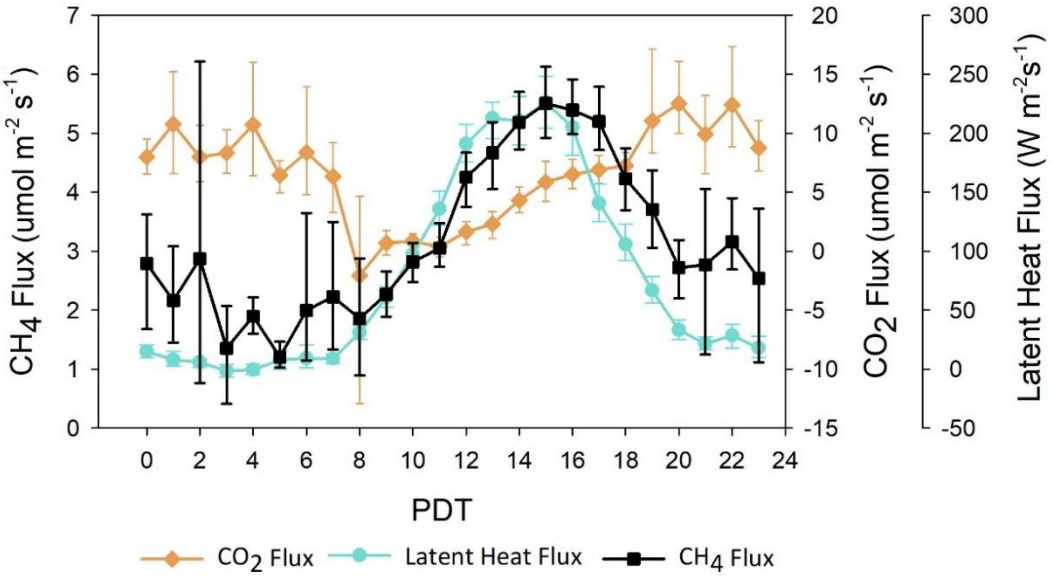

Figure 4.8. Diurnal hourly averaged fluxes of methane, carbon dioxide, and latent heat for the study period. The upper and lower bounds represent the 95% confidence interval in the mean. The uncertainty intervals are calculated through bootstrap re-sampling.

At the diurnal scale, the micrometeorological factors that had the strongest correlations with CH_4 fluxes were air and surface pond temperature, wind speed, and friction velocity based on linear regression models. The micrometeorological factors that had the strongest effects differed between the pre-sedimentation stage (June 2019 - May

2020) and post-sedimentation stage (June 2020 – June 2021). There was a strong diurnal relationship between CH_4 fluxes and surface pond temperature fluxes, especially during the pre-sedimentation stage of manure pond 1 (pond temperature $R^2 = 0.13$, $P < 0.0001$). However, the diurnal connection between CH_4 fluxes and pond temperature weakens post-sedimentation ($R^2 = 0.04$, $P < 0.001$). Methane fluxes and latent heat fluxes follow a similar diurnal pattern ($R^2 = 0.21$, $P < 0.0001$), with peaks during the early afternoon, when pond and air temperatures were also the highest (Figure 4.7). Wind speed also had a significant effect on diurnal CH_4 fluxes during both pre-sedimentation ($R^2 = 0.11$, $P < 0.0001$) and post-sedimentation ($R^2 = 0.19$, $P < 0.0001$) conditions. Friction velocity had a stronger influence on CH_4 fluxes during the post-sedimentation phase ($R^2 = 0.13$, $P < 0.0001$) than during the pre-sedimentation phase ($R^2 = 0.03$, $P < 0.001$) of manure pond 1.

During our study period, CH_4 fluxes from manure pond 1 decreased from 2019 to 2021, with the highest CH_4 fluxes observed during the spring period (March-May) in 2020 (Figure 4.9). Spring CH_4 fluxes decreased on average by 70% from 2020 to 2021 and summer CH_4 fluxes decreased on average by 57% from 2019 to 2021. Monthly CO_2 fluxes increased during the spring season and then decreased during the summer months, when there was vegetation growth in manure pond 1, driving photosynthesis and carbon uptake. Methane fluxes and CO_2 fluxes followed a similar seasonal pattern ($R^2 = 0.47$, $P < 0.01$). In contrast to diurnal CH_4 fluxes, seasonal CH_4 fluxes were not significantly correlated with seasonal latent heat flux ($R^2 = 0.05$, $P = 0.20$). Monthly latent heat fluxes increased during the summer, whereas monthly CH_4 fluxes decreased during the summer.

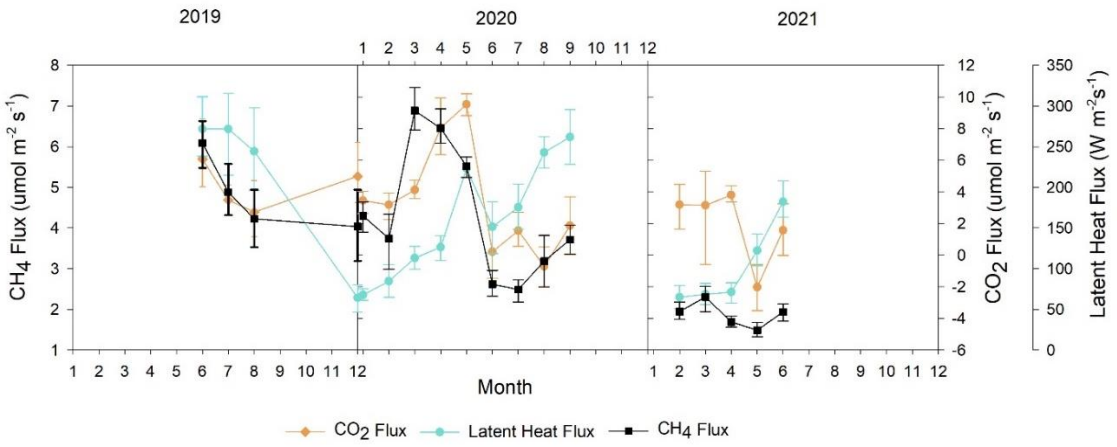

Figure 4.9. Average monthly fluxes of methane, carbon dioxide, and latent heat fluxes. The upper and lower bounds represent the 95% confidence interval in the mean. The uncertainty intervals are calculated through bootstrap re-sampling.

At our study site, precipitation events were highest during the winter and spring seasons. The highest precipitation events occurred during the months of March and April in the year 2020. Daily CH_4 fluxes were also highest during this time (Figure 4.6). Surface and pond temperatures were on average highest during the summer months of August and September. Similarly, incoming shortwave radiation was strongest during the summer months of August and September in 2020. There were no seasonal patterns observed for friction velocity and sensible heat flux.

4.4.3 Methane Emission Predictors

We evaluated which micrometeorological factors could be used to predict CH_4 fluxes from manure lagoons using Akaike's Information Criterion (AIC) (Sakamoto, Y., Ishiguro, M., 1986). Table 4.2 lists the models with the lowest AIC values with their corresponding square root of the mean square prediction error (RMSE). Model 1 represents the best prediction equation for diurnal CH_4 fluxes under all manure pond conditions. Wind

speed (u), friction velocity (u*), surface pond (T_{pond}) and air temperatures (T_{air}), and precipitation (P) were all important factors to estimate diurnal CH_4 fluxes. During the pre-sedimentation stage of manure pond 1, the prediction equation (Model 2) included wind speed, friction velocity, and surface pond and air temperatures. In contrast, during the post-sedimentation stage, the variables that were most relevant to estimate CH_4 fluxes were u, T_{pond} and T_{air} (Model 3). Seasonal CH_4 fluxes during the pre-sedimentation stage are best estimated using P, wind direction, T_{pond} and T_{air} (Model 4). During the post-sedimentation stage, u, u*, and T_{air} are important factors for seasonal CH_4 fluxes (Model 5).

Table 4.2. Methane Prediction Models with Akaike's Information Criterion (AIC), Square Root Mean Prediction Error (RMSE), Coefficient of Determination (R^2), and P-value.

Model	Time Period	Manure Pond 1 Conditions	Prediction Equation[1]	AIC	RMSE	R^2	*P*
1	Diurnal	All	$CH_4 = 2.69 + 1.22 \times u - 10.33\, x\, u* + 0.12 \times T_{pond} - 0.07 \times T_{air} + 4.21 \times P$	1115.8	2.3	0.13	<0.0001
2	Diurnal	Pre-sedimentation	$CH_4 = 3.06 + 0.18 \times T_{pond} + 1.02 \times u - 7.28 \times u* - 0.10\, T_{air}$	470.51	2.3	0.25	<0.0001
3	Diurnal	Post-sedimentation	$CH_4 = 0.64 - 0.07 \times T_{pond} + 0.48 \times u + 0.10\, T_{air}$	90.71	1.41	0.25	<0.0001
4	Seasonal	Pre-sedimentation	$CH_4 = -35.6 + 0.52 \times T_{pond} + 0.14 \times WD - 0.61\, T_{air} + 19.5 \times R$	-19.51	0.16	0.95	<0.01
5	Seasonal	Post-sedimentation	$CH_4 = 6.97 + 1.77 \times u + 0.04\, T_{air} - 34.9 \times u*$	-18.07	1.21	0.84	0.02

[1]Wind speed (u), friction velocity (u*), surface pond temperature (T_{pond}), air temperature T_{air}), precipitation (P), wind direction (WD).

4.4.4 Biogeochemical Conditions

On August 28, 2019, the pH values ranged between 6.9 to 8.3 at manure pond 1. The surface of manure pond 1 had the highest pH values, with the highest pH value at location 1 (L1) near the pond inlet. pH decreased with depth at each sampling location and across the lagoon's surface from location 1 (L1) to location 3 (L3) (Figure 4.10). Pond temperatures were highest at the surface level and closer to the inlet, with a maximum pond temperature of 28º C. The lowest pond temperature, 22.2º C, was observed in location 3 (L3) at a depth of 0.3 m. ORP values ranged from -283 to 15 mV. ORP values were less than -200 mV at all locations at 0.3 m and at location 3 at 0.8 m. The lowest ORP value was observed at a depth of 0.3 m near the inlet. Total solids (TS) ranged from 0.15 to 8%, with the highest TS levels observed at 0.3 m near the inlet. Fixed solids (FS) levels ranged from 49 to 63%, with highest levels observed across the surface of location 2 (60%) and at 0.3 m (63%) at location 3. Volatile solids (VS) ranged from 0 to 4%, with the highest levels observed at 0.3 m near the inlet at location 1 (L1).

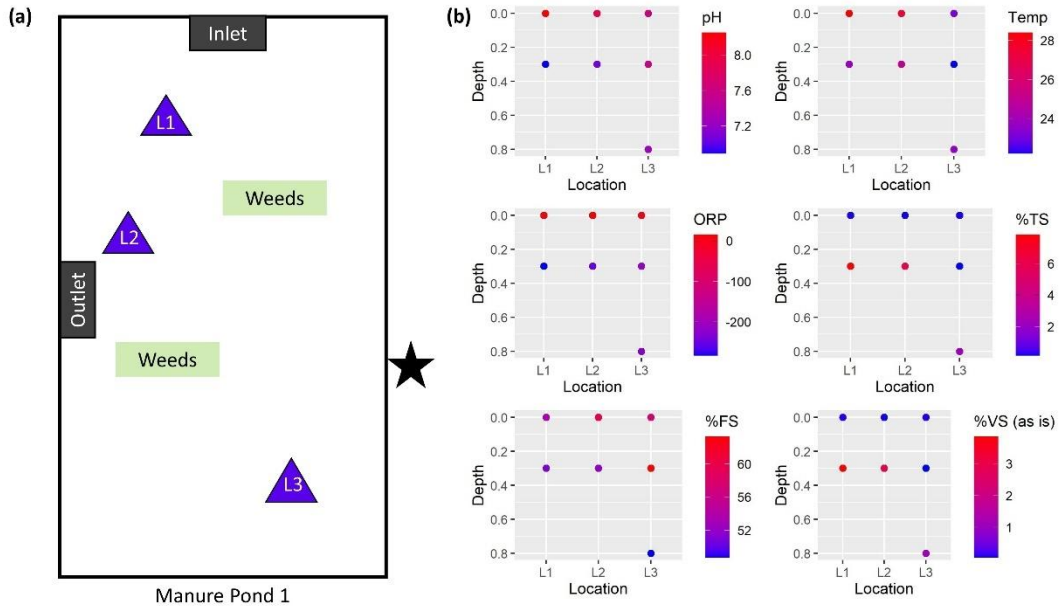

Figure 4.10. Manure pond 1 biogeochemical characteristics sampled in August 2019. (a) Schematic of sampling locations (L1, L2, L3), indicated by purple triangles, on manure pond 1. The location of the eddy covariance tower is represented by the black star. (b) Manure pond biogeochemical characteristics: pH, temperature (Temp), oxidation-reduction potential (ORP), total solids (TS), fixed solids (FS), and volatile solids (VS).

4.5 Discussion

4.5.1 Diurnal and Seasonal Variability in CH_4 Fluxes

Methane fluxes from the manure ponds had a robust diurnal pattern, increasing with air and surface pond temperatures. As such, latent heat flux and CH_4 flux also had a strong positive diurnal relationship, especially during the pre-sedimentation stage. Higher wind speed and friction velocity also increased diurnal maxima of CH_4 fluxes. Rising lagoon temperatures and wind speeds commonly enhance CH_4 emissions by promoting high microbial activity, diffusion, and convection of liquid manure storage (Sommer et al., 2007; Leytem et al., 2017; Amini et al., 2022). Another eddy covariance study also found

that wind speed increased CH_4 fluxes from manure lagoons in California, with a range between 20 to 65 kg $m^{-2}yr^{-1}$.

Seasonal patterns, in contrast, were dominated by other factors such as precipitation events, seasonal variations in substrate availability, and manure management practices. We observed the highest CH_4 fluxes during the spring season of 2020 after heavy precipitation events (6 events > 5 mm/day). Increased CH_4 fluxes during this period was likely driven by perturbation of the pond surface, increased wastewater inputs to the manure pond system, and/or a combination of both. Previous research has shown an increase in CH_4 emissions after a rainfall event as it agitates the surface of the manure pond, releasing an outburst of trapped gas bubbles (ebullition) (Kaharabata & Schuepp, 1998; Minato et al., 2013; Leytem et al., 2017; Arndt et al., 2018; Kupper et al., 2020). A similar case is observed after surface thawing events, wherein trapped CH_4 is released (VanderZaag et al., 2010, 2011; Leytem et al., 2017). In addition, it is likely that during these precipitation events extra manure from the corral surface entered the manure pond system due to the engineering design of the manure pond system. Specifically, sufficiently large rainfall events flush manure deposited in the corral area into the channel that conveys wastewater to the lagoon, increasing the amount of manure substrate deposited to the system

Seasonal changes in substrate availability, sometimes termed the seasonal hysteresis effect, may also explain the rising CH_4 fluxes observed during the spring season. Methanogenesis rates are slowest during the winter season when temperatures are low, leading to a buildup of volatile solids in the manure ponds. As temperatures rise during the spring season, manure ponds release more CH_4 compared to other seasons with comparable

temperatures because of greater availability of substrate due to winter buildups (Chang et al., 2021). Future modeling studies are needed to assess how much of an impact these factors contribute to increased seasonal CH_4 fluxes.

A stark decrease in monthly CH_4 fluxes from 2019 to 2021 was likely driven by changes in CH_4 production and consumption rates and transport pathways. The area covered by crust and vegetation substantially increased from June 2020 to June 2021, providing a favorable environment for CH_4 oxidation under aerobic conditions and slower diffusion rates (Petersen et al., 2005; Petersen & Ambus, 2006; Nielsen et al., 2010).Vegetation with aerenchyma formations may serve as both a conduit to transport CH_4 from the lagoon to the atmosphere or provide an environment for CH_4 oxidation and production (Laanbroek, 2010; Iwata et al., 2018; Knox et al., 2021). Given that CH_4 fluxes drastically decreased after crust formation, there was likely an increase in CH_4 oxidation and a slower diffusion of gases to the atmosphere. Future work is needed to investigate the role of vegetation and crust formation on CH_4 emissions from manure ponds.

Based on manure sampling in August 2019, we assessed that CH_4 was produced deeper in the water column or sludge layer of the manure pond at 0.3 m and 0.8 m, especially closer to the inlet at location 1 and location 2. Neutral pH conditions and low ORP levels less than -200 mV were found at 0.3 m and 0.8 m, providing a conducive environment for methanogenesis. The ORP levels were greater than 0 mV at the surface layer of manure pond, indicative of biomass accumulation, which likely increased occurred during the sedimentation stage (Kaffka & Barzee, 2016). This coincides with the crust layer formation at the surface. The most alkaline conditions were found at the surface at location

1 and location 2, which likely inhibits methanogenesis. In addition, higher TS and VS content was measured near the inlet, at location 1 and location 2 at 0.3 and 0.8 m, providing biodegradable organic matter needed to produce CH_4 (J.D. Wood et al., 2012).

4.5.2 Scaling up Multiple CH_4 Flux methods to Estimate Emissions

We evaluated our eddy covariance CH_4 fluxes by comparing it to other estimates using different techniques. A scaling factor was used to compare between this study's CH_4 flux estimate using the eddy covariance technique with the Thiruvenkatachari et al. (2020) study and the floating chamber pilot study discussed in Section 4.3.6. To best compare to these studies, we only selected daytime CH_4 fluxes (10:00 – 15:00) measured in August 2019, before there was significant crust formation, considering that the Thiruvenkatachari et al. (2020) study measured during the daytime hours (10:00 – 15:00) on August 14, 2018, and the floating chamber pilot study was conducted during the daytime hours (9:30 – 14:00) on August 15, 2019. It is also important to consider that the CH_4 flux footprint (Figure 4.3) of our eddy covariance measurements primarily captures Source Area 3 & Source Area 4 of manure pond 1 (Figure 4.3). As such, we estimate that 24 kg CH_4 d^{-1} (95% confidence interval: 18 – 29 kg d^{-1}) is emitted from Source Area 3 & 4 during the daytime (10:00 – 15:00) in August 2019. To estimate a scaling factor, we compared our eddy covariance's CH_4 fluxes with the Thiruvenkatachari et al. (2020) study's CH_4 emission estimate for Source Area 4. Thiruvenkatachari et al. (2020)'s CH_4 emission estimate is 3.7 times higher than our eddy covariance CH_4 flux estimate for Source Area 4. As such, we estimated CH_4 emissions for the entire manure pond complex (Figure 4.1, manure ponds 1-5) by applying this scaling factor to Thiruvenkatachari et al. (2020)'s CH_4

emission estimates for the rest of the manure pond sources. Thus, we estimate that 117 kg CH_4 d^{-1} is emitted from the manure pond complex (Figure 4.1, Table 4.3, manure ponds 1-5), or 81 g CH_4 $head^{-1}$ d^{-1} using the eddy covariance technique. In comparison, Thiruvenkatachari et al. (2020)'s estimates a total of 387 kg CH_4 d^{-1} is emitted from manure pond 1. Floating chamber measurements were also consistent with the concentration gradient observed in the Thiruvenkatachari et al., (2020) study with CH_4 emission estimates of 172, 89, and 28 kg d^{-1} for Source Area 1, 3, and 4, respectively (Table 4.3; Carranza & Caruso, unpublished data). All methods estimate CH_4 emissions within the same order of magnitude for each of the corresponding areas in manure pond 1 (Table 4.3).

Table 4.3. Methane Emission Estimates Using the Floating Chamber, Dispersion Model, and Eddy Covariance Technique From the Manure Pond Complex.

Manure Pond Source Areas	**Methane Emissions (kg d^{-1})**		
	Floating Chamber	**Dispersion Model (95% confidence limits)**	**Eddy Covariance**
Manure Pond 1 Source Area 1	172	200 (160 – 236)	54
Manure Pond 1 Source Area 2	-	89 (62 – 117)	24
Manure Pond 1 Source Area 3	89	55 (33 – 78)	15
Manure Pond 1 Source Area 4	28	43 (9 – 75)	12
Manure Pond 2	-	-	2.9
Manure Pond 3	-	-	2.9
Manure Pond 4	-	-	2.9
Manure Pond 5	-	-	2.9

As shown in this study, there are both strengths and disadvantages of using the eddy covariance technique to estimate CH_4 fluxes from dairy manure lagoons. An important strength of eddy covariance is that we can estimate CH_4 fluxes at both diurnal and seasonal time-scales. This allows to better predict the most influential drivers of CH_4 fluxes at different time scales and provides important information for manure management strategies. For example, dredging the manure pond during the winter season may substantially reduce CH_4 emissions during the spring season, when CH_4 fluxes were highest. The limitation of the eddy covariance technique is that can prove challenging to capture CH_4 fluxes from the entire manure pond complex when there are changes in the predominant wind direction. In our study, we primarily captured portions of Source Area 3 and 4 based on the CH_4 flux footprint. Moreover, there could be substantial loss of data based on changes in predominant wind direction. As such, we recommend that future studies carefully plan the best location of the eddy covariance tower to avoid significant data loss and consider using multiple eddy covariance towers to fully capture different areas of dairy manure lagoons under different predominant wind directions.

4.6 Conclusion

In summary, CH_4 fluxes from manure lagoons varied across different timescales, both diurnally and seasonally. The primary factors influencing diurnal CH_4 fluxes were also different from those driving the seasonal pattern of CH_4 fluxes. Temperature and wind speed affected diurnal CH_4 fluxes the most. In contrast, seasonal CH_4 fluxes were most likely impacted by precipitation events, changes in substrate availability, and manure management practices. Higher CH_4 fluxes were observed during the spring seasons, when

methanogenesis rates increase with warmer manure pond temperatures and after precipitation events. This suggests that manure management practices, such as dredging manure ponds, during the winter months could potentially have the greatest reduction of CH_4 emissions. Understanding how CH_4 fluxes change over time, and which factors most control CH_4 emissions is important to develop methane reduction strategies in the agricultural sector.

4.7 References

Amini, S., Kuwayama, T., Gong, L., Falk, M., Chen, Y., Mitloehner, Q., Weller, S., Mitloehner, F. M., Patteson, D., Conley, S. A., Scheehle, E., & FitzGibbon, M. (2022). Evaluating California dairy methane emission factors using short-term ground-level and airborne measurements. *Atmospheric Environment: X*, *14*(November 2021), 100171. https://doi.org/10.1016/j.aeaoa.2022.100171

Arndt, C., Leytem, A. B., Hristov, A. N., Zavala-Araiza, D., Cativiela, J. P., Conley, S., Daube, C., Faloona, I., & Herndon, S. C. (2018). Short-term methane emissions from 2 dairy farms in California estimated by different measurement techniques and US Environmental Protection Agency inventory methodology: A case study. *Journal of Dairy Science*, *101*(12), 11461–11479. https://doi.org/10.3168/jds.2017-13881

Aubinet, M., Vesala, T., & Papale, D. (2012). Eddy Covariance: A Pratical Guide to Measurement and Data Analysis. In *Springer*.

Bagtang, M., McCorkle, S., & Scott, B. (2020). *The Generation of Synthetic Diesel and Other Synthetic Petroleum Products Through the Fischer- Tropsch Synthesis Process Via the Gasification of Dairy Manure Solids and Utilization of Biogas* (Issue July).

Baldé, H., VanderZaag, A. C., Burtt, S., Evans, L., Wagner-Riddle, C., Desjardins, R. L., & MacDonald, J. D. (2016). Measured versus modeled methane emissions from separated liquid dairy manure show large model underestimates. *Agriculture, Ecosystems and Environment*, *230*, 261–270. https://doi.org/10.1016/j.agee.2016.06.016

Barber, T. R., Burke, R. A., & Sackett, W. M. (1988). Diffusive flux of methane from warm wetlands. *Global Biogeochemical Cycles*, *2*(4), 411–425. https://doi.org/10.1029/GB002i004p00411CARB. (2020). *California Greenhouse Gas Emissions Inventory: 2000– 2020*.

Chang, K.-Y., Riley, W. J., Knox, S. H., Jackson, R. B., McNicol, G., Poulter, B., Aurela, M., Baldocchi, D., Bansal, S., Bohrer, G., Campbell, D. I., Cescatti, A., Chu, H., Delwiche, K. B., Desai, A. R., Euskirchen, E., Friborg, T., Goeckede, M., Helbig, M., … Zona, D. (2021). Substantial hysteresis in emergent temperature sensitivity of global wetland CH4 emissions. *Nature Communications*, *12*(1), 2266. https://doi.org/10.1038/s41467-021-22452-1

Chanton, J. P., Martens, C. S., & Kelley, C. A. (1989). Gas transport from methane-saturated, tidal freshwater and wetland sediments. *Limnology and Oceanography*, *34*(5), 807–819. https://doi.org/10.4319/lo.1989.34.5.0807

Conrad, R. (1989). Control of methane production in terrestrial ecosystems. In *Exchange of trace gases between terrestrial ecosystems and the atmosphere* (pp. 39–58).

Fan, S.-M., Wofsy, S. C., Bakwin, P. S., Jacob, D. J., & Fitzjarrald, D. R. (1990). Atmosphere-biosphere exchange of CO 2 and O 3 in the central Amazon Forest. *Journal of Geophysical Research*, *95*(D10), 16851. https://doi.org/10.1029/JD095iD10p16851

Foken, T., Göockede, M., Mauder, M., Mahrt, L., Amiro, B., & Munger, W. (2004). Post-Field Data Quality Control. *Handbook of Micrometeorology*, 181–208. https://doi.org/10.1007/1-4020-2265-4_9

Gerardo-Nieto, O., Vega-Peñaranda, A., Gonzalez-Valencia, R., Alfano-Ojeda, Y., & Thalasso, F. (2019). Continuous Measurement of Diffusive and Ebullitive Fluxes of Methane in Aquatic Ecosystems by an Open Dynamic Chamber Method. *Environmental Science & Technology*, *53*, 5159–5167. https://doi.org/10.1021/acs.est.9b00425

Habtewold, J., Gordon, R. J., Wood, J. D., Wagner-Riddle, C., VanderZaag, A. C., & Dunfield, K. E. (2017). Dairy Manure Total Solid Levels Impact CH4 Flux and Abundance of Methanogenic Archaeal Communities. *Journal of Environmental Quality*, *46*(1), 232–236. https://doi.org/10.2134/jeq2016.11.0451

Harper, L. A., Denmead, O. T., & Flesch, T. K. (2011). Micrometeorological techniques for measurement of enteric greenhouse gas emissions. *Animal Feed Science and Technology*, *166–167*, 227–239. https://doi.org/10.1016/j.anifeedsci.2011.04.013

Iwata, H., Hirata, R., Takahashi, Y., Miyabara, Y., Itoh, M., & Iizuka, K. (2018). Partitioning Eddy-Covariance Methane Fluxes from a Shallow Lake into Diffusive and Ebullitive Fluxes. *Boundary-Layer Meteorology*, *169*(3), 413–428. https://doi.org/10.1007/s10546-018-0383-1

Kaffka, S., & Barzee, T. (2016). *Evaluation of Dairy Manure Management Practices for Greenhouse Gas Emissions Mitigation in California*.

Kaharabata, S. K., & Schuepp, P. H. (1998). Methane emissions from aboveground open manure slurry tanks oxygen demand z 218. *Global Biogeochemical Cycles*, *12*(3), 545–554.

Kaharabata, S. K., Schuepp, P. H., & Desjardins, R. L. (1998). Methane emissions from above ground open manure slurry tanks. *Global Biogeochemical Cycles*, *12*(3), 545–554. https://doi.org/10.1029/98GB01866

Kebreab, E., Clark, K., Wagner-Riddle, C., & France, J. (2006). Methane and nitrous oxide emissions from Canadian animal agriculture: A review. *Canadian Journal of Animal Science*, *86*(2), 135–157. https://doi.org/10.4141/A05-010

Kljun, N., Calanca, P., Rotach, M. W., & Schmid, H. P. (2015). A simple two-dimensional parameterisation for Flux Footprint Prediction (FFP). *Geoscientific Model Development*, *8*(11), 3695–3713. https://doi.org/10.5194/gmd-8-3695-2015

Knox, S. H., Bansal, S., McNicol, G., Schafer, K., Sturtevant, C., Ueyama, M., Valach, A. C., Baldocchi, D., Delwiche, K., Desai, A. R., Euskirchen, E., Liu, J., Lohila, A., Malhotra, A., Melling, L., Riley, W., Runkle, B. R. K., Turner, J., Vargas, R., … Jackson, R. B. (2021). Identifying dominant environmental predictors of freshwater wetland methane fluxes across diurnal to seasonal time scales. *Global Change Biology*, *27*(15), 3582–3604. https://doi.org/10.1111/gcb.15661

Koebsch, F., Jurasinski, G., Koch, M., Hofmann, J., & Glatzel, S. (2015). Controls for multi-scale temporal variation in ecosystem methane exchange during the growing season of a permanently inundated fen. *Agricultural and Forest Meteorology*, *204*, 94–105. https://doi.org/10.1016/j.agrformet.2015.02.002

Kupper, T., Häni, C., Neftel, A., Kincaid, C., Bühler, M., Amon, B., & VanderZaag, A. (2020). Ammonia and greenhouse gas emissions from slurry storage - A review. *Agriculture, Ecosystems & Environment*, *300*, 106963. https://doi.org/10.1016/j.agee.2020.106963

Laanbroek, H. J. (2010). Methane emission from natural wetlands: interplay between emergent macrophytes and soil microbial processes. A mini-review. *Annals of Botany*, *105*(1), 141–153. https://doi.org/10.1093/aob/mcp201

Leytem, A. B., Bjorneberg, D. L., Koehn, A. C., Moraes, L. E., Kebreab, E., & Dungan, R. S. (2017). Methane emissions from dairy lagoons in the western United States. *Journal of Dairy Science*, *100*(8), 6785–6803. https://doi.org/10.3168/jds.2017-12777

Liu, Y., & Whitman, W. B. (2008). Metabolic, Phylogenetic, and Ecological Diversity of the Methanogenic Archaea. *Annals of the New York Academy of Sciences*, *1125*(1), 171–189. https://doi.org/10.1196/annals.1419.019

Lorke, A., Bodmer, P., Noss, C., Alshboul, Z., Koschorreck, M., Bastviken, D., & Flury, S. (2015). *Technical note : drifting versus anchored flux chambers for measuring greenhouse gas emissions from running waters*. 7013–7024. https://doi.org/10.5194/bg-12-7013-2015

Marklein, A. R., Meyer, D., Fischer, M. L., Jeong, S., Rafiq, T., Carr, M., & Hopkins, F. M. (2021). Facility-scale inventory of dairy methane emissions in California: implications for mitigation. *Earth System Science Data*, *13*(3), 1151–1166. https://doi.org/10.5194/essd-13-1151-2021

Martinsen, K. T., Kragh, T., & Sand-jensen, K. (2018). Technical note : A simple and cost-efficient automated floating chamber for continuous measurements of carbon dioxide gas flux on lakes. *Biogeosciences*, *15*, 5565–5573. https://doi.org/https://doi.org/10.5194/bg-15-5565-2018

Mauder, M., & Foken, T. (2006). Impact of post-field data processing on eddy covariance flux estimates and energy balance closure. *Meteorologische Zeitschrift*, *15*(6), 597–609. https://doi.org/10.1127/0941-2948/2006/0167

McGinn, S. M. (2013). Developments in micrometeorological methods for methane measurements. *Animal*, *7*(s2), 386–393. https://doi.org/10.1017/S1751731113000657

Miller, D. J., Sun, K., Tao, L., Pan, D., Zondlo, M. A., Nowak, J. B., Liu, Z., Diskin, G., Sachse, G., Beyersdorf, A., Ferrare, R., & Scarino, A. J. (2015). Ammonia and methane dairy emission plumes in the San Joaquin Valley of California from individual feedlot to regional scales. *Journal of Geophysical Research: Atmospheres*, *120*(18), 9718–9738. https://doi.org/10.1002/2015JD023241

Minato, K., Kouda, Y., Yamakawa, M., Hara, S., Tamura, T., & Osada, T. (2013). Determination of GHG and ammonia emissions from stored dairy cattle slurry by using a floating dynamic chamber. *Animal Science Journal*, *84*(2), 165–177. https://doi.org/10.1111/j.1740-0929.2012.01053.x

Moncrieff, J., Clement, R., Finnigan, J., & Meyers, T. (2004). Averaging, Detrending, and Filtering of Eddy Covariance Time Series. In *Handbook of Micrometeorology* (pp. 7–31). Kluwer Academic Publishers. https://doi.org/10.1007/1-4020-2265-4_2

Moncrieff, J., Massheder, J. M., de Bruin, H., Elbers, J., Friborg, T., Heusinkveld, B., Kabat, P., Scott, S., Soegaard, H., & Verhoef, A. (1997). A system to measure surface fluxes of momentum, sensible heat, water vapour and carbon dioxide. *Journal of Hydrology*, *188–189*(1–4), 589–611. https://doi.org/10.1016/S0022-1694(96)03194-0

Morin, T. H., Bohrer, G., Frasson, R. P. d. M., Naor-Azreli, L., Mesi, S., Stefanik, K. C., & Schäfer, K. V. R. (2014). Environmental drivers of methane fluxes from an urban temperate wetland park. *Journal of Geophysical Research: Biogeosciences*, *119*(11), 2188–2208. https://doi.org/10.1002/2014JG002750

Nielsen, D. A., Nielsen, L. P., Schramm, A., & Revsbech, N. P. (2010). Oxygen Distribution and Potential Ammonia Oxidation in Floating, Liquid Manure Crusts. *Journal of Environmental Quality*, *39*(5), 1813–1820. https://doi.org/10.2134/jeq2009.0382

Owen, J. J., & Silver, W. L. (2015). Greenhouse gas emissions from dairy manure management: a review of field-based studies. *Global Change Biology*, *21*(2), 550–565. https://doi.org/10.1111/gcb.12687

Petersen, S. O., & Ambus, P. (2006). Methane Oxidation in Pig and Cattle Slurry Storages, and Effects of Surface Crust Moisture and Methane Availability. *Nutrient Cycling in Agroecosystems*, *74*(1), 1–11. https://doi.org/10.1007/s10705-005-3822-6

Petersen, S. O., Amon, B., & Gattinger, A. (2005). Methane oxidation in slurry storage surface crusts. *Journal of Environmental Quality*, *34*(2), 455–461. https://doi.org/https://doi.org/10.2134/jeq2005.455

Ripley, B. D. (2002). *Modern applied statistics with S*. Springer.

Ro, K. S., & Hunt, P. G. (2006). New Unified Equation for Wind-Driven Surficial Oxygen Transfer into Stationary Water Bodies. *Transactions of the ASABE*, *49*(5), 1615–1622. https://doi.org/10.13031/2013.22020

Saggar, S., Bolan, N. S., Bhandral, R., Hedley, C. B., & Luo, J. (2004). A review of emissions of methane, ammonia, and nitrous oxide from animal excreta deposition and farm effluent application in grazed pastures. *New Zealand Journal of Agricultural Research*, *47*(4), 513–544. https://doi.org/10.1080/00288233.2004.9513618

Sakamoto, Y., Ishiguro, M., and K. G. (1986). *Akaike Information Criterion Statistics.* D. Reidel Publishing Company.

Sommer, S. G., Petersen, S. O., & Møller, H. B. (2004). Algorithms for calculating methane and nitrous oxide emissions from manure management. *Nutrient Cycling in Agroecosystems*, *69*(2), 143–154. https://doi.org/10.1023/B:FRES.0000029678.25083.fa

Sommer, S. G., Petersen, S. O., Sørensen, P., Poulsen, H. D., & Møller, H. B. (2007). Methane and carbon dioxide emissions and nitrogen turnover during liquid manure storage. *Nutrient Cycling in Agroecosystems*, *78*(1), 27–36. https://doi.org/10.1007/s10705-006-9072-4

Thiruvenkatachari, R. R., Carranza, V., Ahangar, F., Marklein, A., Hopkins, F., & Venkatram, A. (2020). Uncertainty in using dispersion models to estimate methane emissions from manure lagoons in dairies. *Agricultural and Forest Meteorology*, *290*, 108011. https://doi.org/10.1016/j.agrformet.2020.108011

VanderZaag, A. C., Gordon, R. J., Jamieson, R. C., Burton, D. L., & Stratton, G. W. (2010). Effects of winter storage conditions and subsequent agitation on gaseous emissions from liquid dairy manure. *Canadian Journal of Soil Science*, *90*(1), 229–239. https://doi.org/10.4141/CJSS09040

VanderZaag, A. C., Wagner-Riddle, C., Park, K. H., & Gordon, R. J. (2011). Methane emissions from stored liquid dairy manure in a cold climate. *Animal Feed Science and Technology*, *166–167*, 581–589. https://doi.org/10.1016/j.anifeedsci.2011.04.041

Webb, E. K., Pearman, G. I., & Leuning, R. (1980). Correction of flux measurements for density effects due to heat and water vapour transfer. *Quarterly Journal of the Royal Meteorological Society*, *106*(447), 85–100. https://doi.org/10.1002/qj.49710644707

Whalen, S. C. (2005). Biogeochemistry of Methane Exchange between Natural Wetlands and the Atmosphere. *Environmental Engineering Science*, *22*(1), 73–94. https://doi.org/10.1089/ees.2005.22.73

Wilczak, J. M., Oncley, S. P., & Stage, S. A. (2001). Sonic anemometer tilt correction algorithms. *Boundary-Layer Meteorology*, *99*, 127–150.

Wood, J.D., Gordon, R. J., Wagner-Riddle, C., Dunfield, K. E., & Madani, A. (2012). Relationships between Dairy Slurry Total Solids, Gas Emissions, and Surface Crusts. *Journal of Environmental Quality*, *41*(3), 694–704. https://doi.org/10.2134/jeq2011.0333

Wood, Jeffrey D., Gordon, R. J., & Wagner-Riddle, C. (2013). Biases in discrete CH4 and N2O sampling protocols associated with temporal variation of gas fluxes from manure storage systems. *Agricultural and Forest Meteorology*, *171–172*, 295–305. https://doi.org/10.1016/j.agrformet.2012.12.014

You, Y., Staebler, R. M., Moussa, S. G., Beck, J., & Mittermeier, R. L. (2021). Methane emissions from an oil sands tailings pond: a quantitative comparison of fluxes derived by different methods. *Atmospheric Measurement Techniques*, *14*(3), 1879–1892. https://doi.org/10.5194/amt-14-1879-2021

5. Conclusion

The research presented here examined the CH_4, N_2O, and NH_3 emission trends from dairy farms at different timescales and from distinct source areas. Each project advances our understanding of CH_4 emissions from California dairy farms. In addition, it delivers effective source apportionment techniques that can be used to identify sources of emissions in mixed-source regions. The result from this research is critical to our understanding of seasonal and diurnal CH_4 fluxes from dairy manure lagoons in the state of California. Additionally, stable carbon isotopes of CH_4 and enhancement ratios between trace gases, may be used to evaluate the effectiveness of mitigation strategies as California moves toward meeting GHG reduction goals.

I have shown that $\delta^{13}C$ measurements of atmospheric CH_4 using a mobile platform can be used for source attribution of enteric and manure methane. My findings show that CH_4 from manure lagoons is more enriched in $\delta^{13}C$ than enteric fermentation emissions on average by $14 \pm 2‰$. A potential strategy to track the effectiveness of mitigation efforts is to measure $\delta^{13}C_{CH4}$ and quantify enteric: manure ratios over time. A recommended area of research is to gather more measurements of $\delta^{13}C$ and $\delta^{2}H$ of CH_4 and $\delta^{13}C\text{-}CO_2$ to disentangle and detect the CH_4 generation processes that drive manure lagoon emissions. This research is also important to the body of knowledge dedicated to investigating the sources and processes responsible for the increasing global mole fraction of atmospheric CH_4. An important area of future research is to investigate how $\delta^{13}C_{CH4}$ signatures change with mitigation efforts.

In the second body of research, we demonstrate that enhancement ratios can be used to characterize and identify emission sources from dairy farms. Animal housing (e.g.,

freestall barns, corrals), wet manure management (e.g., manure lagoons), dry manure management (e.g., dry bedding), silage piles, and cropland had distinct enhancement ratios (ΔNH_3:ΔCH_4 and ΔN_2O:ΔCH_4). Enhancement ratios for each source vary among seasons, underscoring the importance of seasonal studies. Dry bedding, crops, silage were characterized by relatively high NH_3 to CH_4 enhancement ratios. In contrast, crops, silage, and corrals had relatively high N_2O to CH_4 enhancement ratios. The highest enhancement ratios were observed in the summer and autumn. Enhancement ratios are particularly useful for source attribution of an emission plume in a mixed-source region. Future work is needed to identify which dairy management practices and physicochemical and meteorological factors influence the relative contributions of CH_4, NH_3, and N_2O emissions the most.

Lastly, the last body of research investigated how CH_4 fluxes from manure lagoons varied across different timescales, both diurnally and seasonally. The primary factors influencing diurnal CH_4 fluxes were different from those influencing the seasonal pattern of CH_4 fluxes. In particular, temperature and wind speed greatly influenced diurnal CH_4 fluxes. In comparison, seasonal CH_4 fluxes were most likely impacted by precipitation events, changes in substrate availability, and manure management practices. Higher CH_4 fluxes were observed during the spring season, after precipitation events that agitated the manure lagoon surface and when methanogenesis rates increased with warmer manure pond temperatures. Dredging the manure ponds during the winter months could potentially have the greatest reduction of CH_4 emissions. Future research should measure long-term seasonal CH_4 fluxes at a dairy farm in the SJV of California.

Appendix A1: Isotopic Signatures of Methane Emissions from Dairy Farms in California's San Joaquin Valley

A1.1 Introduction

The first part of Appendix A1 includes additional detail about the calibration method for CRDS measurements, dilution experiment described in section 2.3.4, an example of a time series plot of the comparison between the mobile laboratory sampling technique using CRDS with analysis of whole-air samples analyzed with IRMS. The second part includes isotopic signatures downwind of dairy farms (Table 2.4) with time series plots of the CH_4 hotspot, Keeling plots, location of the CH_4 measurements, wind direction, and CH_4 flux footprints of the CH_4 hotspots estimated by the Eulerian numerical dispersion model. The data is averaged to 15 sec intervals.

A1.2 Calibration Method

As discussed in section 2.3, trace gas mole fractions and isotope ratios were corrected using low and high custom gas mixtures that were measured before and after each measurement period. The low and high custom gas mixtures were each measured for a minimum of three minutes after values reached stabilization. The design of the mobile laboratory allowed for simultaneous measurements of the custom gas mixtures by both the Picarro G2210-*i* and Picarro G2401. Depending on the availability of calibration tanks for each campaign period, the low custom gas mixtures had CH_4 mole fractions that ranged from 1.92 ppm to 4.07 ppm and high custom gas mixtures with CH_4 mole fractions that

ranged from 3.02 ppm to 9.91 ppm. The isotopic values of the gas mixtures were -39.5‰ (Fall 2018, Spring 2019, Summer 2019), -40.7‰ (Fall 2019), and -38.5‰ (Winter 2020). We then used a two-point calibration method to adjust the observations with an offset based on the relationship between the observed and expected values. For the IRMS measurements, we used standards B-iso and H-iso. The $\delta^{13}C$ and δD of B-iso are -55.6‰ and -247‰, respectively, and for H-iso, the $\delta^{13}C$ and δD is-28.5‰ and -156‰, respectively.

A1.3 Dilution Experiment

A dilution experiment was conducted on January 20, 2021 to analyze the precision of $\delta^{13}C$-CH_4 sampled with the CRDS instrument at varying CH_4 mole fractions. CH_4 levels and measurement timing (15 second intervals) were chosen to mimic downwind plume sampling of dairies (section 2.4.2). Details of this experiment are described in section 2.3.4. Figure S1 show the Keeling plot of the dilution experiment measurements.

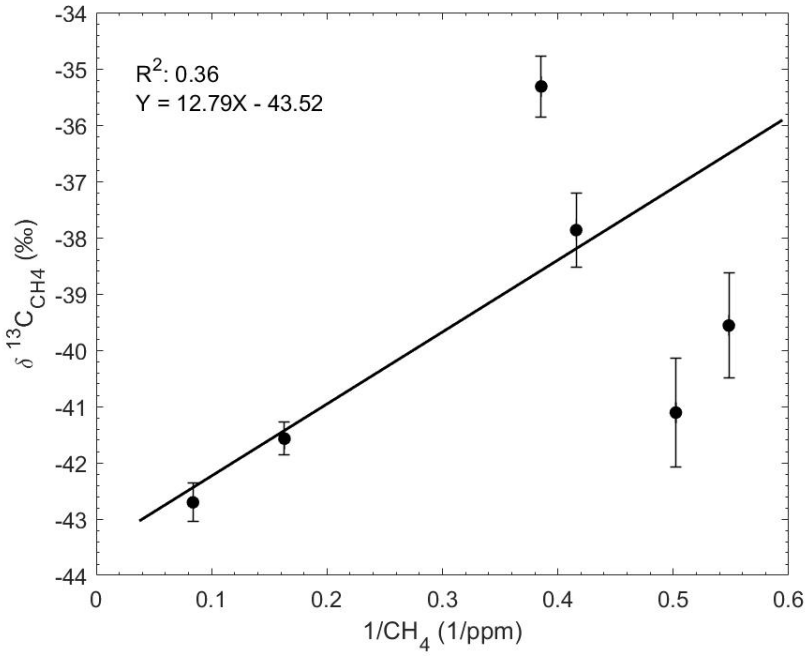

Figure S1. Keeling plot of dilution experiment measurements.

A1.3 Comparison between CRDS and IRMS Measurements

In addition to the analysis discussed in section 2.4, we explored how the isotopic composition measured by the CRDS changes with different time intervals (30 sec, 60 sec, 180 sec) in comparison to observations reported in Table 2.1. We found that the isotopic composition remains within the range reported by the IRMS for CH_4 mole fractions below 30 ppm, the reported upper limit for $\delta^{13}C_{CH4}$ measurements by the Picarro G2210-i. Accordingly, CH_4 mole fractions above 30 ppm were excluded from the farm-scale and downwind plume sampling analyses. Below is an example of a time series showing the comparison between CRDS and IRMS observations downwind of the primary lagoon. While CH_4 mole fractions varied across the measurement period, $\delta^{13}C_{CH4}$ remained

relatively constant, showing the influence of just the measured CH_4 source on the isotopic signature despite increasing dilution of the plume.

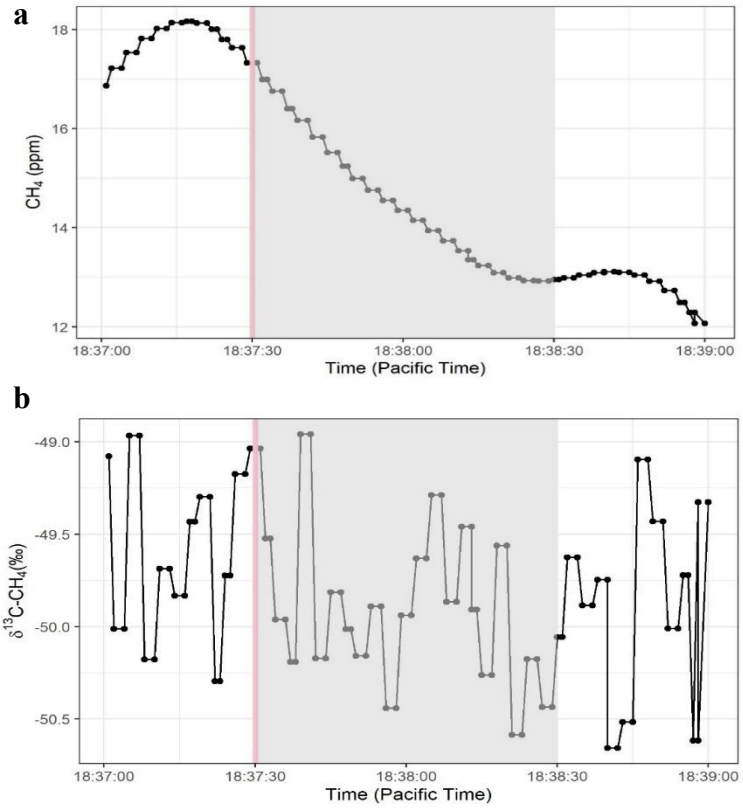

Figure S2. An example showing the comparison between CRDS and IRMS observations on March 25, 2019 from 18:37:30 - 18:38:30, downwind of the primary lagoon. The gray region indicates the time interval used to calculate the mean CH_4 mole fraction reported in Table 2.1 and the pink line indicates the approximate time of sample collection used for the IRMS method. a) Time series of CH_4 mole fraction measured by the CRDS. b) Time series of the CRDS $\delta^{13}C$-CH_4 observations.

A1.4 Downwind Plume Sampling

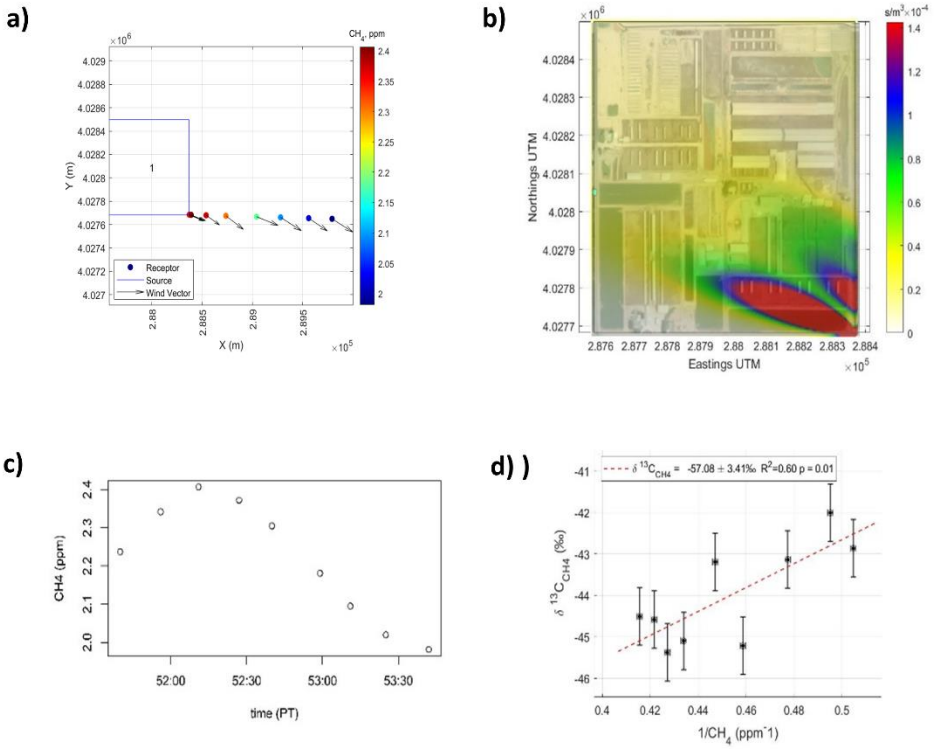

Figure S3. Isotopic signatures downwind of Dairy I on June 25th, 2019 from 15:51:40-15:53:50. a) Mobile platform measurements of 15-sec averaged CH_4 mole fractions (Receptor) downwind of Dairy I (Source). b) Methane flux footprint of Dairy I using the mobile survey shown in (a). The color gradient shows the relative contribution from the upwind areas where CH_4 was emitted. (c) Time series plot using 15-second averages from the mobile survey shown in (a). (d) Keeling plot using 15-second averages from the mobile survey shown in (a).

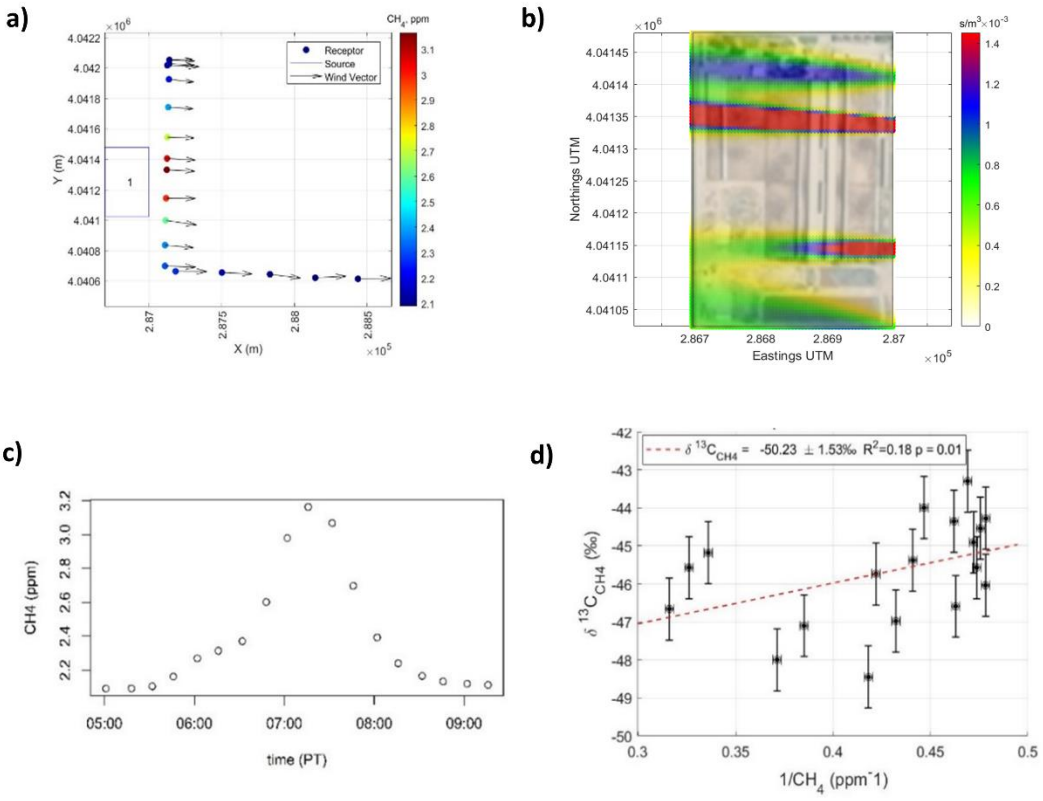

Figure S4. Isotopic signatures downwind of Dairy II on September 21st, 2018 from 18:05:01-18:09:30. a) Mobile platform measurements of 15-sec averaged CH_4 mole fractions (Receptor) downwind of Dairy II (Source). b) Methane flux footprint of Dairy II using the mobile survey shown in (a). The color gradient shows the relative contribution from the upwind areas where CH_4 was emitted. (c) Time series plot using 15-second averages from the mobile survey shown in (a). (d) Keeling plot using 15-second averages from the mobile survey shown in (a).

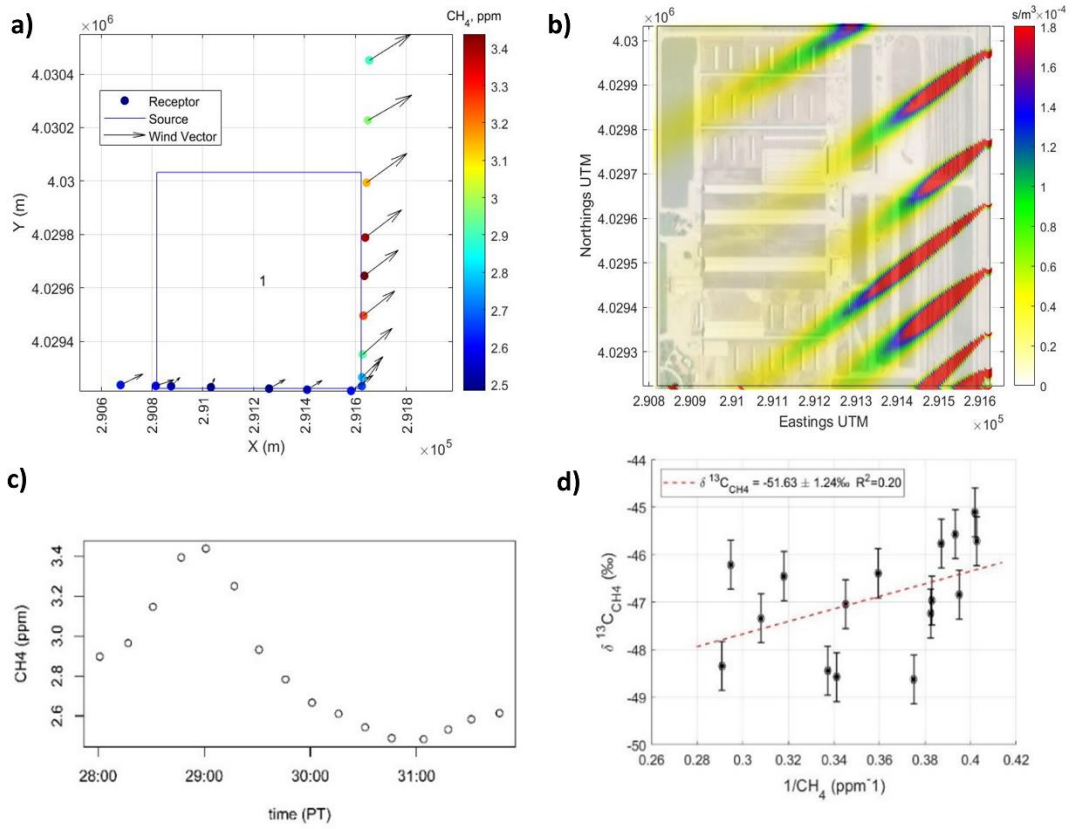

Figure S5. Isotopic signatures downwind of Dairy III on March 24th, 2019 from 13:28:01-13:32:00. a) Mobile platform measurements of 15-sec averaged CH_4 mole fractions (Receptor) downwind of Dairy III (Source). b) Methane flux footprint of Dairy III using the mobile survey shown in (a). The color gradient shows the relative contribution from the upwind areas where CH_4 was emitted. (c) Time series plot using 15-second averages from the mobile survey shown in (a). (d) Keeling plot using 15-second averages from the mobile survey shown in (a).

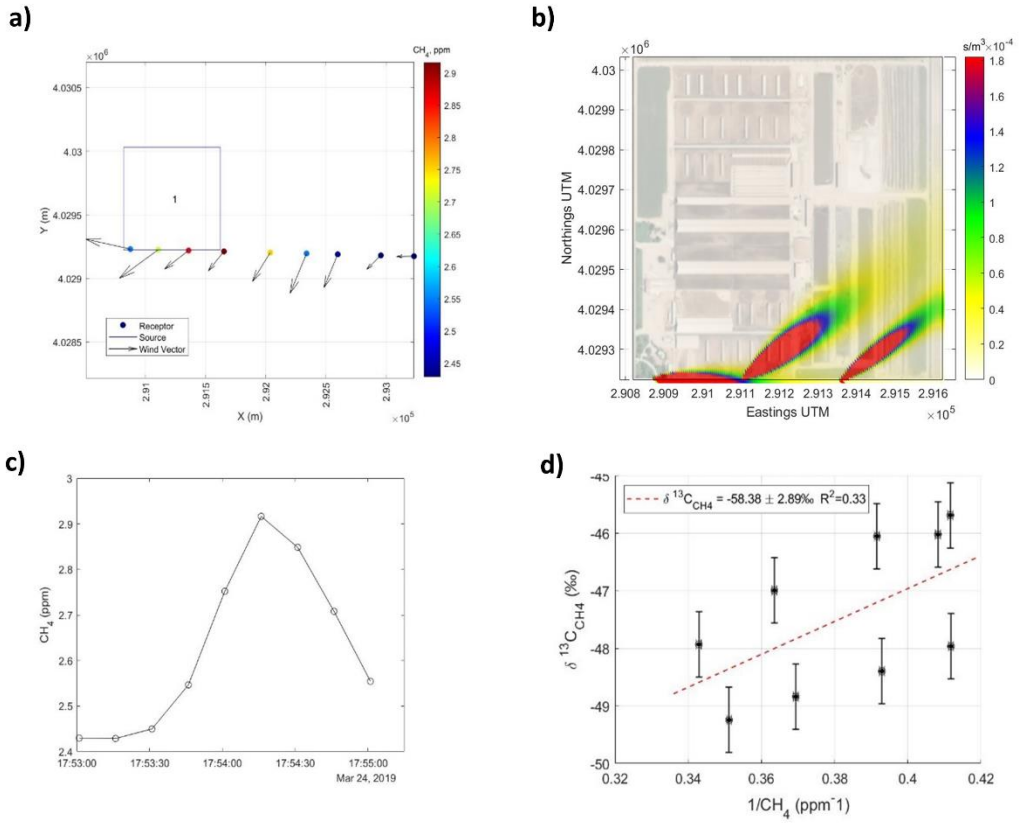

Figure S6. Isotopic signatures downwind of Dairy III on March 24th, 2019 from 17:53:01-17:55:13. a) Mobile platform measurements of 15-sec averaged CH_4 mole fractions (Receptor) downwind of Dairy III (Source). b) Methane flux footprint of Dairy III using the mobile survey shown in (a). The color gradient shows the relative contribution from the upwind areas where CH_4 was emitted. (c) Time series plot using 15-second averages from the mobile survey shown in (a). (d) Keeling plot using 15-second averages from the mobile survey shown in (a).

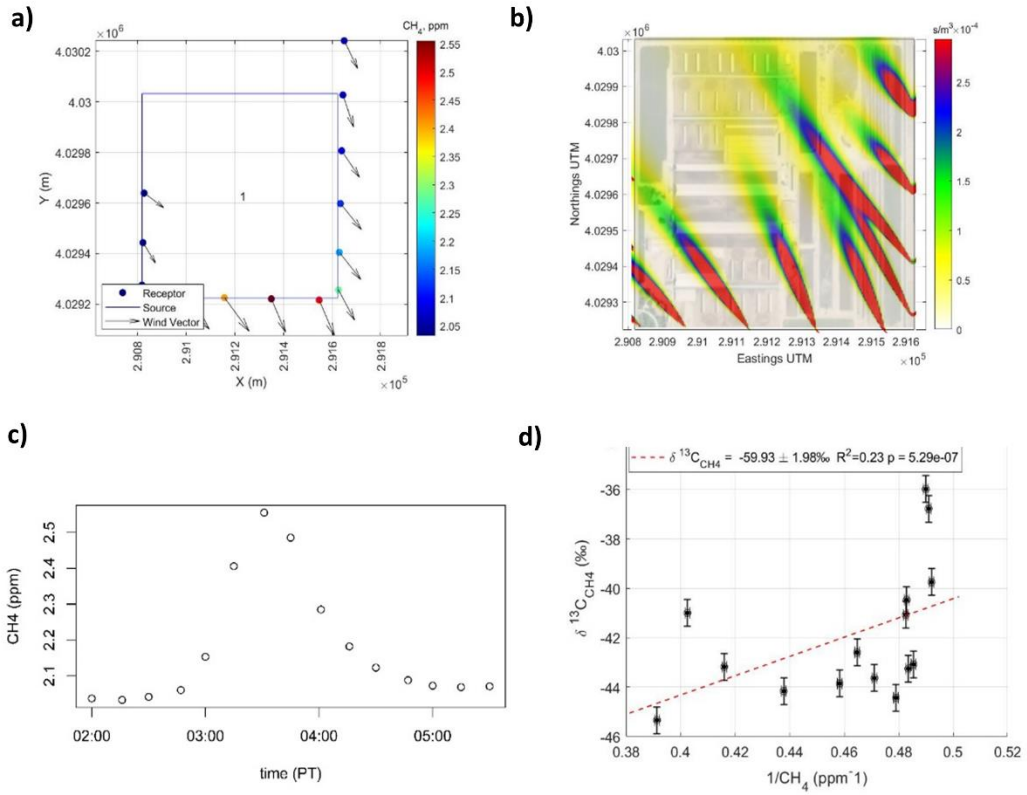

Figure S7. Isotopic signatures downwind of Dairy III on June 25th, 2019 from 14:02:00-14:05:30. a) Mobile platform measurements of 15-sec averaged CH_4 mole fractions (Receptor) downwind of Dairy III (Source). b) Methane flux footprint of Dairy III using the mobile survey shown in (a). The color gradient shows the relative contribution from the upwind areas where CH_4 was emitted. (c) Time series plot using 15-second averages from the mobile survey shown in (a). (d) Keeling plot using 15-second averages from the mobile survey shown in (a).

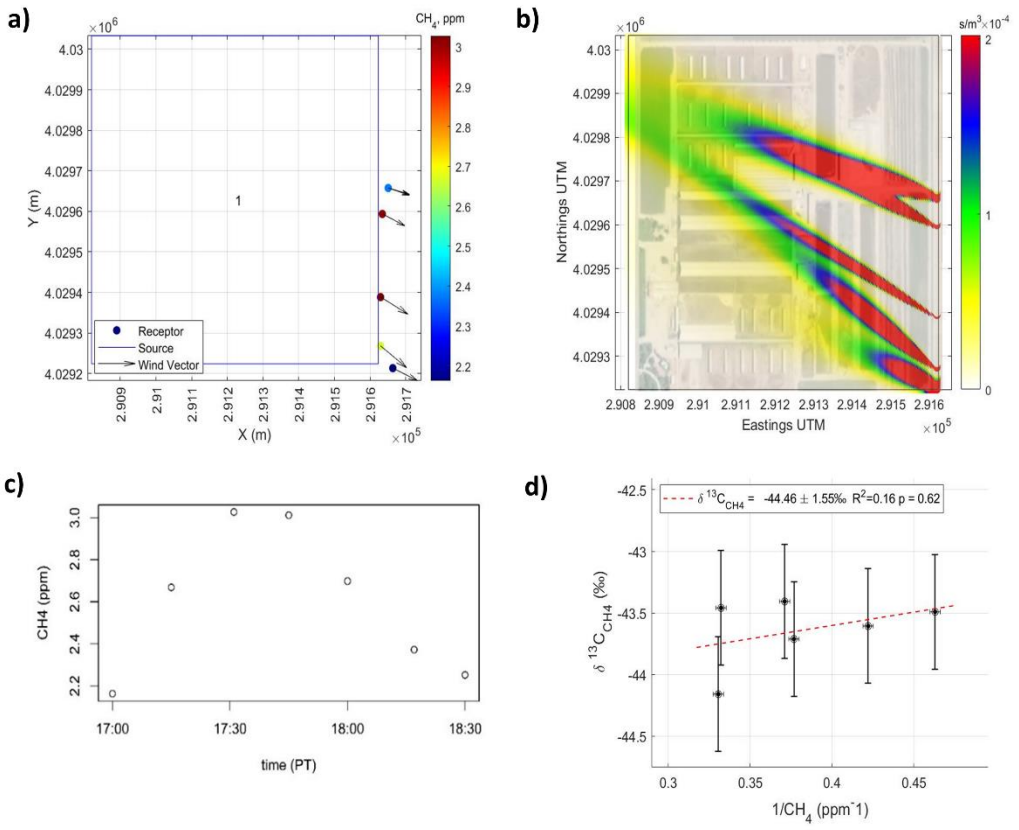

Figure S8. Isotopic signatures downwind of Dairy III on June 25th, 2019 from 15:17:00-15:18:28. a) Mobile platform measurements of 15-sec averaged CH_4 mole fractions (Receptor) downwind of Dairy III (Source). b) Methane flux footprint of Dairy III using the mobile survey shown in (a). The color gradient shows the relative contribution from the upwind areas where CH_4 was emitted. (c) Time series plot using 15-second averages from the mobile survey shown in (a). (d) Keeling plot using 15-second averages from the mobile survey shown in (a).

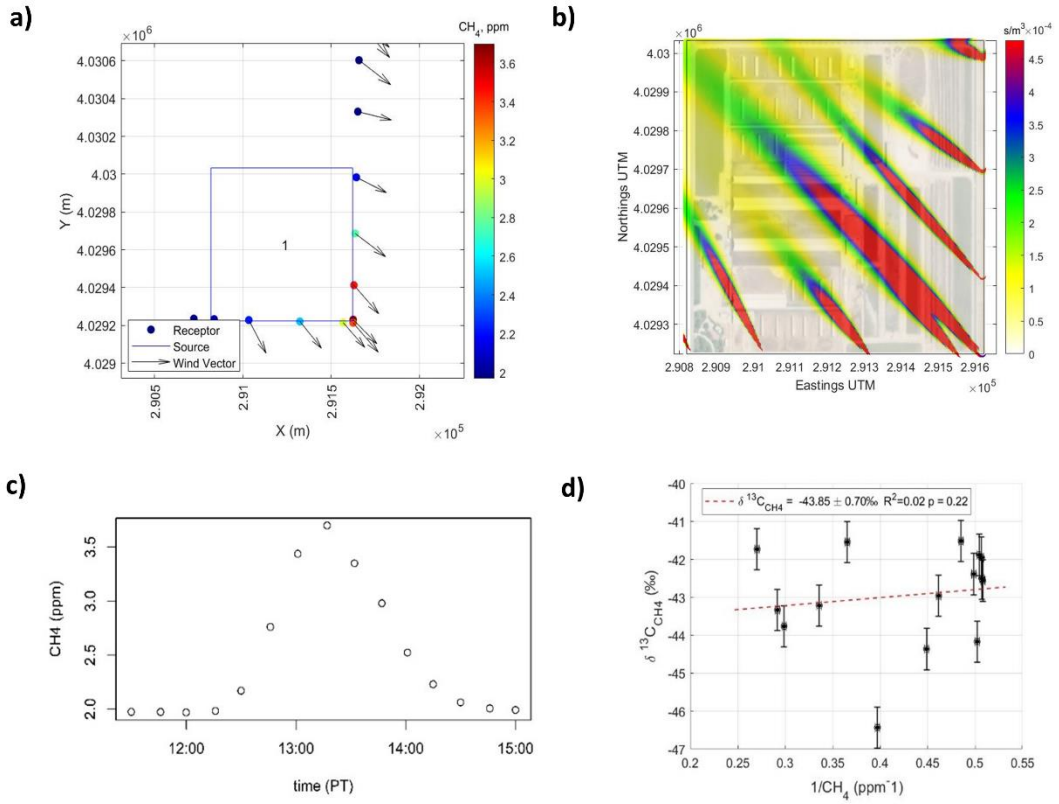

Figure S9. Isotopic signatures downwind of Dairy III on June 25th, 2019 from 17:11:30-17:15:00. a) Mobile platform measurements of 15-sec averaged CH_4 mole fractions (Receptor) downwind of Dairy III (Source). b) Methane flux footprint of Dairy III using the mobile survey shown in (a). The color gradient shows the relative contribution from the upwind areas where CH_4 was emitted. (c) Time series plot using 15-second averages from the mobile survey shown in (a). (d) Keeling plot using 15-second averages from the mobile survey shown in (a).

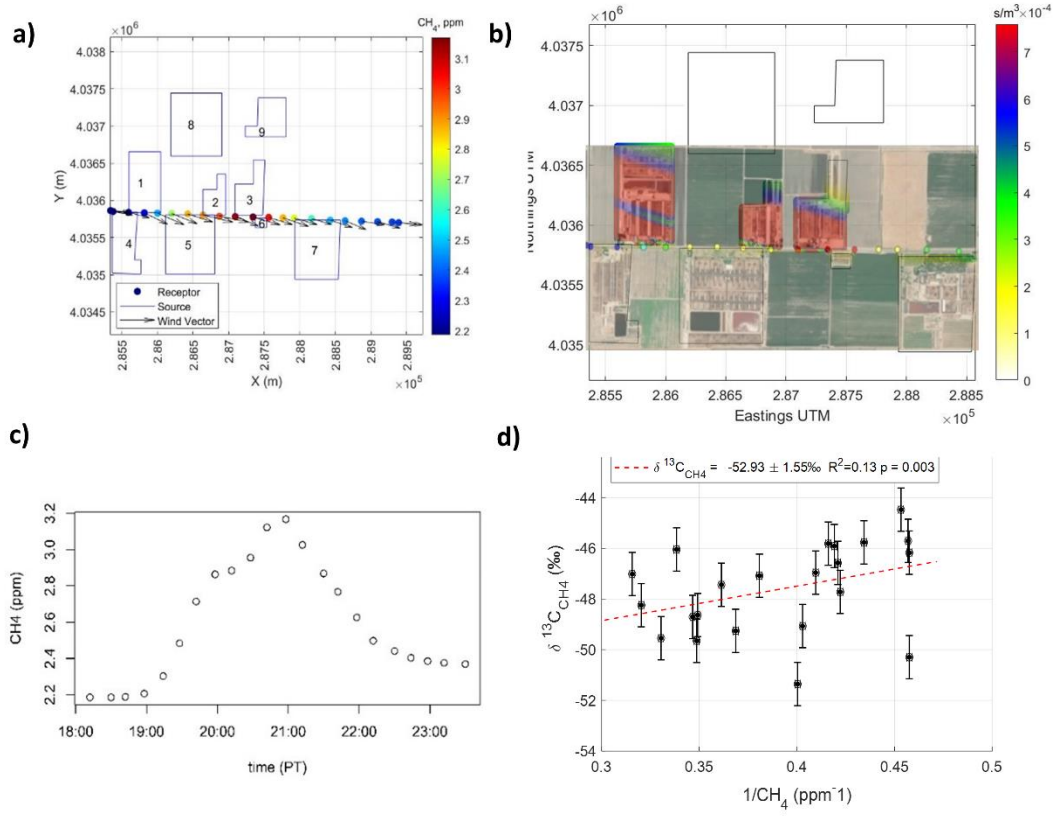

Figure S10. Isotopic signatures downwind of the Dairy Cluster on September 21st, 2018 from 17:18:12-17:23:36. a) Mobile platform measurements of 15-sec averaged CH_4 mole fractions (Receptor) downwind of the Dairy Cluster (Source). b) Methane flux footprints of the Dairy Cluster using the mobile survey shown in (a). The color gradient shows the relative contribution from the upwind areas where CH_4 was emitted. (c) Time series plot using 15-second averages from the mobile survey shown in (a). (d) Keeling plot using 15-second averages from the mobile survey shown in (a).

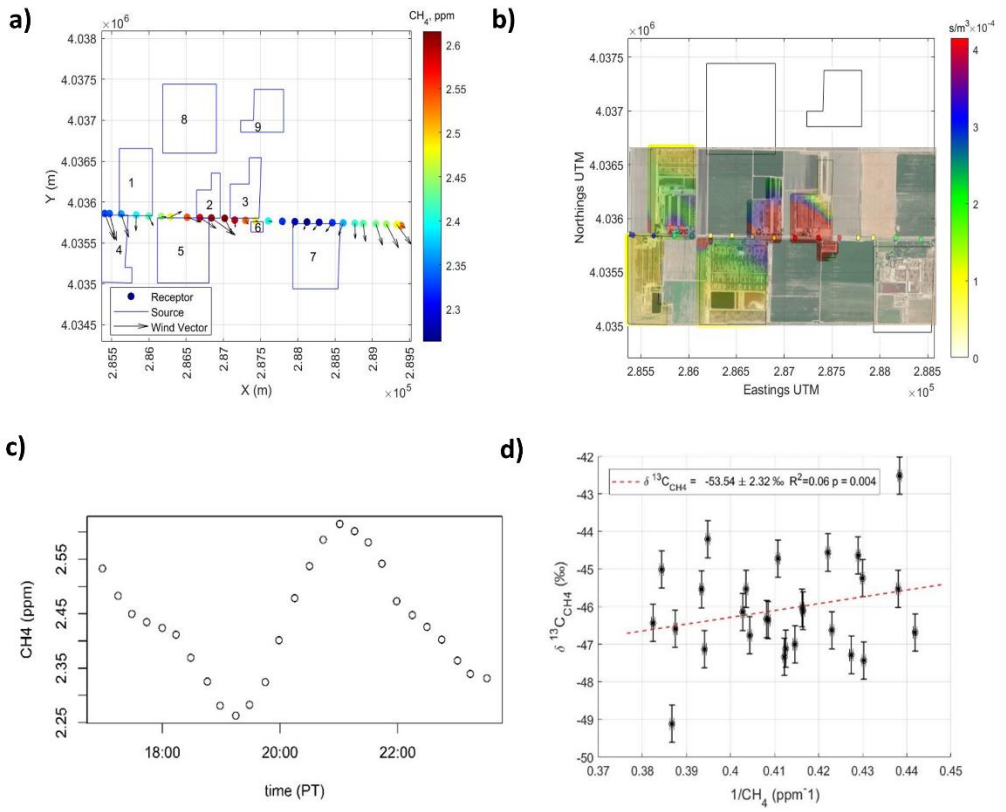

Figure S11. Isotopic signatures downwind of the Dairy Cluster on March 24th, 2019 from 14:16:59-14:23:34. a) Mobile platform measurements of 15-sec averaged CH_4 mole fractions (Receptor) downwind of the Dairy Cluster (Source). b) Methane flux footprints of the Dairy Cluster using the mobile survey shown in (a). The color gradient shows the relative contribution from the upwind areas where CH_4 was emitted. (c) Time series plot using 15-second averages from the mobile survey shown in (a). (d) Keeling plot using 15-second averages from the mobile survey shown in (a).

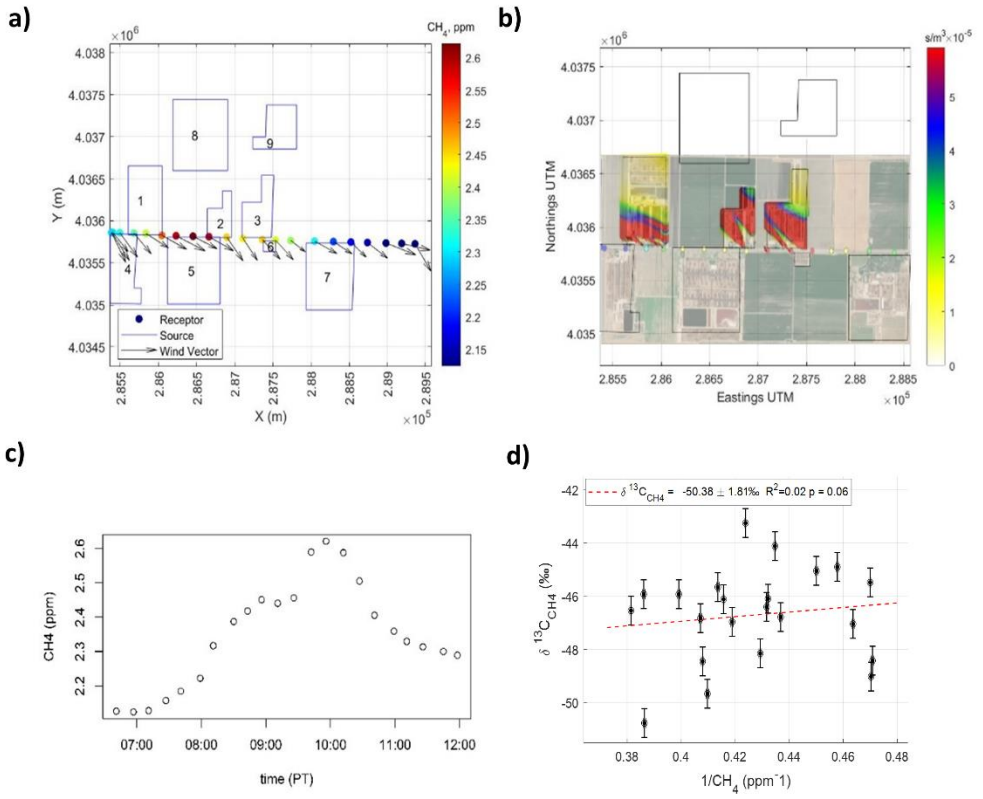

Figure S12. Isotopic signatures downwind of the Dairy Cluster on June 24th, 2019 from 16:06:41-16:12:05. a) Mobile platform measurements of 15-sec averaged CH_4 mole fractions (Receptor) downwind of the Dairy Cluster (Source). b) Methane flux footprints of the Dairy Cluster using the mobile survey shown in (a). The color gradient shows the relative contribution from the upwind areas where CH_4 was emitted. (c) Time series plot using 15-second averages from the mobile survey shown in (a). (d) Keeling plot using 15-second averages from the mobile survey shown in (a).

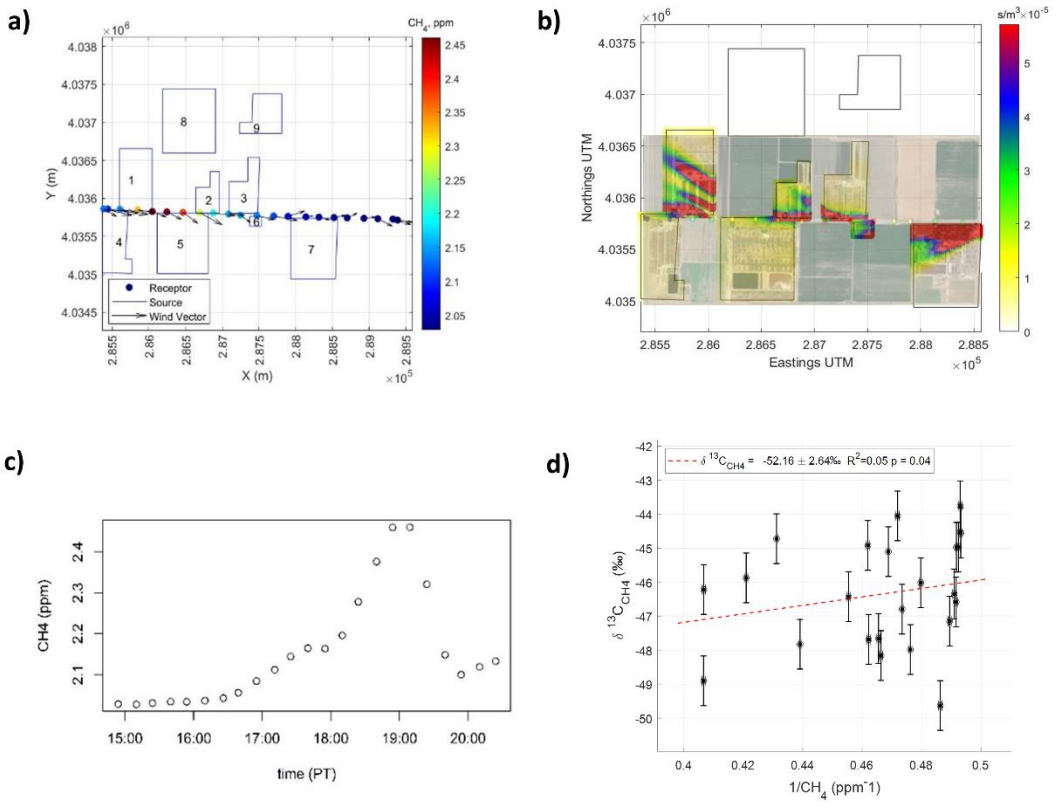

Figure S13. Isotopic signatures downwind of the Dairy Cluster on June 25th, 2019 from 14:14:54-14:20:28. a) Mobile platform measurements of 15-sec averaged CH_4 mole fractions (Receptor) downwind of the Dairy Cluster (Source). b) Methane flux footprints of the Dairy Cluster using the mobile survey shown in (a). The color gradient shows the relative contribution from the upwind areas where CH_4 was emitted. (c) Time series plot using 15-second averages from the mobile survey shown in (a). (d) Keeling plot using 15-second averages from the mobile survey shown in (a).